The Synthesis of α-Tocopentaenol (αT5), a Fluorescent Analogue of α-Tocopherol

By

Andrew Hildering

A Thesis

Submitted to the Department of Chemistry

In partial fulfillment of the requirements for the degree of

Master of Science

Supervised by

Professor Jeffrey K. Atkinson

December, 2016

Brock University

St. Catharines, Ontario

Acknowledgements

First, I would like to thank my supervisor, Dr. Jeffrey Atkinson, for allowing me to pursue my MSc thesis under his supervision. It was because of his constant support, understanding and guidance throughout my time in his lab that I have made it this far in my studies. The experience has been great, and I am able to thank him for the extensive knowledge I have gained through my two years of graduate studies.

I also would like to express my respect and admiration to my thesis committee members: Dr. Tomas Hudlicky, and Dr. Travis Dudding. The two of you were always more than willing to give me helpful advice, and allow me to use your equipment. The concepts and subjects you taught helped me immensely through my studies, and will hopefully continue to help me in the future.

I would like to further extend my thanks to Mr. Rasvan Simionescu, and Mrs. Liqun Qiu for all their time and assistance in the acquisition and interpretation of spectra.

I wish to thank my group members and all the co-workers I have had the privilege of working with: Mikel Ghelfi, Nick Krueger, Candace Panagabko, Parthajit Mukherjee, Matilda Baptist, Ravi Shekar, Nico Bonanno, and Cody Wilson for their constructive suggestions and discussions.

Last, but not least, I would like to thank both my family and friends for their constant support and guidance.

Abstract

This thesis is focused on the investigation of synthesizing a fluorescent analogue of vitamin E, α-tocopentaenol (αT5). α-Tocopentaenol contains five conjugated double bonds across the phytyl tail, resulting in its fluorescence characteristics. Different methodologies of preparation were attempted to synthesize an all *trans*-configuration in the five-conjugated double bonds. Unfortunately, across the C3' bond on the tail, geometric isomers were obtained. However, TBSO-αT5 was produced in what appeared to be ≈ 2:1 *E:Z* mixture across the C3' bond (having the four other olefins with *trans*-configurations). α-Tocopentaenol showed a strong absorbance in ethanol with a maximum λ_{ab}= 338 nm. This compound is stable as an oil, stored at -78˚C and protected from light for over a month with minimal degradation. Because αT5 resembles the naturally occurring form of the vitamin E, this analogue will enhance our ability to study the biological activity of vitamin E and will create an easy method of monitoring its presence in solution and cells.

Table of Contents

Acknowledgements ii

Abstract iii

List of Abbreviations vii

List of Tables viii

List of Figures viii

List of Schemes x

1. Introduction 1

1.1. Bioavailability and Bioactivity of Vitamin E 3

1.2. Structure and Function of Human Tocopherol Transfer Protein 7

1.3. Antioxidant Functions of Vitamin E 11

1.3.1 Factors Affecting the Antioxidant Activities of Vitamin E 16

1.4. Fluorescent Derivatives of Vitamin E 18

1.4.1 NBD, AO, NMA, and DAN Analogues 18

1.4.2 BODIPY Analogues 23

1.4.3 α-Tocohexaenol Analogue 26

1.5. Aims and Objectives 29

2. Results and Discussion 31

2.1. Design of a Fluorescent Analogue of Vitamin E 31

2.2. Synthesis of Intermediate (5) Through Zincke Aldehyde Formation 32

2.2.1 Preparation of (3) By Nucleophilic Attack of a Secondary Amine to the Activated Pyridine 32

2.2.2 Preparation of the Unsaturated Stannyl Aldehdye (5) 34

2.3. (S)- α –Trolox® as Starting Material 35

2.3.1 Manipulation of (*S*)- α –Trolox 35

2.3.2 Chain Elongation of Compound (10) Via Wittig Reactions 36

2.3.3 Hydrogenation vs Reduction and Oxidation 38

2.4. Olefin Cleavage of α-Tocotrienol 41

2.4.1 Ozonolysis of TBSO-αT3 43

2.4.2 $RuCl_3$ Oxidative Cleavage of αT3 45
2.4.3 OsO_4 Oxidative Cleavage of αT3 (Lemieux-Johnson Oxidation) 46
2.5. Production of an (E)-Vinyl Halide 47
2.5.1 Synthesis of Compound (30) using diethyl (1-iodoethyl)phosphonate 47
2.5.2 New Approach: Corey-Fuchs Modification 49
2.5.3 Hydrozirconation: Schwartz Reagent 51
2.6. Stille Coupling of Compounds (25) and (5) 54
2.7. Final Attempts at Correcting the C3'/C4' Geometry 60
2.7.1 Takai Olefination 60
2.7.2 Potassium Azodicarboxylate (PAD) Reduction 62
2.9. Stability of αT5 67
3. Conclusions and Future Work 68
4. Experimental 70
4.1. Synthesis of 1-(2,4-dinitrophenyl)-3-methylpyridin-1-ium chloride (2) 72
4.2. Synthesis of (2*E*,4*E*)-5-(dimethylamino)-2-methylpenta-2,4-dienal (3) 73
4.3. Synthesis of (2*E*,4*E*)-5-(dibutylamino)-2-methylpenta-2,4-dienal (4) 74
4.4. Synthesis of (2*E*,4*E*)-2-methyl-5-(tributylstannyl)penta-2,4-dienal (5) 75
4.5. Synthesis of Racemic methyl 6-hydroxy-2,5,7,8-tetramethylchroman-2-carboxylate (8) 76
4.6. Synthesis of (*S*)-methyl 6-hydroxy-2,5,7,8-tetramethylchroman-2-carboxylate (8) 77
4.7. Synthesis of (*S*)-methyl 6-((*tert*-butyldimethylsilyl)oxy)-2,5,7,8-tetramethylchroman-2-carboxylate (9) 78
4.8. Synthesis of (*S*)-6-((*tert*-butyldimethylsilyl)oxy)-2,5,7,8-tetramethylchroman-2-carbaldehyde (10) 79
4.9. Synthesis of (*S*,*E*)-ethyl 3-(6-((*tert*-butyldimethylsilyl)oxy)-2,5,7,8-tetramethylchroman-2-yl)acrylate (14) 80
4.10. Modified synthesis of (*S*,*E*)-ethyl 3-(6-((*tert*-butyldimethylsilyl)oxy)-2,5,7,8-tetramethylchroman-2-yl)acrylate (14) 81
4.11. Synthesis of *tert*-butyldimethyl(((*R*)-2,5,7,8-tetramethyl-2-((3*E*,7*E*)-4,8,12-trimethyltrideca-3,7,11-trien-1-yl)chroman-6-yl)oxy)silane (20) 82

4.12. Synthesis of (*S*)-3-(6-((*tert*-butyldimethylsilyl)oxy)-2,5,7,8-tetramethylchroman-2-yl)propanal (21) **83**
4.13. Synthesis of (*R*,*E*)-*tert*-butyl((2-(4-iodopent-3-en-1-yl)-2,5,7,8-tetramethylchroman-6-yl)oxy)dimethylsilane (30) **84**
4.14. Synthesis of (*R*,*E/Z*)-*tert*-butyl((2-(4-iodopent-3-en-1-yl)-2,5,7,8-tetramethylchroman-6-yl)oxy)dimethylsilane (30) **86**
4.15. Synthesis of diethyl (1-iodoethyl)phosphonate (32) **87**
4.16. Synthesis of (*R*)-*tert*-butyl((2-(4,4-dibromobut-3-en-1-yl)-2,5,7,8-tetramethylchroman-6-yl)oxy)dimethylsilane (33) **88**
4.17. Synthesis of (*R*)-*tert*-butyldimethyl((2,5,7,8-tetramethyl-2-(pent-3-yn-1-yl)chroman-6-yl)oxy)silane (34) **89**
4.18. Synthesis of (2*E*,4*E*,6*E*)-9-((*R*)-6-((*tert*-butyldimethylsilyl)oxy)-2,5,7,8-tetramethylchroman-2-yl)-2,6-dimethylnona-2,4,6-trienal (36) **91**
4.19. Synthesis of tributyl(3-methylbut-2-en-1-yl)phosphorane (37) **92**
4.20. Synthesis of *tert*-butyldimethyl(((*R*)-2,5,7,8-tetramethyl-2-((3*E*,5*E*,7*E*,9*E*)-4,8,12-trimethyltrideca-3,5,7,9,11-pentaen-1-yl)chroman-6-yl)oxy)silane (38) **93**
4.21. Synthesis of (*R*,*E*)-*tert*-butyl((2-(4-iodobut-3-en-1-yl)-2,5,7,8-tetramethylchroman-6-yl)oxy)dimethylsilane (40) **94**
4.22. Synthesis of *tert*-butyl(((2*S*)-2-(3-iodobutyl)-2,5,7,8-tetramethylchroman-6-yl)oxy)dimethylsilane (41) **96**

5. References **97**

6. VITA **114**

7. Appendix **115**

List of Abbreviations

AVED	Ataxia with isolated vitamin E deficiency
DMF	*N,N*-dimethylformamide
DIBAL-H	Diisobutyl aluminum hydride
HPLC	High performance liquid chromatography
IR	Infrared spectrometry
LAH	Lithium aluminum hydride
LHMDS	Lithium hexamethyldisilylamide
MS	Mass spectrometry
NMR	Nuclear magnetic resonance
PAD	Potassium azodicarboxylate
TBAF	Tetrabutylammonium fluoride
TBS	*tert*-butyldimethylsilyl ether
THF	Tetrahydrofuran
TLC	Thin layer chromatography
TTP	Tocopherol transfer protein

List of Tables

Table 1. Screening results for the oxidative cleavage of αT3 under various conditions 46
Table 2. Various Stille reaction conditions with the corresponding yields in the synthesis of (32) 56

List of Figures

Figure 1 Chemical structures of tocopherols and tocotrienols. 2
Figure 2. Simon metabolites: Top: α-tocopheronic acid, bottom: α-tocopherono lactone 5
Figure 3. Initial ω-hydroxylation, followed by a series of β-oxidation of α -tocopherol to yield water soluble α-CEHC 7
Figure 4. Drawing of the interactions of αT with the residues in the αTTP binding pocket. Hydrogen bonds are depicted with the dotted lines, and Van der Waal forces by the arcs.[27] 10
Figure 5. A comparison of the open (left) and closed (right) conformations of αTTP. Hydrophobic residues are yellow, basic; blue, acidic; red, polar; cyan. The hydrophobic key residues of the 'lid' (residues 198-221) are depicted in light gray.[27] 11
Figure 6. Radical chain reaction mechanism of lipid peroxidation 13
Figure 7. Coenzyme Q; ubiquinol, ubisemiquinone, and ubiquinone. 16
Figure 8. Fluorescent analogues of α-tocopherol. 18
Figure 9. Spectral characteristics of C9-NBD-αT; excitation and emission spectra recorded in methanol. Fluorescence excitation (solid line; monitored at 533 nm), and emission (dashed line; excitation at 466 nm) were monitored in 0.22 μM NBD-TOH.[57] 21

Figure 10. Time dependent change in fluorescence energy transfer between the lipid bilayer and NBD-tocopherol. Fluorescence monitored at 575 nm, with excitation at 466 nm.[59] 23
Figure 11. Chemical structure of BODIPY α-tocopherol analogue 24
Figure 12. Second generation BODIPY α-tocopherol analogue 25
Figure 13. Excitation and emission spectra of the second generation BODIPY analogue 25
Figure 14. αT6 absorbance spectra in ethanol (blue) and hexane (green). 27
Figure 15. Chemical structures of αT6, a fluorescent derivative of α-tocopherol and Fe-AOX-6, an inhibitor of lipid peroxidation. 27
Figure 16. Target molecule: αT5 ((*R*)-2,5,7,8-tetramethyl-2-((3*E*,5*E*,7*E*,9*E*)-4,8,12-trimethyltrideca-3,5,7,9,11-pentaen-1-yl)chroman-6-ol 29
Figure 17. Cartoon illustration of α-tocopentaenol and α-tocopherol in a phospholipid membrane. 30
Figure 18. Retrosynthesis of αT5 via α-tocotrienol and (*S*)- α-Trolox® 31
Figure 19. General overview of converting Trolox® to a one-carbon aldehyde (10). 35
Figure 20. Product observed on first attempt at the Wittig reaction in scheme 2B 37
Figure 21. Oxidative cleave of αT3 would result in the three-carbon intermediate needed for chain elongation, and could be performed in a one-step reaction. 42
Figure 22. Various methods to oxidatively cleave an olefin; 1[78], 2[79], 3[80], 4[81] 42
Figure 23. Expected products from an oxidative cleavage of αT3: a three-carbon aldehyde (21), acetone (28), and 4-oxopentanal (29). Due to the low boiling points of (28) and (29), those products were not isolated during purification. 45
Figure 24. Target intermediate, with the vinyl halide having (E)-geometry 47
Figure 25. Representation of diethyl (1-iodoethyl)phosphonate 48
Figure 26. Reduced alkene obtained via hydrozirconation of alkyne (34) 52
Figure 27. Top: Non-stabilized ylides favour (Z)-olefins, whereas stabilized ylides favour (E)-olefins (bottom). 58

Figure 28. Removal of the methyl group at C4' position would allow for a different pathway in attempts of obtaining (E)-geometry across that bond. The omission of the methyl group would not affect the binding to TTP. 60
Figure 29. Typical reaction conditions used in the Takai Olefination. 60
Figure 30. The reaction mechanism proposed by Takai. Chromium (II) is oxidized to chromium (III) after substitution of both iodine atoms. The geminal carbodianion acts as a nucleophile on the aldehyde. Following elimination of both chromium-bearing groups, the vinyl halide is formed. 61
Figure 31. Highlighting H_1 and H_2 in both the cis and trans- olefins. See Figure 29 and 30 for ^{1}HNMR analysis before and after PAD reduction. 63
Figure 32. ^{1}HNMR of an inseparable mixture of (*E*) and (*Z*)-40 before PAD reduction 64
Figure 33. ^{1}HNMR of an inseparable mixture of (*E*) and (*Z*)-40 after PAD reduction 65
Figure 34. Corey's method of producing (Z)-specific olefins from propargylic alcohols. Only after substitution of iodine, is the trans-geometry instilled. 66
Figure 35. UV-Vis absorption of TBSO-αT5 in ethanol (concentration 9.07 μM). 66
Figure 36. Future attempts at establishing correct (*E*)-geometry across the C3' bond using hydrostannylation methods 68

List of Schemes

Scheme 1. Pathway following the Zincke aldehyde reaction, whereby an activated pyridine is prone to nucleophilic addition.. 32
Scheme 2. A) Esterification, protection and DIBAL reduction lead to compound (10).. 36
Scheme 3. Competing pathways of forming the P-O bond with the use of this phosphonium ylide. 37
Scheme 4. Four products obtained from the LAH reduction of (14). 38

Scheme 5. Isomerization of α, β-unsaturated alcohol to the saturated aldehyde (21) 39
Scheme 6. Microwave reaction of trimethylhydroquinone (20), methyl methacrylate (21), and formaldehyde (22) to produce racemic (8).. 40
Scheme 7. Lemieux Johnson Oxidation of an olefin 43
Scheme 8. Use of phosphonium ylide (27) would obtain compound (26) with the unwanted geomtry. 48
Scheme 9. Schlosser Modification of the Wittig reaction. (E)-geometry is produced when $R_2 \neq$ methyl/Hydrogen. As a result, this method could not be used. 49
Scheme 10. Corey–Fuchs modification for the production of an internal alkyne (34). 50
Scheme 11. *In situ* synthesis of Schwartz reagent during the reaction produced a mixture of three compounds, viewed as a single spot on TLC. 54
Scheme 12. Optimized Stille coupling conditons between vinyl halide (26) and (5). 55
Scheme 13. Wittig reaction between (36) and phosphonium salt (37) produced TBSO- αT6 in a 26% yield. 59
Scheme 14. Reaction conditions used for the Takai olefination. 62
Scheme 15. Thought process for using PAD as a reductant on the olefin. 63

1. Introduction

The history of vitamin E begins nearly a century ago when, in 1922, Dr. Herbert M. Evans and Dr. Katharine S. Bishop discovered that rats were unable to reproduce when fed a semi-synthetic purified diet of lard.[1] Interestingly, fertility was restored when the rats were given wheat germ as part of their diet. It was concluded that diets prepared from purified materials lacked a substance needed for normal growth, and natural foods contained a compound that was essential for reproduction. Upon lipid extraction and isolation of this unknown compound, vitamin E was discovered.[1,2]

Vitamin E is a term that encompasses eight fat-soluble antioxidants consisting of four tocopherols (α, β, γ, and δ) and four tocotrienols (α, β, γ, and δ) **(Figure 1)**.

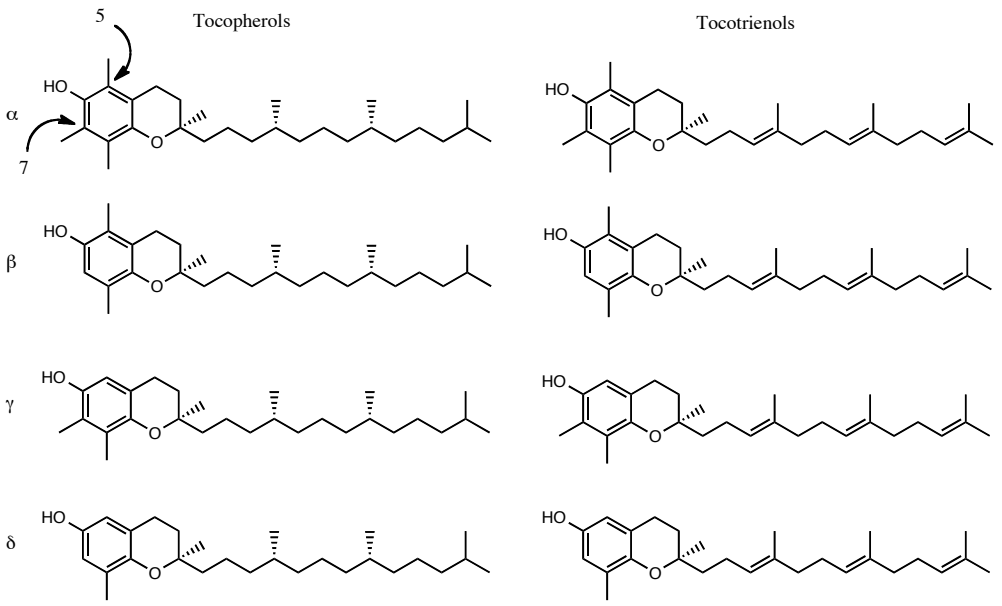

Figure 1 Chemical structures of tocopherols and tocotrienols.

Both the tocopherols and tocotrienols contain a chroman ring portion, which depending on the position and numbering of the methyl substituents at positions 5 and 7 on the aromatic ring, defines the different forms of the vitamin.[3] The absence or presence of these methyl groups contributes to each molecule's respective antioxidant properties.[4,5] Attached to the chroman is a chain (consisting of 16 carbons) known as the phytyl tail that is primarily responsible for the hydrophobic nature of these compounds. The slight difference between tocopherols and tocotrienols lies in the saturation of the phytyl tail; tocopherol is fully saturated with two chiral centers (C4' and C8'), whereas tocotrienols are unsaturated at positions 3', 7' and 11'.[4]

Arguably, vitamin E's most noteworthy characteristic is the donation of its phenolic hydrogen atom to a reactive radical species, protecting against lipid peroxidation in membranes. α-Tocopherol (αT) donates a hydrogen atom to

peroxyl radicals, creating a lipid hydroperoxide and an α-tocopheroxyl radical that has one of two fates: a further one-electron oxidation to produce α-tocopheryl quinone, or predominately, it is reduced / recycled by vitamin C. Both fates lead to a more stable compound than that of the oxygen containing radical, and halt any further damage that could harm the membrane, ultimately protecting cell integrity.[5,6]

Apart from antioxidant properties, much is still unknown about tocopherols. Vitamin E has been a conundrum of nutritional chemistry for over ninety years. Since the discovery of vitamin E, certain questions involving the mechanism of transport and delivery to tissues remain partially unanswered. Because of the hydrophobic property of vitamin E, a central challenge *in vivo* is the transport and delivery of this molecule to specific environments and tissues. To visualize the transport of tocopherols, fluorescent probes have been incorporated at the terminus of the phytyl tail.[7] These probes act as reporters of the cellular location of vitamin E.[8] Still, the mechanism as to how α-tocopherol transfer protein (αTTP) selectively mediates tocopherol secretion from liver cells is still not very well understood.[9]

1.1. Bioavailability and Bioactivity of Vitamin E

Vitamin E is an essential nutrient that cannot be synthesized in mammals and must be acquired through diet.[3] Vitamin E consumption is obtained from vegetable oils, nuts, and wheat germ.[10] Because of the availability and consumption of particular plant products in North America (particularly soy oil), γ-tocopherol (γT) accounts for roughly 70% of the vitamin E obtained in the US diet.[3] However,

because of different food preferences, individuals in Europe have a lower intake of γT. Sunflower oil (5mg γT /100g) and olive oil (0.7mg γT /100g) predominate in the diet of Europeans, whereas in the US, soybean (80mg γT /100g) and corn oils (60mg γT /100g) are mainly consumed.[11]

The majority of research has focused on tocopherols because of their retention at higher concentrations within human plasma (α-tocopherol; 10-15μg/ml, γ-tocopherol; 3-5μg/ml),[12,13] whereas tocotrienol concentrations are significantly lower (≈0.7μg/ml).[14] However, despite γT being the most consumed form of vitamin E amongst North Americans, αT, is the most potent and biologically active antioxidant (accounts for ≈ 90% of the vitamin E in both human and animal tissue; including serum levels).[15]

In the past, the higher plasma levels of αT over other isoforms led researchers to hypothesize that the absorption efficiencies of these vitamins varied within the small intestine. By using deuterium-labeled tocopherols, researchers examined this hypothesis and concluded that there is no noticeable difference. After ingestion, all isoforms are absorbed with equal efficiencies.[3,9,16] Following gastrointestinal absorption, all forms of vitamin E are packaged and discharged into chylomicrons (vesicles responsible for the transfer of fat-soluble compounds from the intestine to the liver). Only once these nutrients enter the liver is there any discrimination between the compounds.[3]

α-Tocopherol is selectively retained as a result of the α-tocopherol transfer protein (αTTP). α-Tocopherol transfer protein, a 32 kDa cytosolic protein, is highly expressed in the liver, and controls the transfer of αT from hepatocytes by re-

secreting the tocopherol into plasma on very-low density lipoproteins (VLDL), allowing for distribution through the plasma to target tissues.[17] However, αTTP is highly selective for αT, while all other forms of vitamin E are essentially metabolized and excreted.[6]

Excess vitamin E beyond the body's needs, is metabolized before excretion. For a long time the only known urinary metabolites were the "Simon metabolites", first observed in 1956 (**Figure 2**).[18] These metabolites encompass α-tocopheronic acid and its lactone, and are excreted in urine as glucuronides or sulfates. Additionally, these metabolites had a shortened side chain and opened chroman ring.[19] Opening of the chroman ring is initiated by the α-tocopheroxyl radical intermediate (after αT acts as an antioxidant, donating the phenolic hydrogen atom). However, these metabolites are thought to be an artifact arising during sample preparations and formed by chemical or enzymatic hydrolysis. In the absence of oxygen, Simon metabolites were not observed.[20] The spontaneous oxidation of carboxyethyl hydroxychromans (see below) would lead to these Simon metabolites.

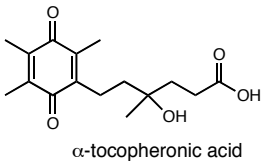

α-tocopheronic acid

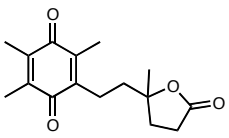

α-tocopherono lactone

Figure 2. Simon metabolites: Top: α-tocopheronic acid, bottom: α-tocopherono lactone

Carboxyethyl hydroxychromans (CEHC's) are the other class of vitamin E metabolites found in urine and blood.[21] This process of degradation is catalyzed by cytochrome P450 monooxygenase enzymes (**Figure 3**). In contrast to αT, the seven other forms of vitamin E are efficiently degraded by cytochrome P450 monooxygenases and secreted into bile then excreted in feces. Parker originally studied the necessity of these monooxygenases by demonstrating that inhibition of the P450 complexes by ketoconazole diminished the build-up of the water soluble tocopherol metabolites.[22] In the initial step, cytochrome P450 catalyzed ω-hydroxylation produces the corresponding 13-hydroxyl-tocopherol/tocotrienols. Further oxidation of the terminal hydroxyl, performed by microsomal dehydrogenases, produces the water-soluble carboxylic acid derivative. β-Oxidation, a five step chain shortening process, ultimately produces carboxyethyl hydroxychromans (CEHC's).[23] CEHC's have been shown to be produced by α, γ, and δ- tocopherols, and α, and γ-tocotrienols.[6] Only approximately 1-3% of consumed *RRR*-α-tocopherol appears as α-CEHC in urine (as opposed to 50% of γ-tocopherol).[24]

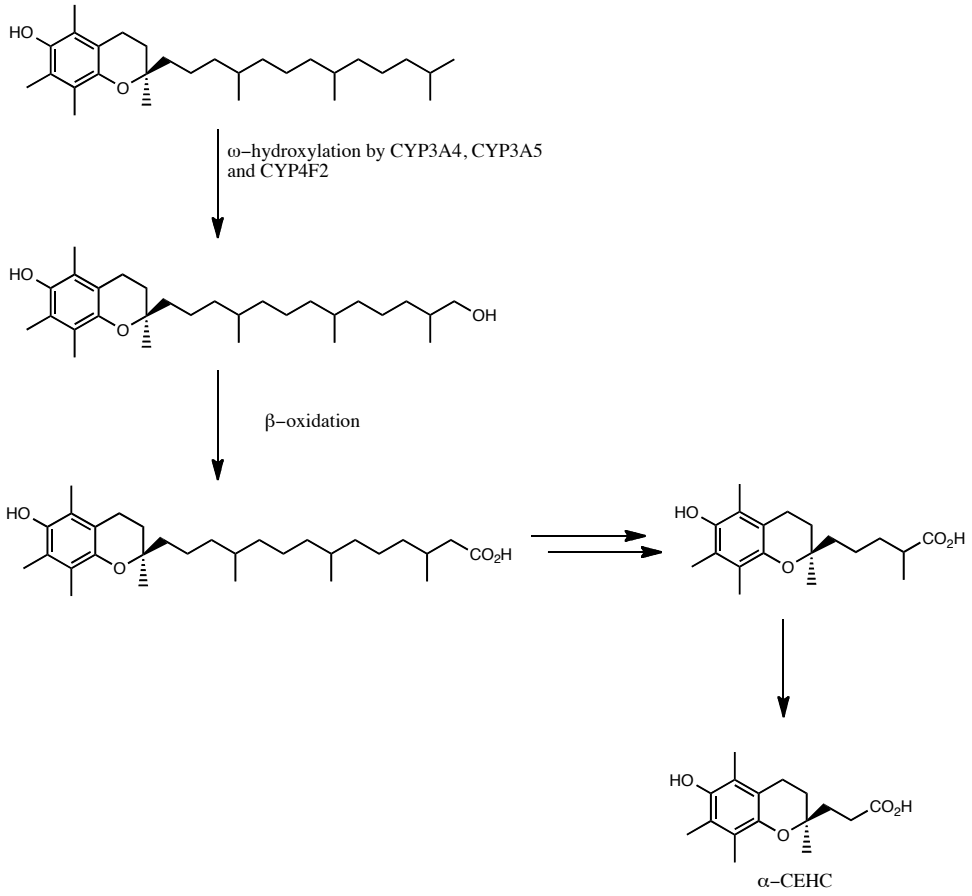

Figure 3. Initial ω-hydroxylation, followed by a series of β-oxidation of α -tocopherol to yield water soluble α-CEHC

1.2. Structure and Function of Human Tocopherol Transfer Protein

α-Tocopherol transfer protein is important for maintaining normal and sufficient levels of αT in humans. Vitamin E deficiency is known to occur when the *hTTP* gene suffers mutations, several of which have been shown to result in ataxia with vitamin E deficiency (AVED).[25] AVED is an autosomal recessive neurodegenerative disease that prevents the body taking up vitamin E in the diet. Symptoms of AVED include: the inability to coordinate movements and speech, the loss of reflexes in the legs, and peripheral neuropathy.[26] The failure of αTTP to

transfer αT from the liver to nascent very low density lipoproteins (VLDL) is thought to be the cause of low vitamin E serum levels in patients with AVED. α-Tocopherol transfer protein is believed to incorporate αT in VLDLs, however, the mechanism of αTTP assisted loading of VLDL with αT is still unknown.[9]

α-Tocopherol transfer protein is considered a member of the SEC14-like protein superfamily, containing a CRAL-TRIO domain. The yeast phosphatidylinositol/ phosphatidylcholine transfer protein (Sec14), cellular retinaldehyde binding protein (CRALBP) and supernatant protein factor (SPF) are also part of this family. All members of this family can facilitate the *in vitro* transfer of their specific lipid ligands from one membrane to another.[27] It was found that many forms of vitamin E (including all tocopherols, α-tocotrienol, Trolox, phenol protected αT, αT quinone, *etc*.) bound to αTTP at a much lower K_d than Sec14, SPF and CRALBP. All other homologous proteins bound to αT, but at much lower affinities (> 10 fold K_d) than αTTP. As a result, it was suggested only αTTP can act as a competent mediator of αT transport.[28]

An *in vitro* study performed by Hosomi *et al*. showed the specificity that αTTP has for αT. *RRR*-α-Tocopherol had 100% specificity compared to βT (38%), γT (9%) and δT (2%).[28] Panagabko *et al.* measured the dissociation constants, K_d, in a radiolabeled binding assay that showed αT had a five-fold greater affinity for αTTP than the βT and fully ten-fold greater than γT.[28] α-Tocopherol had the greatest affinity to αTTP because of its full methyl substituted chromanol ring.[28] The presence of the methyl groups increase the hydrophobic interactions and packing density in the αTTP binding pocket. When methyl groups are absent, these

properties decrease, lowering the affinity to αTTP. As supporting evidence, Fersht showed there was a loss of 1.3 kcal/mol in binding energy when a methylene group was removed from a chymotrypsin inhibitor in a highly hydrophobic pocket.[29] This number can be used as a rough comparison of the methyl group interactions in the hydrophobic pocket of αTTP.[27]

Additional properties important for recognition for binding to αTTP are a phytyl tail and the *R*-configuration where the phytyl tail attaches to the chromanol ring (C2 position).[30] The preferential binding of *RRR*-αT or γT to αTTP is shown by the 3-fold increase of the half-life of *RRR*- αT (57 ± 19 hours) compared to that of *SRR*.[31] Therefore, only natural *RRR*- αT or 2*R*-αT (obtained from a mixture of all racemic αT found in supplements) are retained by the body.[31]

To be an effective transfer protein, it is reasonable to assume that αTTP should bind to membranes reversibly and sequester its hydrophobic ligand from the aqueous medium (**Figure 4**). α-Tocopherol transfer protein exists in both an open and closed conformation (**Figure 5**). When in the closed form, the lid (residues 198-221 on αTTP that are exposed to the solvent) is directly interacting with the phytyl tail of αT. When the protein is membrane-bound and the lid opens, new hydrophobic interactions occur on the membrane surface and αT is released into the bilayer. Similarly, when αT binds to αTTP, closing of the lid shuttles αT into the empty binding site and pushes any water molecules out through an additional tunnel located at the back of the binding site.[27]

α-Tocopherol transfer protein facilitates the transfer of αT between donor and acceptor hydrophobic environments. α-Tocopherol transfer protein is

responsible for transferring αT from liposomes to mitochondria, microsomes, and erythrocytes. Unfortunately, the molecular mechanism by which this happens is unclear.[32] It has been speculated that αTTP distributes ligand transfer to intracellular organelles to similar pathways as Sec14p. Atkinson demonstrated that αTTP can transfer tocopherol between synthetic lipid bilayers, indicating (at least *in vitro*) that additional proteins may not be required.[8]

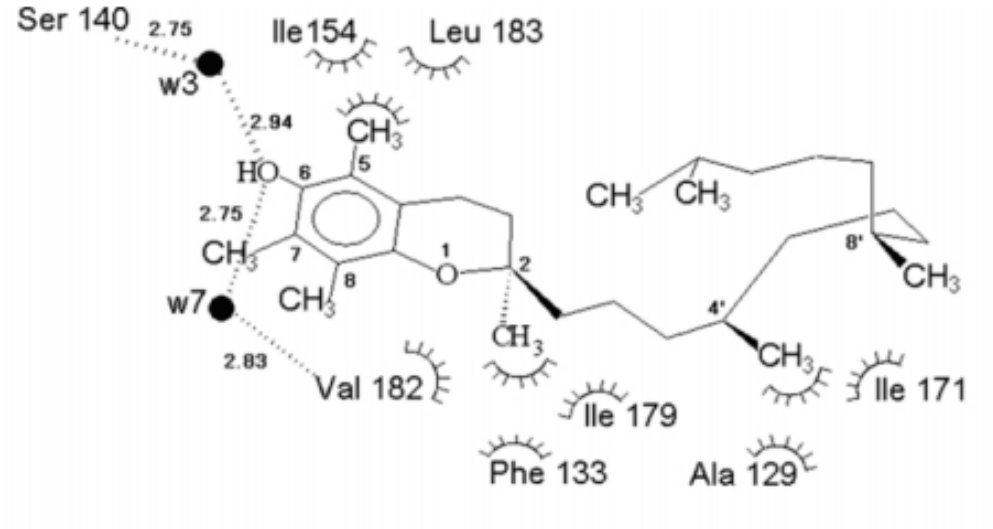

Figure 4. Drawing of the interactions of αT with the residues in the αTTP binding pocket. Hydrogen bonds are depicted with the dotted lines, and Van der Waal forces by the arcs.[27]

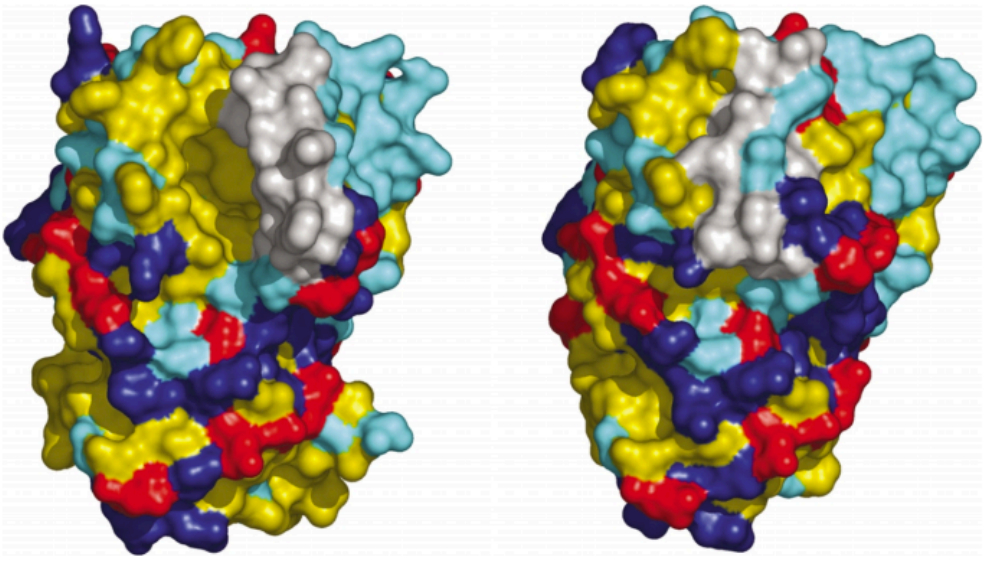

Figure 5. A comparison of the open (left) and closed (right) conformations of αTTP. Hydrophobic residues are yellow, basic; blue, acidic; red, polar; cyan. The hydrophobic key residues of the 'lid' (residues 198-221) are depicted in light gray.[27]

1.3. Antioxidant Functions of Vitamin E

Oxygen is essential to aerobic life yet, paradoxically, it can also be very toxic to cells. Cells that are exposed to molecular oxygen are at risk of being damaged by free radical species derived from oxygen, such as superoxide or hydroxyl radicals. These radicals can abstract a hydrogen atom from lipids located in the cell membrane, in a process known as lipid peroxidation.[33,34–37]

Lipids are fundamental components of cell membranes, maintaining structural integrity and participating in cell signaling processes. Unfortunately, under oxidative stress, lipids can be damaged by reactive oxygen species (ROS).[38,39] Reactive oxygen species arise from biochemical reactions, exposure to some

environmental pollutants, and consumption of certain drugs and toxins. Cellular components of our body can be adversely affected under oxidatively stressful conditions. When the oxidative stress increases, cells stimulate the production of antioxidants (both enzymatic and non-enzymatic) as a primary defense system that efficiently neutralize the ROS.[40]

Enzymatic antioxidant processes use metal cofactors in breaking down the ROS. Superoxide dismutases (SODs) catalyze the breakdown of superoxide into hydrogen peroxide and oxygen. SODs are located in the mitochondria and cytosol, and use copper, zinc or manganese cofactors. Additionally, catalase converts hydrogen peroxide to water and oxygen and glutathione peroxidases (present in cytoplasm and extracellularly) convert hydrogen peroxide to water. Various peroxidases catalyze the reduction of hydroperoxides, and peroxynitrites.[41] Non-enzymatic antioxidants, such as vitamin E, vitamin C, carotenoids, and glutathione work by reacting with the ROS, acting as reducing electron sources, terminating the ROS. However, under high oxidative stress, lipid peroxidation rates increase and the overwhelming amount of ROS is too much for the antioxidant defense. As a result cell apoptosis may be triggered.[42]

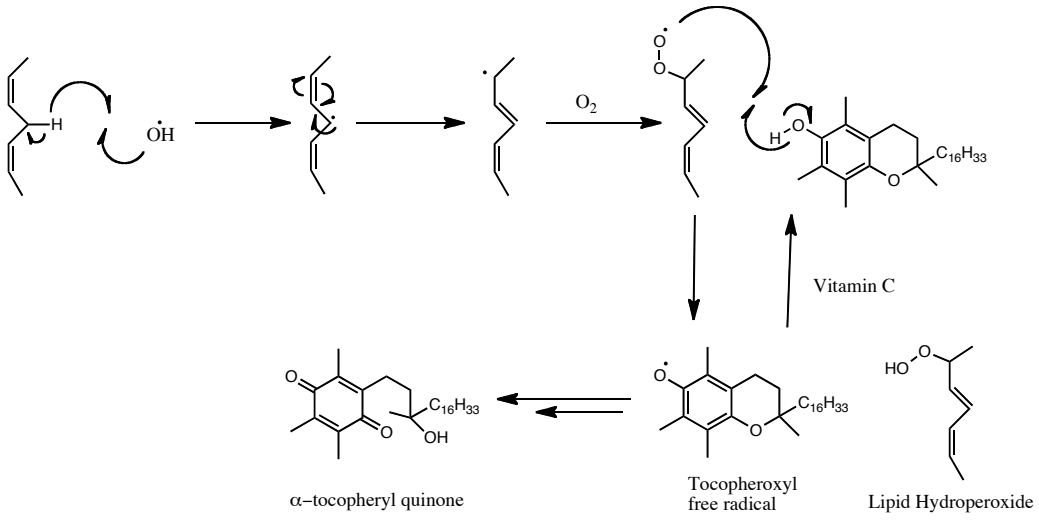

Figure 6. Radical chain reaction mechanism of lipid peroxidation

Peroxidation of polyunsaturated fatty acids consists of three reactions: initiation, chain propagation, and chain termination (**Figure 6**).[34] In the initiation phase, hydrogen abstraction by a ROS creates a short-lived carbon centered radical. Several forms of molecules are known to abstract the initial hydrogen: these species include alkoxy or hydroxy radicals (initiated from redox chemistry of Cu^{2+} and Fe^{2+}), UV radiation, and other initiators such as superoxide, nitric oxide and peroxynitrite.[37] In the case of transition metals, such as Fe^{2+}, and to a lesser extent, Cu^{2+}, it has been found that these metals have enough sufficiently reducing redox potential to result in decomposition of hydroperoxides. These metals participate in one electron redox cycles, resulting in peroxyl and alkoxyl radicals.[43] However, O_2^-, and •OH are the main culprits for initiating lipid peroxidation. These hydroxyl radicals can be generated by a Fenton-catalyzed Haber-Weiss reaction, where the iron acts as a catalytic mediator between H_2O_2 and superoxide anion.[44]

After the radical initiator is formed, the hydrogen abstraction occurs at the bis-allylic position, since this is where the weakest hydrogen bond (73 kcal/mol *vs* 88 kcal/mol for an allylic hydrogen) is located.[45,46,47] This methylene hydrogen abstraction by the peroxyl radical occurs with a rate of about 100^{-1} M s^{-1} and is viewed to be the rate-limiting step in autoxidation.[34] *In vitro*, this hydrogen abstraction can be mimicked and studied on linoleic acid or methyl linoleate.[46] Upon hydrogen abstraction, isomerization rapidly occurs to form the more stable conjugated diene. During this propagation phase, molecular oxygen reacts quickly with the isomerized carbon radical to form the lipid peroxyradical (ROO•). This addition of oxygen happens extremely fast and the rate of addition is only restricted by the length of time it takes oxygen to diffuse to the site of the radical (10^9 M^{-1} s^{-1}).[34,48]

Because peroxyl radicals have half-lives ranging between milliseconds to seconds, if no antioxidant is present the peroxyl radical can abstract a hydrogen atom from an adjacent lipid molecule producing a chain reaction. Continuation of multiple propagation steps will consume valuable polyunsaturated fats and result in a high concentration of the lipid hydroperoxide (ROOH). Even though this H-atom abstraction by peroxyl radicals is the slowest of the autooxidation steps, it is facilitated by the close proximity of neighboring lipids.[49]

The evidence suggesting the importance of vitamin E in protecting cell membranes is highlighted by the fact that it is the only major lipid-soluble, chain-breaking antioxidant located in tissues, red cells, and blood. Granted, β-carotene does have some antioxidant activity, but it is much less efficient and is thought to be

important in areas of the cell where there is very low oxygen partial pressure.[49] Lemoyne attempted to prove the antioxidant effects of αT by studying the concentrations of exhaled pentane. Pentane is a minor product formed during fragmentation of the fatty acyl peroxyl radicals.[44] Human test subjects who had been given vitamin E had a reduced amount of pentane in their breath samples. Such evidence strongly supports the prevention of lipid peroxidation by vitamin E.[50]

The prevention of lipid peroxidation is associated with the phenol moiety on vitamin E. The phenolic hydrogen bond is weaker (≈78 kcal/mol)[51] than the bis-allylic C-H bond of the fatty acid. As a result, vitamin E prevents the destructive propagation process by donating its phenolic hydrogen, terminating the process before another lipid can react. The antioxidant reaction, with αT as the hydrogen donor, has a rate of 3.8×10^6 M^{-1} s^{-1}.[52] The stable α-tocopheroxyl radical (**Figure 6**) that is formed moves freely, and may react with other lipid peroxyl radicals, forming a non-radical species.[53] Thus, the chain reaction of free radical–induced membrane oxidation is interrupted, and cell membrane integrity is protected.[34]

The tocopheroxyl radical can be reduced (regenerating tocopherol) by vitamin C or coenzyme Q.[33] It is thought that the α-tocopheroxyl radical is less reactive than the oxygen-containing radicals, and can "float" to the top of the membrane near the aqueous environment. Vitamin C is also an antioxidant and in *vitro* evidence demonstrates the proficiency of vitamin C to reduce tocopheroxyl radical back to vitamin E. However, *in vivo* studies proving the recycling of vitamin E by vitamin C is lacking as well as controversial.[33,54–56]

The possibility of the regeneration of αT through coenzyme Q is also possible. If αT and coenzyme were to work together, a redox cycling process would occur; as shown[49]:

$TO\bullet + QH_2 \rightarrow TOH + HQ\bullet$ (1)

$TO\bullet + HQ\bullet \rightarrow TOH + Q$ (2)

where QH_2, HQ• and Q are ubiquinol, ubisemiquinione, and ubiquinone, respectively (**Figure 7**).

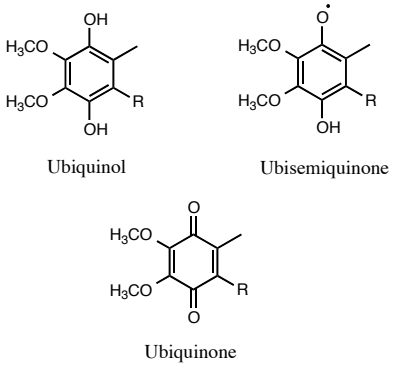

Figure 7. Coenzyme Q; ubiquinol, ubisemiquinone, and ubiquinone.

1.3.1 Factors Affecting the Antioxidant Activities of Vitamin E

Certain factors determine the antioxidant activity of vitamin E. These factors include: i) how well vitamin E reacts with free radicals, and ii) the concentration and localization of vitamin E in a cell. The rate that a phenolic antioxidant reacts with a peroxyl radical is directly related to their antioxidant efficiency. α -Tocopherol reacts ≈200 times faster with a peroxyl radical than the commercial antioxidant, butylated hydroxytoluene (BHT).[57] Because αT reacts with peroxyl radicals at a much faster rate than polyunsaturated fatty acids, 'catalytic' amounts of αT can

protect the cell membrane. Studies indicate one αT per 1000 lipid molecules is present in cell membranes.[58]

Ingold and co-workers were able to determine the rate constants for H-atom abstraction and the corresponding bond dissociation energy (BDE) of the phenolic hydrogen.[57,59] They discovered that all forms of vitamin E would be good chain-terminating antioxidants *in vivo,* through *in vitro* studies. However, αT had the largest rate constant for H-atom transfer to a peroxyl radical (3.2×10^6 $M^{-1}s^{-1}$)[57], indicating it was the most efficient antioxidant. Two factors are responsible for αT's properties to be the most potent antioxidant: the steric effects surrounding the hydroxyl group, and the BDE of the phenolic hydrogen. Not surprisingly, having *tert*-butyl groups in the *ortho* positions with respect to the hydroxyl group, decreases reactivity that is due to steric crowding. However, in the case of vitamin E, the steric crowding is almost negligible and the BDE must be the discerning factor.[23]

A low BDE makes for a stronger antioxidant in both kinetic and thermodynamic respects. In the inhibition step, hydroperoxide (ROO-H bond) has a BDE of 88 kcal/mol. For an antioxidant to be efficient, the phenolic hydroxyl BDE must be <88 kcal/mol. In the case of αT, the BDE is 78.2 kcal/mol, βT; 78.7 kcal/mol, γT; 80.7 kcal/mol, δT; 81.7 kcal/mol.[23] With respect to vitamin E, three factors decrease BDE: an alkoxy group in the *para* position, alkyl substituents positioned on the aromatic ring, and the electron donating effects of the methyl (and alkoxy) groups are greater in the *ortho* and *para* than *meta*-positions. These factors of αT's structure weaken its BDE, enabling it to be an effective antioxidant.[23]

1.4. Fluorescent Derivatives of Vitamin E

1.4.1 NBD, AO, NMA, and DAN Analogues

A series of fluorescent analogues of αT has been synthesized in attempt to study both the mechanisms by which αTTP assists the secretion of αT from hepatocytes to carrier lipoproteins and mode of transport between various intracellular sites.[7] Current techniques attempting to study these issues involve the use of tissue or plasma extraction followed by chromatography and mass spectrometry. As a result of extraction, all time and spatial movement of tocopherol is lost. Additionally, extensive manipulations, poor kinetic resolution, and low signal-to-noise make this method unfavorable for tracking the movement of the vitamin in tissues, let alone cells.[7,60]

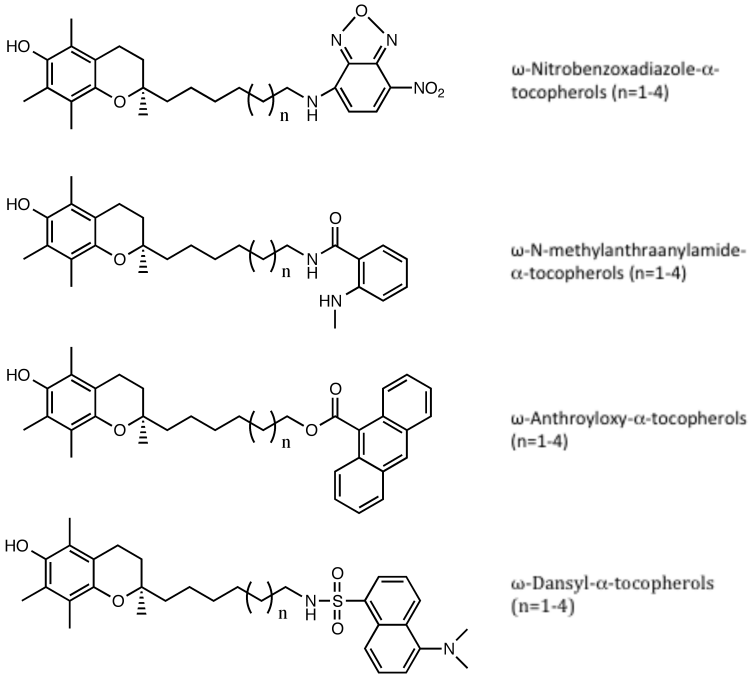

Figure 8. Fluorescent analogues of α-tocopherol.

α -Tocopherol is weakly fluorescent, having a $\lambda_{abs} \approx 290$ nm and $\lambda_{em} \approx 330$ nm in ethanol.[7] Unfortunately, various cell components (ie., tryptophan $\lambda_{abs} \approx 280$ nm) overlap the absorption spectra in this range, preventing any selective monitoring of tocopherol. Preparation of a fluorescently labeled tocopherol would overcome many of these issues. Previous work has prepared fluorescent substrate analogues for fatty acids and sterols which have been used as useful probes in binding assays and to clarify their intracellular transfer mechanisms.[7] Based on these promising results, the synthesis of fluorescently labeled tocopherols was initiated by Nava *et al.* in 2006.[7]

The most important design manipulation made sure the fluorophore did not interfere with the chromanol head portion of the molecule. As previously stated, αT had the highest affinity to αTTP because of the additional methyl groups located on the chroman ring. Any modification of the methyl groups would interfere with binding and decrease affinity towards αTTP. The phytyl tail became the only viable option for the placement of the fluorophore. Since the methyl groups on the phytyl tail are not needed for binding, they were omitted for simplicity sake.[7]

Sixteen compounds with varying chain lengths and fluorophores were synthesized (**Figure 8**).[7] These molecules were then used in fluorescent resonance energy transfer (FRET) assays. FRET is a radiationless distance-dependent transfer of energy between a donor and an acceptor molecule.[61] In the most successful assays, NBD-αT fluorophore is used as the donor molecule that absorbs incident light energy. This energy is then transferred to the acceptor vesicle containing the match fluorophore tetramethylrhodamine isothiocyanate PE-conjugate (TRITC-PE).

The transfer of energy occurs without any molecular interaction or any conversion to thermal energy. As a result the donors fluorescence and excited state lifetime decays, and *vice versa* for the acceptor.[61]

For the fluorescent analogue to be of use it must bind specifically and reversibly to αTTP, mimicking the natural form of vitamin E. Despite the anthroyloxy (AO) derivatives being weakly fluorescent in aqueous solutions, they exhibited non-specific binding to αTTP and the K_d values could not be determined.[60] Dansyl (DAN) and *N*-methylanthraniliate (NMA) also retained fluorescence in aqueous medium, rendering our ability to decipher between free and bound ligands difficult. The non-specific binding of these analogues may be attributed to the high polarity of the fluorophore moieties not being accepted in the hydrophobic pocket of αTTP. Contrarily, C9-NBD-αT was found to bind specifically and reversibly (K_d = 8.5 ± 6.3 nM), and lacked fluorescence in an aqueous environment.[60] Among the analogues of different chain lengths C6 to C9, the C9 analogue showed the highest affinity to αTTP. Therefore, the C9-NBD analogue was used in all subsequent transport assays and imaging microscopy.[60]

The fluorescent C9-NBD-αT derivative aided in the study of ligand binding and transfer activities of αTTP. In methanol, this analogue has a maximum absorption at 466 nm, and fluorescence at 533 nm (**Figure 9**). When bound to αTTP, the ligand fluorescence and excitation intensity increase by ≈ 50x. As noted previously, this drastic increase is a result of the ligand moving from a polar aqueous environment, to the hydrophobic pocket of αTTP. Binding results in a "blue

shift", whereby free ligand to bound ligand has an excitation shift from 474 nm to 466 nm, and emission maxima from 547 to 526 nm.[60]

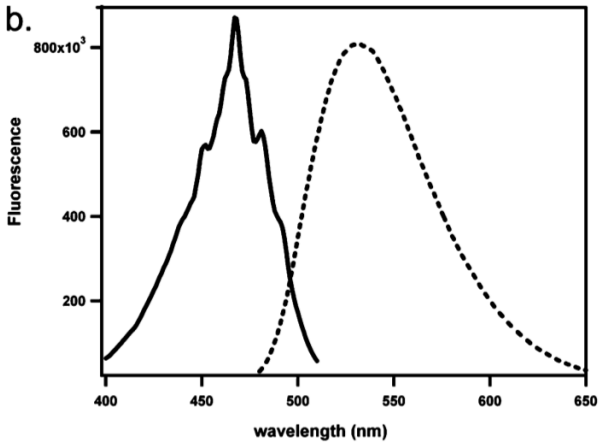

Figure 9. Spectral characteristics of C9-NBD-αT; excitation and emission spectra recorded in methanol. Fluorescence excitation (solid line; monitored at 533 nm), and emission (dashed line; excitation at 466 nm) were monitored in 0.22 μM NBD-TOH.[60]

Competitive binding assays demonstrated that with addition of unlabeled αT, the C9-NBD-αT is displaced from the binding site and its fluorescence greatly decreased (i.e., αT competitively binds more efficiently to the hydrophobic pocket of αTTP, displacing the analogue).[60] In contrast, the fluorescence signal of the C9-NBD-αT bound to αTTP is not diminished when a neutral lipid such as cholesterol is introduced. Thus, C9-NBD-αT binds to αTTP's active site with affinity close to that of the natural αT. However, when a mutated αTTP, with a mutation where lysine 59 is replaced by tryptophan, (this mutation is found in patients experiencing AVED) is studied in binding assays, a 5 fold lower affinity of binding between the derivative αT and αTTP is observed (71 ± 19 nM). This data demonstrates the effectiveness of the C9-NBD-αT to respond and report perturbations in the αTTP binding pocket.[60]

After showing that C9-NBD-αT can bind specifically and reversibly to αTTP, additional studies were performed by Atkinson's group that analyzed the transfer of the ligand from protein to a lipid bilayer.[62] More specifically, the association between the protein and the membrane for this ligand transfer were studied. There were two possible mechanisms by which ligand transfer could occur. In one scenario, αTTP could physically interact with the lipid bilayer and extract αT into the hydrophobic binding pocket. In this case, the rate of ligand binding would be dependent on the protein concentration. In the second plausible mechanism, αT may passively diffuse from the membrane, to the aqueous environment where αTTP would bind. This process would be rate limiting by the spontaneous ligand dissociation to the aqueous medium.[62]

The task of deciphering between the two mechanisms was accomplished by the introduction of C9-NBD-αT bound to αTTP into sonicated phospholipid vesicles that contained a fluorescent phospholipid derivative. The phospholipid derivative was chosen to be a FRET acceptor of the emission of NBD. When the NBD-aT is present in the TRITCE-PE labeled membrane, fluorescence of NBD is quenched, and TRITCE-PE fluorescence is increased. Addition of αTTP secretes NBD-αT and as result, NBD fluorescence is restored. What was found was a direct dependence of protein (αTTP) concentration to the reaction rate. With 5 μM of αTTP, the rate was observed to be 8.7 ± 0.4 s, with a decrease to 3.9 ± 0.2 s when 30 μM of αTTP was present. As shown (**Figure 10**), there is decrease in fluorescence between NBD-tocopherol and TRITC-PE lipids. Because the rate was dependent on αTTP

concentration, it is concluded αTTP directly interacts with the membrane, binding αT.[62]

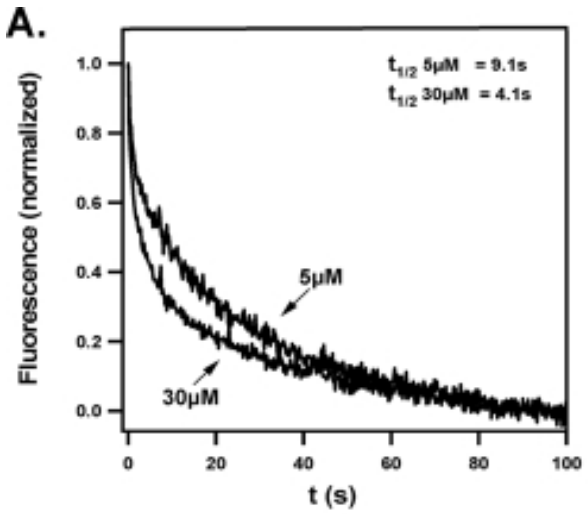

Figure 10. Time dependent change in fluorescence energy transfer between the lipid bilayer and NBD-tocopherol. Fluorescence monitored at 575 nm, with excitation at 466 nm.[62]

1.4.2 BODIPY Analogues

Despite the great utility of the NBD-analogues, they are susceptible to photobleaching during prolonged exposure to the illumination used in confocal microscopy and time resolved *in vitro* FRET assays. To resolve this problem, an αT derivative containing a dipyrromethene boron difluoride (BODIPY) fluorophore was established and published in 2010 (**Figure 11**).[63] Unlike NBD, this BODIPY analogue is not as susceptible to photobleaching, and does not contain any polar functionality; preventing unfavorable binding in the hydrophobic pocket of αTTP.

The polarity of the NBD fluorophore can accelerate fast intermembrane transfer of phospholipid derivatives (PC and PE lipids)[64], and to disrupt the behavior of modified NBD-acyl chains. Both these characteristics are undesired when dealing with αTTP, a protein designed to transfer hydrophobic compounds from one membrane to another.[63] Taking these properties into account, BODIPY-αT was produced as a second-generation derivative.

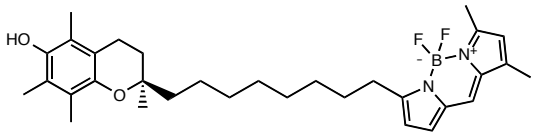

Figure 11. Chemical structure of BODIPY α-tocopherol analogue

Besides their non-polar characteristic, BODIPY lipids were previously used because of the tremendous photostability, large extinction coefficient and high quantum yields (λ_{ex}= 507 nm, λ_{em}= 511nm, ε_{507}= 83,000 $M^{-1}cm^{-1}$).[63,65] Additionally, the lipophilicity of BODIPY allows easy transfer through cell membranes.[63,66] For BODIPY-αT to be of any utility, it must bind specifically and reversibly to αTTP. Varying chain lengths (C6-8) were studied, and the C8 chain was found to have the highest affinity to αTTP (K_d = 94 ± 3 nM). Similar to NBD-αT-analogues, competitive binding assays were studied, wherein it was shown that αT specifically competed for the BODIPY analogue in the binding pocket of αTTP.[63]

In 2016, Ghelifi *et al.* published an enhanced BODIPY-αT analogue; one that combined the photostability of BODIPY with an extended chromophore that absorbed light at a longer wavelength (**Figure 12**).[67] The combination of these two properties will allow better fluorescence tracking in tissues and cells. By increasing

conjugation along the phytyl tail, the UV-vis absorption was shifted to longer wavelengths (λ_{ex}= 571nm, λ_{em}= 583 nm) (**Figure 13**). Even though the maximum fluorescence of this analogue was less than the original αT-BODIPY when bound to αTTP (1/10th the fluorescence), the binding to αTTP was exceptional (K_d= 8.7 nM).[67]

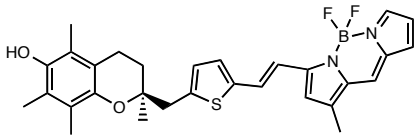

Figure 12. Second generation BODIPY α-tocopherol analogue

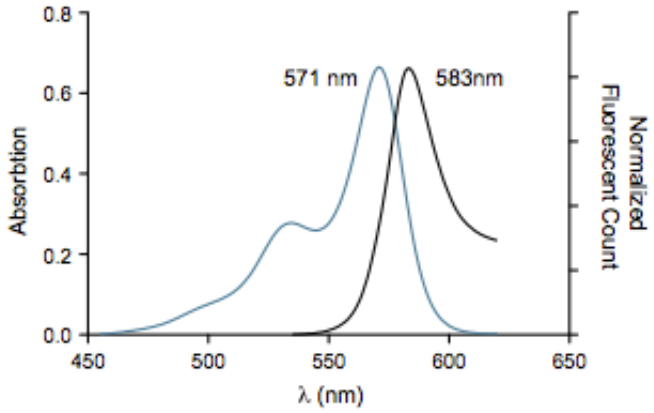

Figure 13. Excitation and emission spectra of the second generation BODIPY analogue

The McA-RH7777 cell line was used to test ligand tracking by fluorescence microscopy. This cell line expresses the human αTTP gene by activation of the tetracyclin promoter through the addition of doxycycline. Without doxycline present, cells do not express αTTP and can be used as a control. When αTTP is present, there is an accompanying 30% reduction in the cellular area of fluorescence of the BODIPY analogue, illustrating that this analogue can be used to study the

secretion of the ligand from cultured cells when the transcription of αTTP is active. Equally as important, after 20 minutes of exposure, there was a lack of photobleaching. As comparison, C9-NBD-αT had a 50% emission bleach during this time.[67] In the future, this BODIPY compound will be used in studies on the uptake and transport of αT in neurons.

1.4.3 α-Tocohexaenol Analogue

Despite all these useful fluorescent derivatives, the addition of any fluorescent probe may alter the overall properties of αT. A polyunsaturated analogue of αT lacking the bulky fluorophore, but keeping its fluorescence properties would mimic the natural form of αT to a greater extent. Additionally, the conjugation would allow the phytyl tail to be sensitive to oxidative stress that occurs in phospholipid membranes. The synthesis of α-tocohexaenol (αT6) (**Figure 15**) accomplished these characteristics. The concept of αT6 was similar in many regards to a compound known as Fe-AOX-6 (**Figure 15**).[68] Fe-AOX-6 was used for studying the inhibition of lipid peroxidation and ROS.[68]

The only difference between αT6 and Fe-AOX-6 was the saturation on C9 of the phytyl tail (**Figure 15**). Fe-AOX-6 had an absorption wavelength maximum ≈300nm, which overlaps with cellular chromophores. αT6's fully conjugated carbon chain would resolve this issue. In ethanol, αT6's observed absorption maximum occurs at 368 nm and its fluorescence emission maximum is at 523 nm (**Figure 14**).[69] These fluorescent characteristics do not interfere with other endogenous cellular components. It is noteworthy that αT6 has a K_d of 540 ± 35 nM. This

relatively high K_d (in comparison to natural αT's k_d of 25 ± 2.8 nM)[28] is probably a result of the rigidity of αT6 phytyl tail.

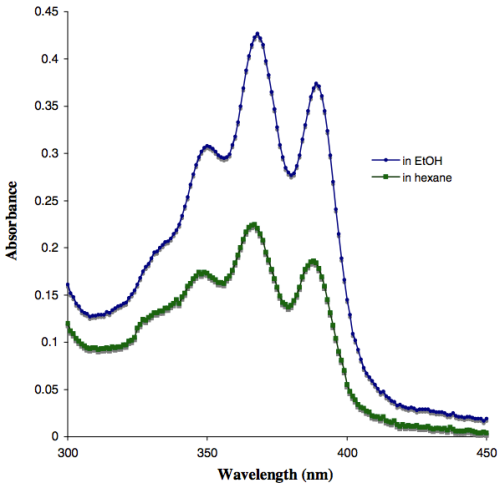

Figure 14. αT6 absorbance spectra in ethanol (blue) and hexane (green).

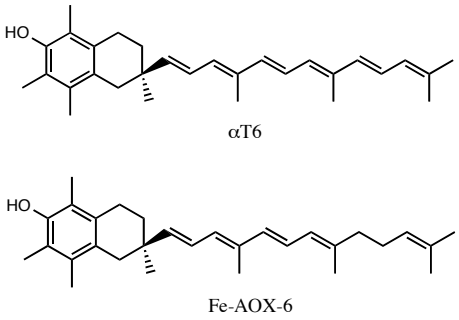

Figure 15. Chemical structures of αT6, a fluorescent derivative of α-tocopherol and Fe-AOX-6, an inhibitor of lipid peroxidation.

When the side chain of αT6 is exposed to peroxidative stress, peroxyl radicals add to the conjugated π-system in a manner similar to what is thought to occur with β-carotene. The disruption of conjugation results in a loss of fluorescence. In this respect, this αT analogue can act as an oxidatively sensitive

membrane probe. Having a similar structure as αT would allow for accurate location and behavior as the natural form. More specifically, it could show 'differential' loss of fluorescence to the regions in the membrane that are enduring greater oxidative stress.[69]

Proof of concept was performed in *in vitro* studies. When placed in a soy PC vesicle and exposed to AMVN (2,4-dimethylvaleronitrile, a radical initiator), the fluorescence decreased. α-Tocohexaenol successfully acted as an *in vitro* peroxidatively sensitive membrane probe. When αT6 and AMVN are present together, there was no lag phase in the loss of fluorescence. However, in the presence of excess αT, αT6 competes with tocopherol and has a delayed loss of fluorescence. Because of these promising preliminary studies, αT6 had plans to be used as a probe for the turnover of tocopherol at sites of high peroxidative activity. Unfortunately, the properties of this compound make it very sensitive to oxygen, light, acid, *etc*. It even rapidly degraded on storage at -20˚C in the dark. Therefore, no further tests could be performed.[69] However, as presented in this thesis, synthesis of α-tocopentaenol (αT5), a more stable compound that retains fluorescence, would allow us to use it as a peroxidatively sensitive probe in the future.

1.5. Aims and Objectives

The synthetic work of this thesis will focus on the investigation of the first synthesis of α-tocopentaenol (αT5), a fluorescent analogue of αT (**Figure 16**). Similar to Yongsheng Wangs work in producing αT6, I aim to produce a fluorescent oxidatively sensitive membrane probe that resembles natural αT. α-Tocopentaenol lacks conjugation at the C1 position on the carbon tail. By lessening the number of conjugated double bonds, we assume there will be an increase in stability. Removal of the C1′ alkene will prevent delocalization of the phenoxyl radical to the phytyl tail. Moreover, the free rotation around this C1′-C2′ bond allows flexibility when binding to αTTP, in theory this might increase the affinity of αT5 in comparison to αT6.

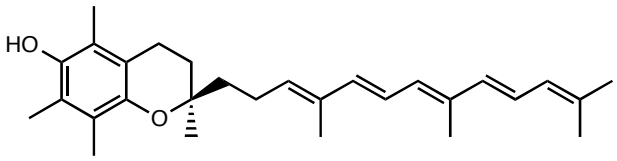

Figure 16. Target molecule: αT5 ((*R*)-2,5,7,8-tetramethyl-2-((3*E*,5*E*,7*E*,9*E*)-4,8,12-trimethyltrideca-3,5,7,9,11-pentaen-1-yl)chroman-6-ol

As the goal is to prepare a molecule as a fluorescence probe of tocopherol biochemistry, a suitable analogue had to be synthesized with consideration of the following requirements:

1) The analogue should mimic the structure of natural αT as much as possible
2) The analogue should have suitable fluorescent characteristics

α-Tocopentaenol meets these requirements and would have a λ_{max} > 300nm. According to Fieser-Kuhn rules, the absorption wavelength of this compound is calculated to be 337 nm.[70]

As shown (**Figure 17**), when αT5 is to be placed in a membrane, the orientation of the phytyl tail and chromanol ring will mimic that of the natural form of αT. This resemblance will allow us to accurately determine locations in the membrane where oxidative stress is high by usingin microscopy to record the areas of fluorescence loss. Additionally, because αT5 lacks a bulky polar fluorophore, a more accurate behavior and location to αT can be determined.

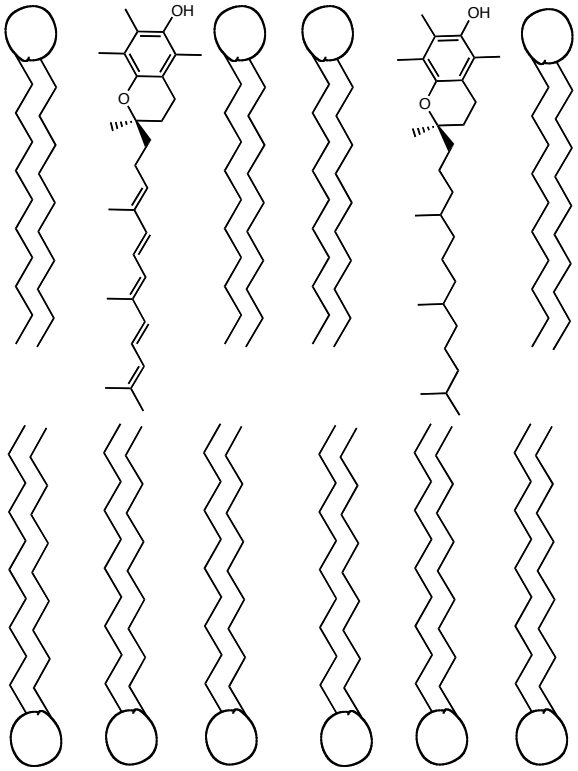

Figure 17. Cartoon illustration of α-tocopentaenol and α-tocopherol in a phospholipid membrane.

2. Results and Discussion

2.1. Design of a Fluorescent Analogue of Vitamin E

The overall synthetic approach has to start with a cheap, commercially accessible compound, or a compound that was in large quantities within our laboratory. For these reasons, (*S*)-α-Trolox® and natural α-tocotrienol were used as starting materials (**Figure 18**). Manipulations using (*S*)-α-Trolox® would require the complete synthesis of the phytyl tail, while having the chromanol ring already intact. Contrarily, α-tocotrienol would keep the chromanol ring intact, but the break-down of the phytyl tail would be necessary before synthesis of the new phytyl tail. Both (*S*)-Trolox and α-tocotrienol would also ensure correct (*R*)-stereochemistry at the C2 carbon on the pyran ring.

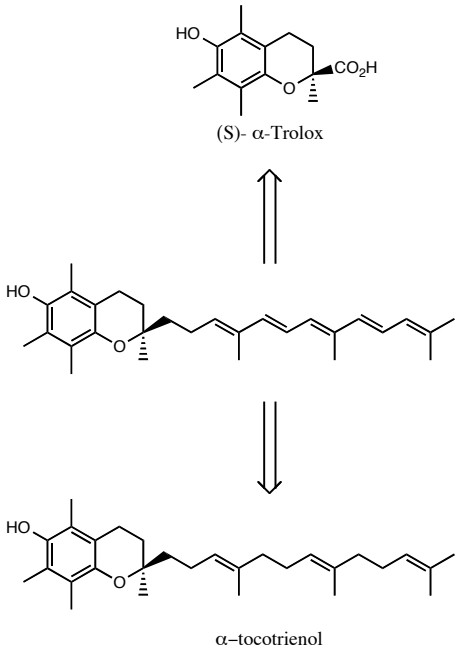

Figure 18. Retrosynthesis of αT5 via α-tocotrienol and (*S*)- α-Trolox®

2.2. Synthesis of Intermediate (5) Through Zincke Aldehyde Formation

2.2.1 Preparation of (3) By Nucleophilic Attack of a Secondary Amine to the Activated Pyridine

Initial plans for the synthesis began with 3-methyl pyridine. In this portion of the synthesis, the target molecule was a tributylstannyl unsaturated aldehyde (**5**) (**Scheme 1**). This compound would be a key intermediate in a Stille reaction needed for chain elongation of the phytyl tail.

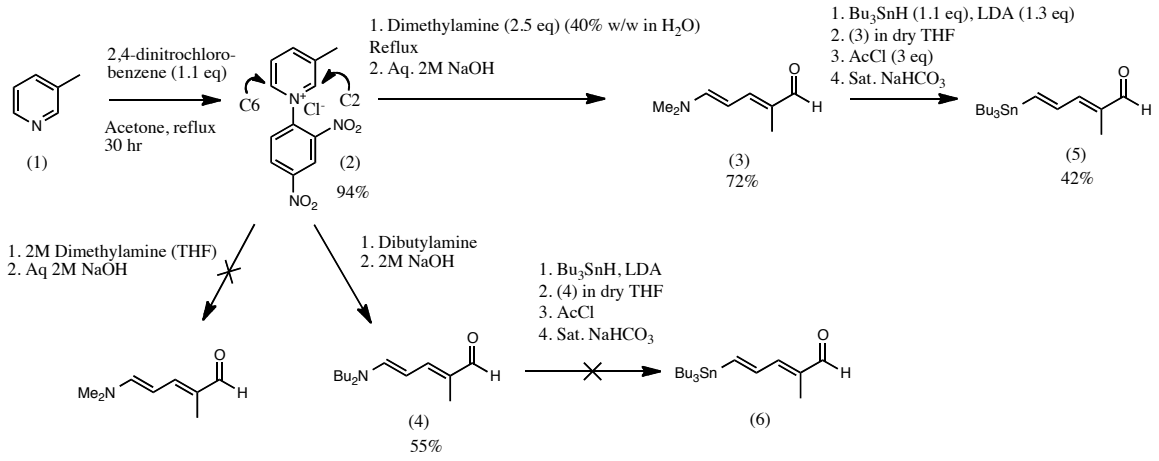

Scheme 1. Pathway following the Zincke aldehyde reaction, whereby an activated pyridine is prone to nucleophilic addition. The resulting unsaturated dimethyl amine can undergo substitution with lithium tributyltin to produce a key intermediate (5).

Early reaction conditions attempted followed those of the Zincke reaction.[71] Zincke aldehydes are prepared by a reaction involving an activated pyridium salt with two equivalents of a secondary amine. Through use of a secondary amine, the terminal iminum group is hydrolyzed under basic conditions to generate an aldehyde.[71]

In the first step, 3-methyl pyridine (**1**) is activated using 2,4-dinitrochloro-benzene. The corresponding Zincke salt (**2**) is prone to nucleophilic addition.[72] In the case of unsymmetrical 3-methyl pyridium salt there are two possible locations for an attack (C2 and C6). When a nucleophile such as HO^- is used, the hydroxide usually reacts at the C2 position. However, in the case of a larger amine nucleophile, an exclusive attack occurs at the C6 carbon.[72] These results are a result of the steric interactions with the pyridine-3-methyl substituent to the nucleophile. However, electronics effects of the pyridine-3-substituent have no affect on where the nucleophile will attack. Another explanation for regioselective nucleophilic addition may be because only one of the ring opening products is stable.[72]

When (**2**) was allowed to react with an old sample of dimethyl amine (in THF), no reaction occurred despite repeated attempts. However, when a new bottle of a 40% w/w dimethyl amine was reacted with the Zincke salt, (**3**) was cleanly generated in a 72% yield. Similarly, the dibutylamine analogue can be produced in a 55% yield. In both reactions, 2,4-dinitroaniline is made as a byproduct; column chromatography with hexane/EtOAc elutes compound (**3**) first, whereas DCM/hexane elutes 2,4-dintroaniline first. In the latter case, the nature (acidity, most likely) of the compound contributes strongly to the 'cracking' the silica column prior to the elution of compound (**3**), resulting in very poor chromatographic separation.

Zincke aldehyde (**3**), can be converted to the corresponding tributylstannyl unsaturated aldehyde by tributylstannyl lithium.[73] Zincke aldehydes are good electrophiles, and organo-stannanes can add in a conjugated manner. However, to

have dimethylamide anion act as a leaving group in such fashion is not typical. The loss of dimethylamine and production of the stannyl aldehyde is only possible in the presence of a quenching agent, such as acetyl chloride, AcCl. The reaction appears to proceed through a 1,6-stannyllithium addition to the aldehyde, then elimination of $-NMe_2$ which is rapidly quenched by AcCl or MeI. In the absence of a quenching agent, no product is observed.[73]

2.2.2 Preparation of the Unsaturated Stannyl Aldehdye (5)

The first attempt of producing the stannyl aldehyde (5) was performed by following exact methods mentioned in Vanderwal's paper.[73] This attempt resembled the method written in the experimental, but with one vital change. In the original attempt, the addition of AcCl was done at room temperature. However, when the reaction was performed multiple times under such conditions, only trace amounts of product were ever observed. The unsaturated aldehyde seemed to polymerize or degrade, as evidenced by a low R_f spot on the TLC. After contacting Vanderwal, author of the paper that described this methodology, it was suggested that the best way to ensure reproducibility was to quench the reaction with acetyl chloride all at once. Furthermore, the reaction (including the work-up) should be performed at -20˚C. When the new reaction conditions were attempted, 42% of (**5**) was isolated. Because of the aldehyde moiety, the compound is reasonably stable towards protodestannylation (a problem that plagues other stannyldienes)[74] and can be stored in the freezer for prolonged periods.

2.3. (S)-α-Trolox® as Starting Material

2.3.1 Manipulation of (*S*)-α Trolox

(*S*)-α–Trolox® (**7**) was used as the starting material for the second precursor. (*S*)-α-Trolox® is commercially available, but our batch was graciously donated by Thomas Netscher (DSM, Basel, CH). It should be noted: (*S*)-α-Trolox® is used to obtain (*R*)-αT5, as the designation of the configuration at C2 changes after alteration of the carboxylic acid moiety of Trolox®.

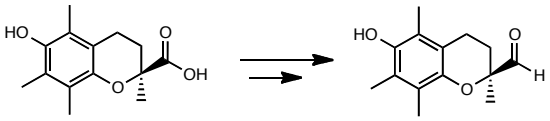

Figure 19. General overview of converting Trolox® to a one-carbon aldehyde (10).

Simple manipulations of the acid would ultimately produce an aldehyde (**10**) (**Figure 19).** In order to obtain intermediate (**10**), one of two routes was chosen: esterification and reduction to an aldehyde, or complete reduction of the acid to an alcohol, and re-oxidation to an aldehyde. The first reaction was an esterification of Trolox® using an excess of methanol. After a clean and easy esterification, protection of the C6 phenol using *tert*-butyldimethylsilyl chloride (TBSCl) was performed.

After protection, partial reduction using DIBAL gave intermediate (**10**). It is worth noting that control of the temperature so as not to exceed -60˚C is very important. At temperatures greater than -60˚C, there is a risk of fully reducing the aldehyde to the corresponding alcohol. The production of this aldehyde group is necessary for further chain elongation steps.

2.3.2 Chain Elongation of Compound (10) Via Wittig Reactions

With compound (**10**) in hand, a Wittig reaction containing an unprotected alcohol present on the phosphonium salt (**11**) was performed in the hope of obtaining the unsaturated alcohol (**12**) (**Scheme 2**). After the first attempt, and upon purification and isolation of the products, it was soon realized that this reaction had two competing reaction intermediates (**Scheme 3**). Prior to the reaction, a literature review showed similar Wittig reactions containing an unprotected alcohol on the phosphonium salt (albeit none of two carbons in length) proceeded without difficulty.[75] The only stipulation was an excess (2.1 eq) of base must be used. After purification it was apparent as to why the phosphonium salt (**11**) was not seen in literature. When the salt is two carbons in length, both alkoxides have an equal chance of reacting with the phosphorous (**Scheme 3**).

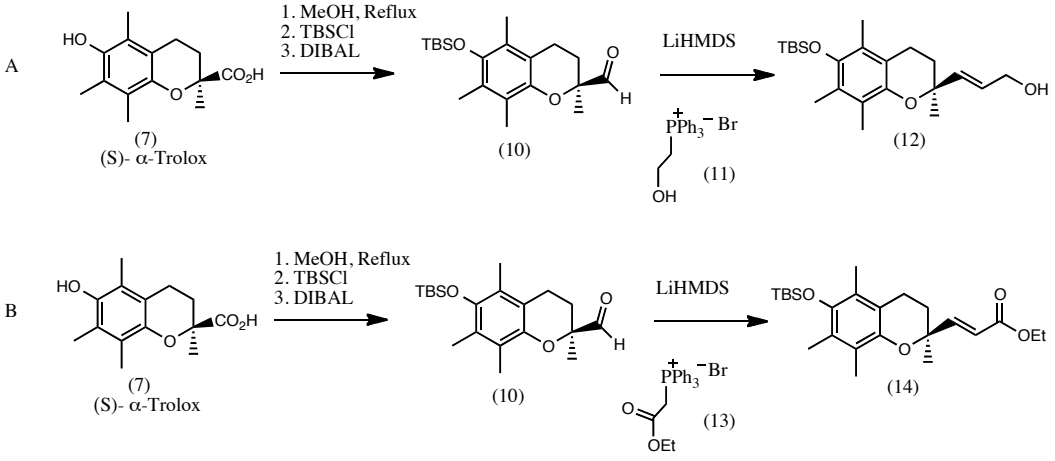

Scheme 2. A) Esterification, protection and DIBAL reduction lead to compound (10). When phosphonium ylide (11) was used, competing pathways resulted in a reduction in yield of (12). B) Switching to an ester phosphonium ylide (13), lead to clean conversion to (14).

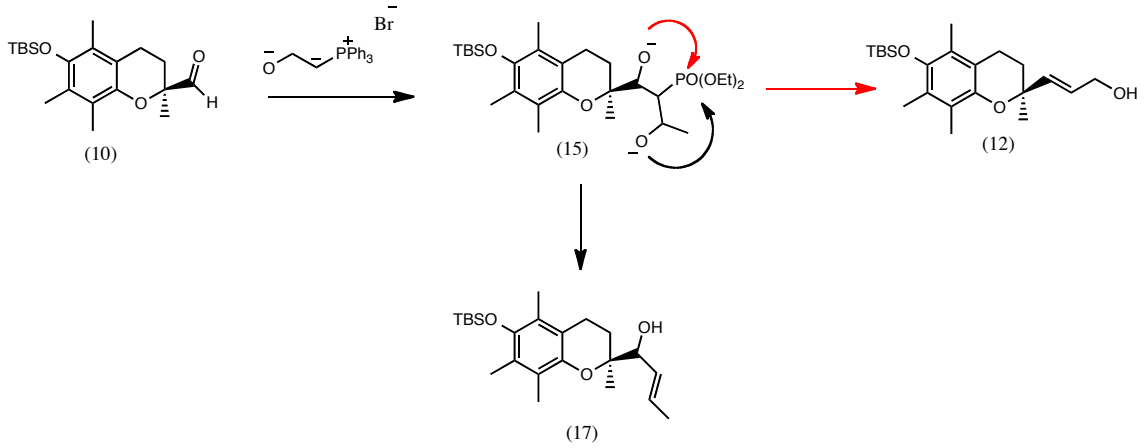

Scheme 3. Competing pathways of forming the P-O bond with the use of this phosphonium ylide.

To avoid these competing reactions, the ester analogue of the phosphonium salt (**13**) was used. The first attempt was done with compound (**10**) and the corresponding 2-carbon ester phosphonium salt (**13**) in THF. After 44 hours of stirring, there was complete consumption of starting material. On a 155 mg scale, only 15 mg of (**14**) was isolated. However, 45 mg of (**18**) (**Figure 20**) was isolated. During the formation of the phosphonium ylide, it was noted that the color was only a very pale yellow, as opposed to the original bright yellow/orange that many of the previous ylides exhibited. Repeating the procedure using the phosphonium ylide suspended in DMSO, and reduction of stirring to only 4 hours, cleanly produced (**14**) in an 84% yield, with no (**18**) present. The geometry of the alkene was not examined as it was of no importance to us; later steps would reduce the alkene.

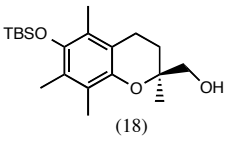

Figure 20. Product observed on first attempt at the Wittig reaction in scheme 2B

Because an ester phosphonium salt had to be used in the prior step, an additional reduction step of the ester to the terminal alcohol had to be employed. The simplest route to achieve this was performed by the addition of a powerful reducing agent; lithium aluminum hydride (LAH).

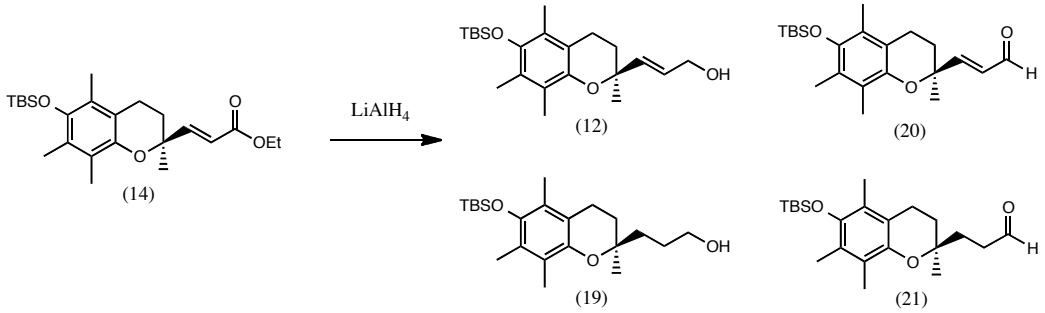

Scheme 4. Four products obtained from the LAH reduction of (14).

Four products were observed from the corresponding reduction (**Scheme 4**). Compounds (**20**) and (**21**) were unexpected, as it was thought a strong reducing agent such as LAH would fully reduce the ester to an alcohol. If the reaction were to be repeated, longer reaction time or ensuring the use of purified LAH (recrystallize in diethyl ether) would resolve this issue. The other two compounds isolated, (**12**), and (**19**), are a result of two mechanistic options for the reduction of an α, β-unsaturated carbonyl. Both 1,2 and 1,4-reduction may occur; 1,4-reduction leading to compound (**19**) and a 1,2-reduction leading to compound (**12**).

2.3.3 Hydrogenation vs Reduction and Oxidation

At this point in the synthesis, decisions had to be made on a future protocol for creating the three-carbon aldehyde. Two plausible routes would yield the same

product. The first one was based on hydrogenation of (**12**) in hopes of yielding the aldehyde directly (**Scheme 5**). Compounds that posses an α, β-unsaturated alcohol have a tendency of directly isomerizing to the saturated aldehyde through the use of select catalysts.[76] The redox isomerization of allylic alcohols to aldehydes is a well-designed shortcut to useful compounds. Various transition metal complexes act as viable catalysts: Rh, Ni, Ir, Mo, Co, Fe, Os, Pd, and Pt. In most cases, ruthenium and palladium are known to be the most efficient of the catalysts.[76]

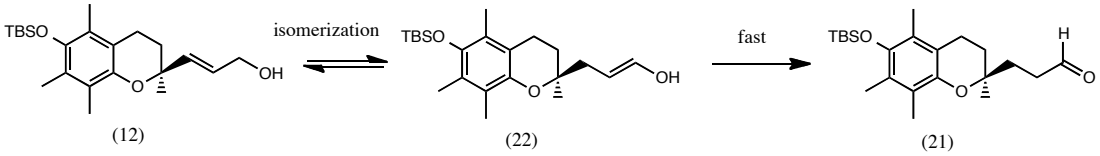

(12) (22) (21)

Scheme 5. Isomerization of α, β-unsaturated alcohol to the saturated aldehyde (21)

Through the use of titania supported palladium (Pd/TiO_2) at 303K and 0.01 MPa partial hydrogen pressure, α, β-unsaturated alcohols have been observed to convert to the corresponding unsaturated aldehydes.[77] The catalytic activity and selectivity are dependent on both steric and electronic effects of the substrate. Higher yields (80%) of the corresponding aldehyde were obtained with smaller chain length alcohols such as 2-propen-1-ol. Once longer chain lengths are introduced, the yield decreases. This was proposed to be a consequence of steric effects crowding the olefinic bond.[77]

The second possible route to obtain (**21**) would be based on the oxidization of the alcohol to the aldehyde, followed by hydrogenation to reduce the olefin. Both routes would produce the target intermediate and the only deciding factor would be which route provided the highest yield. However, neither attempts were tried, as it

was during this point of the synthesis where a critical decision had to be made. Unfortunately, the amount of unsaturated alcohol/saturated alcohol (**Scheme 4**) in storage would not have been enough to continue through the full synthesis. Furthermore, all the (*S*)-Trolox® in our possession had been consumed.

Granted, production of pure (*S*)-Trolox® is possible through multiple microwave reactions[78] (**Scheme 6**), but the method is inefficient and time consuming. Additionally, multiple manipulations including the resolution of racemic Trolox® is needed, whereby the highest yield obtained in our hands was 30%.[79] Trolox® is commercially available, but the cost ($285/5g of racemate is prohibitive at the scale we wished to work on).

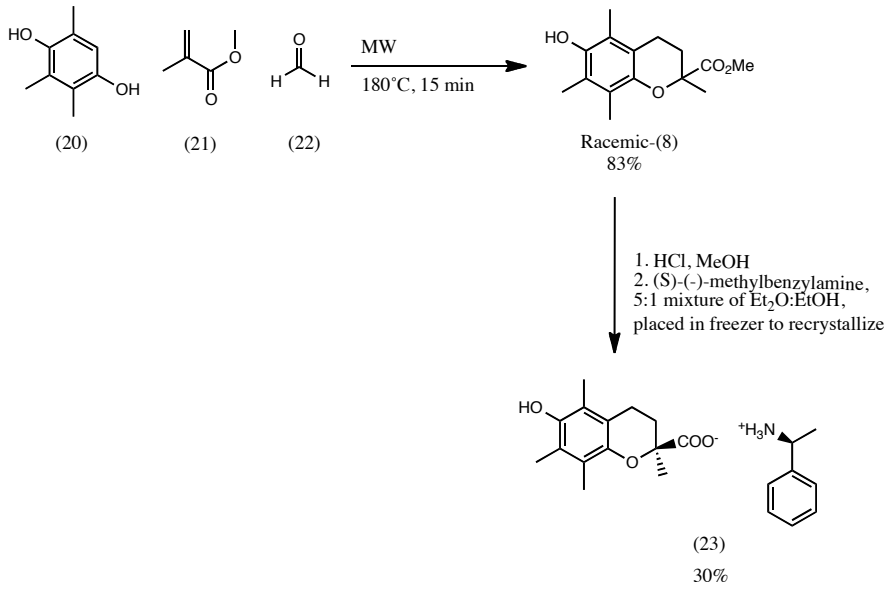

Scheme 6. Microwave reaction of trimethylhydroquinone (20), methyl methacrylate (21), and formaldehyde (22) to produce racemic (8). Resolution of racemic Trolox® results in a 30% yield of the pure (S)-Trolox® methylbenzylamine salt (23).

It is worth noting that these microwave reactions could only be performed on a one-gram scale. It was after multiple microwave reactions, synthesizing more

than 10 g of racemic Trolox® when the question arose whether it would be preferable and possible to cleave α-tocotrienol (αT3), directly producing (**21**) (**Figure 21**). If possible, intermediate (**21**) could be formed in a one-step process with correct stereochemistry at the C2 position of the pyran ring. Because, only natural tocopherols/tocotrienols are sold in a mixture of palm oil, the correct (*R*)-configuration would already be present in the molecule. As a promising option, this route was further explored.

2.4. Olefin Cleavage of α-Tocotrienol

All natural forms of vitamin E used in this synthesis were obtained from a commercial palm kernel oil product TOCOMIN®. This mixture of tocopherol/tocotrienols contained predominately γ, α, and δ- tocopherols/ tocotrienols. Column chromatography was used to separate and purify these compounds. The compounds isolated after purification contained identical mass spectra and ^{1}H- and ^{13}C-NMR as those previously reported.[80] Gradient column chromatography with 1-5% EtOAc in hexanes was used during the separation. From the mixture, concerning tocotrienols, approximately 10% was α-tocotrienol, 20% γ-tocotrienol, and 5% δ-tocotrienol.

Originally, the biggest downfall of this route is the isolation of pure αT3. The mixture of palm oil available to us consists of approximately 10% αT3. To make matters worse, all available forms of vitamin E have very similar R_f values and separation via column chromatography would be difficult. Therefore, in order to

obtain a sufficient amount of αT3 to be used as a starting material, multiple columns must be performed.

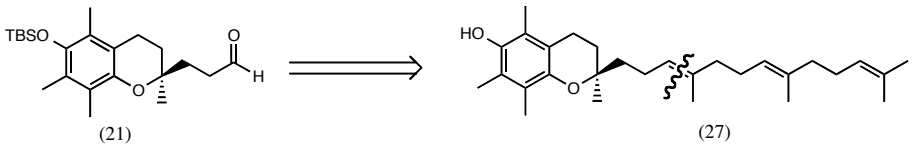

Figure 21. Oxidative cleave of αT3 would result in the three-carbon intermediate needed for chain elongation, and could be performed in a one-step reaction.

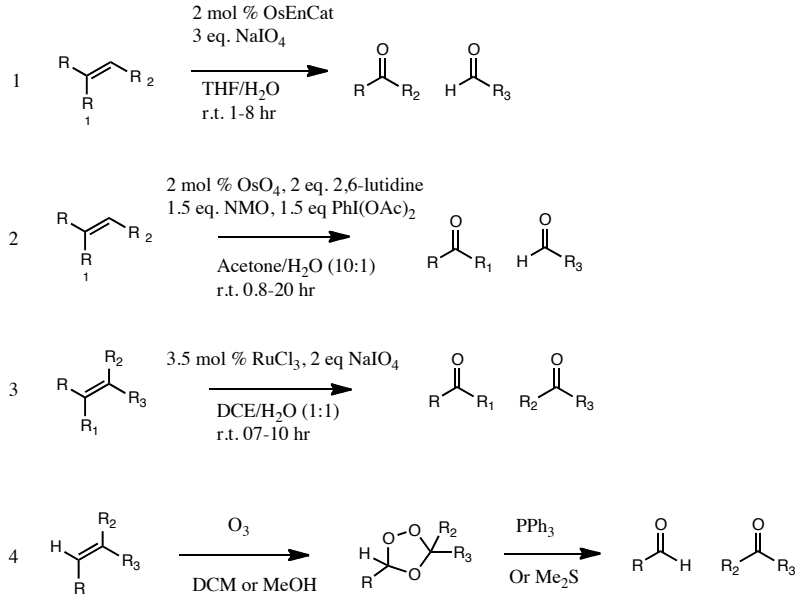

Figure 22. Various methods to oxidatively cleave an olefin; 1[81], 2[82], 3[83], 4[84]

After the necessary amount of αT3 was isolated, it was protected with TBSCl. There are many known ways of cleaving olefins, and oxidizing them to the corresponding aldehydes[81,82,83,84] (**Figure 22**). The Lemieux-Johnson oxidative cleavage of double bonds was discovered by R.U. Lemieux, and W. S. Johnson in 1956.[85] This two-step reaction occurs in the presence of osmium tetroxide and

sodium periodate.[85] In the first step the alkene undergoes dihydroxylation by osmium tetroxide, followed by the oxidative cleavage with periodate (**Scheme 7**). The use of excess sodium periodate regenerates the osmium (VIII) species, allowing osmium tetroxide to be used in catalytic amounts.

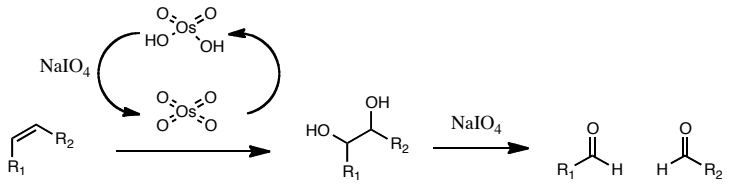

Scheme 7. Lemieux Johnson Oxidation of an olefin

The original Lemieux-Johnson reaction has a tendency of producing many unwanted side products, resulting in difficult purification and lower yields.[86] These characteristics combined with the high toxicity of osmium tetroxide diminished the attractiveness of this approach. Similar results of the Lemieux-Johnson oxidation can be achieved through the process of ozonolysis. Ozonolysis oxidatively cleaves unsaturated bonds into the corresponding carbonyl groups.[87] Unlike the Lemieux-Johnson oxidation where the reaction concludes at an aldehyde, ozonolysis allows for diversity whereby, depending on the work-up, alcohols, aldehydes, ketones or carboxylic acids can be synthesized. The overall reaction occurs in a short time-span (2-5 min) and avoids the use of carcinogenic compounds like OsO_4.

2.4.1 Ozonolysis of TBSO-αT3

Ozonolysis was therefore the first reaction attempted in cleaving αT3. For a typical reaction, ozone is bubbled with substrate in a solution of DCM or MeOH at

-78˚C. When the reaction turns a blue (DCM) or grey (MeOH) color, the reaction is saturated with ozone, and the reaction has gone to completion-- producing the ozonide intermediate.[84] After such time, a reductive work-up is required. In our case, triphenylphosphine or dimethyl sulfide was used to produce the corresponding aldehyde. Sodium borohydride could be used to make an alcohol, and hydrogen peroxide, the carboxylic acid.

Using αT3 as the substrate, ozonolysis was performed multiple times in an attempt to synthesize the corresponding aldehyde. In theory, three different products should be created in this reaction: the three-carbon aldehyde connected to the chromanol ring (**21**), acetone (**28**), and 2 molecules of 4-oxopentanal (**29**) (**Figure 23**). All attempts were done in DCM or DCM/MeOH mixture. Both solutions turned their corresponding blue/violet color after ≈ 2 minutes of ozone bubbling through (-78˚C). After which, PPh_3 or Me_2S was added and the mixture was allowed to warm up to room temperature and stir overnight. All attempts produced what appeared to be a streak of degraded compound near the bottom of the TLC plate; no (**21**) was observed. Degradation was likely a result of using too high a concentration of ozone in the solution. After ozone cleaved the alkenes on αT3, the chromanol ring would be prone to oxidative cleavage.[88] If this reaction were to be performed again, one would have to calculate the concentration at which αT3 should be dissolved in solution, allowing ozone to react with the phytyl tail olefins and stopping the reaction after such time.

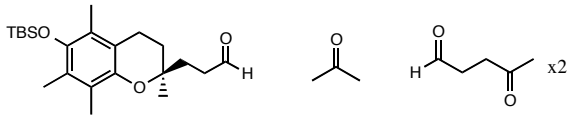

Figure 23. Expected products from an oxidative cleavage of αT3: a three-carbon aldehyde (21), acetone (28), and 4-oxopentanal (29). Due to the low boiling points of (28) and (29), those products were not isolated during purification.

2.4.2 $RuCl_3$ Oxidative Cleavage of αT3

After failure to produce (**21**) through ozonolysis, a variant of the Lemieux-Johnson oxidation was attempted.[83] For safety considerations significant attention has been placed on finding alternative routes to oxidative cleavage of olefins. One such method used ruthenium trichloride to convert double bonds to aldehydes.[83] In Yang's paper, various olefins were exposed to ruthenium trichloride; many of which were aliphatic olefins. According to the paper, substrates containing only a single aliphatic olefin produced their corresponding aldehyde in yields between 50-80% with reaction times ranging from 0.7-3.5 hours. However, the sole example of a compound containing two double bonds, when exposed to ruthenium trichloride, yielded only 38% of the corresponding product. In this latter example, twice the amount (or 4 eq) of periodate was needed. In the case of α-tocotrienol, it contains three double bonds, and therefore there was doubt on how clean the reaction would proceed. In any case, an attempt was made using identical conditions recorded in the paper.[83] Rather unsurprisingly, no (**21**) was observed.

2.4.3 OsO_4 Oxidative Cleavage of αT3 (Lemieux-Johnson Oxidation)

As we had no success with ozonolysis and $RuCl_3$, we returned to using osmium tetroxide (**Table 1**). Knowing that typical osmium cleavage resulted in lower yields, an alternative procedure was used.[86] The only difference in comparison to typical reaction conditions was the addition of 2,6-lutidine. Without 2,6-lutidine, their reaction medium was found to be pH 2. By buffering the reaction media with various bases (where 2,6-lutidine was found to be superior), yields increased from 40-60% to 80-90%. It appeared that this base suppressed side reactions and accelerated the rate of formation of the desired compound.[86]

Table 1. Screening results for the oxidative cleavage of αT3 under various conditions

OsO_4	$NaIO_4$	2,6-lutidine	Yield of (18)
6 mol %	11 eq	6 eq	54%
4 mol %	6 eq	6 eq	42%
4 mol %	11 eq	6 eq	50%

As shown (**Table 1**), the best results were obtained when 11 equivalents of periodate was used. The osmium catalyst amount was lowered from 6 to 4 mol % with no significant decrease in the yield.

After screening for the best reaction conditions with pure αT3, a mixture of both αT3 and αT were run under same conditions. In theory, αT should not be affected during this reaction, and separation of (**21**) from αT would be immensely

easier than separation of αT3 from αT. As predicted, yields were maintained and TBSO-αT was easily separated from (**21**).

2.5. Production of an (*E*)-Vinyl Halide

2.5.1 Synthesis of Compound (30) using diethyl (1-iodoethyl)phosphonate

With compound (**21**) in hand, the next step was to produce compound (**30**), having the vinylic iodine with correct (*E*)-geometry (**Figure 24**). The original plan was to find a Wittig-like reaction that could directly make this compound. Unfortunately, typical Wittig reactions for producing similar structures favour the (*Z*)-isomer.[89] (*E*)-alkenes can be made through the Horner-Wadsworth-Emmons modification, but product formation would result in an ester moiety (where in our case, an iodo moiety is needed).[90,91]

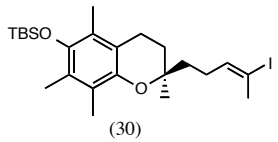

(30)

Figure 24. Target intermediate, with the vinyl halide having (E)-geometry

The first thought was to produce a Wittig reagent (**31**) as shown (**Scheme 8**). By using such a reagent, the vinylic halide (**30**) could be directly obtained.[89] Unfortunately, the use of the phosphonium ylide leads to a strong preference for the (*Z*)-iodoalkene and results in modest yields (30-40%).[89,92]

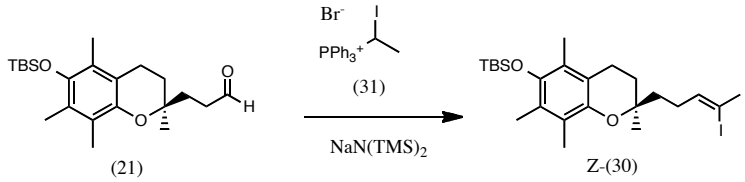

Scheme 8. Use of phosphonium ylide (27) would obtain compound (26) with the unwanted geomtry.

We also considered the possibility of producing (**32**).[93] As opposed to the triphenylphosphine salt (**31**), which produces an unstabilized ylid, (**32**) contains a phosphonate group (**Figure 25**), which, being more electron withdrawing, should lead to a more stable ylide intermediate. If this is true, then (*E*)-(**30**) could possibly be produced in a single reaction step. However, there was the concern that there was no prior report of a Wittig reaction with such a reagent. Phosphonate (**32**) was made in a useful 44% yield. Only a single attempt at a Wittig reaction with (**21**) was performed with (**32**). After consumption of the starting material, the TLC had a bottom spot (streak), with no sign of (**30**). As this was not a promising result, further attempts at this reaction were placed on hold.

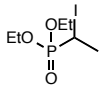

Figure 25. Representation of diethyl (1-iodoethyl)phosphonate

One of the few other approaches to direct formation of (**30**) is through the Schlosser modification of the Wittig reaction (**Scheme 9**). In 1966, Schlosser and Christmann discovered that the *erythro*-betaine can be converted into the *threo*

betaine by the addition of phenyllithium at low temperatures.[94] Upon acidic work-up, the desired (*E*)-alkene is formed.

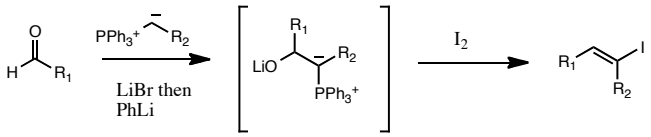

Scheme 9. Schlosser Modification of the Wittig reaction. (E)-geometry is produced when $R_2 \neq$ methyl/Hydrogen. As a result, this method could not be used.

Given the ongoing challenge of developing simple approaches to the stereocontrolled synthesis of trisubstituted alkenes, and the importance of iodoolefins as precursors, screening of various organometallic intermediates of the Schlosser modification was studied.[95] Under the conditions shown in **Scheme 9**, high geometrical integrity was retained in production of (*E*)-alkenes. Iodination of the β-oxido ylides resulted in high geometrical purity and yields only when $R_2 \neq$ methyl. The stereoselective outcome is highly sensitive to the size of the alkyl moiety. Increasing chain lengths result in higher selectivity, and only when a methyl group is not present is the (*E*)-geometry obtained.[95] With a methyl group, there is a significant preference towards (*Z*)-iodoolefin.[95]

2.5.2 New Approach: Corey-Fuchs Modification

As noted in the previous section, it is problematic when, as in our case, a methyl group was wanted at the C4′ position of the phytyl tail. Because the incorporation of the selective (*E*)-iodination across a double bond in a single step was unsuccessful with a methyl group[95], this procedure was never even attempted.

Multiple manipulations would be required to obtain the target intermediate. The new route would follow a Corey-Fuchs modification, whereby an aldehyde is converted to an alkyne via a one-carbon extension (**Scheme 10**).[96] This modification requires a two-step process. The first step is similar to a Wittig reaction (producing a dibromoalkene (**33**)). This step requires at least 2 equivalents of triphenylphosphine to be used. One equivalent is responsible for forming the ylide, and the second equivalent is both a reducing agent and a bromine scavenger. In the second step, treatment of the dibromoalkene with a lithium base creates a bromoalkyne species via dehydrohalogenation where a metal-halogen exchange yields the alkyne product. If methyl iodide is used prior to aqueous work up, one can generate an internal alkyne (**34**). However, in the absence of an electrophilic reactant, a terminal alkyne will be generated.[96]

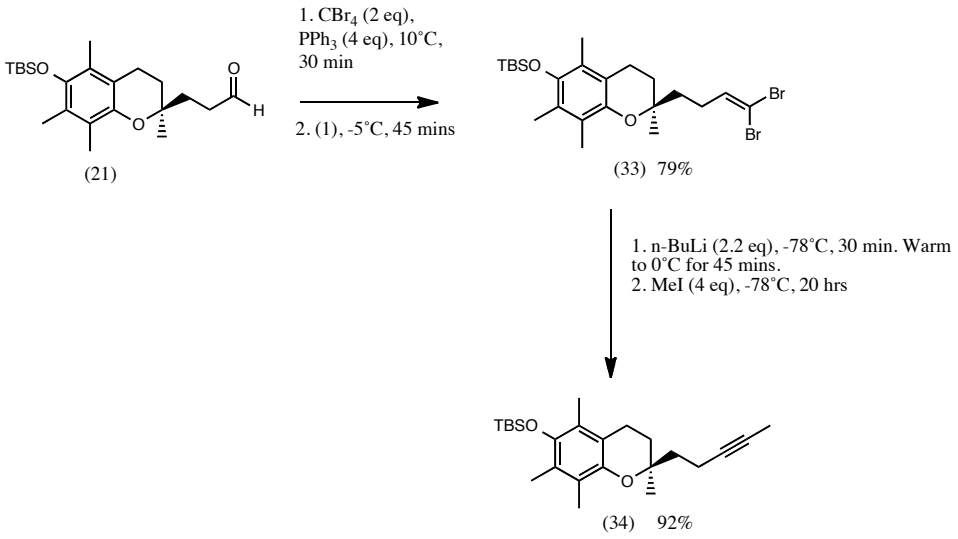

Scheme 10. Corey–Fuchs modification for the production of an internal alkyne (34).

Alkyne (**34**) would allow for extra flexibility for establishing the (*E*)-iodoolefin. One way to accomplish this is through the use of Schwartz reagent ($ZrCp_2HCl$).[97] The first report of $ZrCp_2HCl$ was in 1970 where Wailes hydrozirconated alkenes/alkynes.[98] Four years later, Schwartz and co-workers reacted the zirconocene species with inorganic electrophiles.[97]

2.5.3 Hydrozirconation: Schwartz Reagent

One well-known application in organozirconium chemistry is in the synthesis of (*E*)-vinyl halides via the use of Schwartz reagent and halogenation.[99] Schwartz reagent is a zirconocene complex, $ZrCp_2HCl$, having 16 *d*-electrons and one empty valence shell for coordination. As a result, during hydrozirconation, the π-bond of the olefin initiates interaction with the zirconium empty orbital. π-Backbonding is not possible as the complex does not have d electrons.[97,100]

Stereospecific *cis*-hydrometalation happens with high regioselectivity with respect to the least sterically hindered vinylzirconium species. Extra equivalents of Schwartz regent increase the regioselectivity via the development of a dimetalated alkyl intermediate which undergoes β-hydride elimination at the more sterically encumbered position.[100,101,99]

Premade Schwartz reagent was purchased from Sigma Aldrich for this hydrozirconation reaction. When the reactants were stirred in THF for an hour at 50˚C, using an excess of Schwartz reagent (2.6 eq), a 7:1 mixture in favor of (*E*)-iodoolefin was obtained (albeit in a 25% yield). Increasing the reaction time (3 h),

and temperature (60˚C) yielded 30% of product. Altering the stoichiometry (2-4 eq) did not have any effect on the yield nor the *E/Z* product ratio.

A period of time had passed (≈ month) when the same reaction was attempted using the same batch of Schwartz reagent. The fully reduced alkene was the only product observed and, regrettably, it has the same R_f value as the iodo-alkene. Any change in methods such as: solvent (DCM), equivalencies (1.8-4), temperature (room temperature, 40˚C, 60˚C), reaction times (1-8 hours), and re-sublimation of iodine, all resulted in the same over-reduced product (**35**) (**Figure 26**). Even though the Schwartz reagent was stored in a glove box, it was presumed that the reagent had gone bad over time, as it has been noted to have a very short shelf-life (20 days under N_2).[99,102]

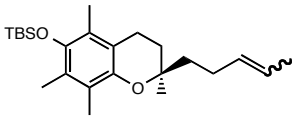

(35)

Figure 26. Reduced alkene obtained via hydrozirconation of alkyne (34)

The most plausible method to remediate this problem was to generate the Schwartz reagent *in situ* (**Scheme 11**). The *in situ* method requires a reduction of $ZrCp_2Cl_2$ using a hydride source ($LiAlH_4$, Red-Al, $LiEt_3BH$, *etc.*).[103,104] When choosing the hydride source, one has to be careful not to choose a reagent that could result in over-reducing the zirconium species to $ZrCp_2H_2$. For such reasons LAH is not recommended because it is difficult to control the extent of reduction. The use of Red-Al restricts over-reduction, but the by-product NaCl contaminates the reaction mixture, inhibiting hydrozirconation.[99]

In our case, LiAlH(O*t*-Bu)$_3$ was used as a means to prevent any unwanted reactions to occur. LiAlH(O*t*-Bu)$_3$ only has one hydride to donate and over-reduction should be prevented. The procedure followed was a one-pot, three-component process with short reaction times.[102] As opposed to prior reaction conditions that needed to be performed at -78˚C,[105] these reactions were done at room temperature. Only four substrates were screened in the original reference, all of which generated their corresponding (*E*)-iodoolefins in 90%+ yields.[102]

$ZrCp_2Cl_2$ (1.4 eq) and (**34**) were dissolved in dry THF. At room temperature, LiAlH(O*t*-Bu)$_3$ (1.4 eq) was added all at once. This solution was allowed to stir for 15 min. After this time, I_2 was added at room temperature and the mixture was allowed to stir for an additional 15 min. Upon work-up and isolation, there was an approximately 2:1 mixture of *E* to *Z* (**30**), approximately 15% of the fully reduced (**35**), and 6% of the regioisomer *R*-30, all of which appeared at the same R_f. The equivalents of LiAlH(O*t*-Bu)$_3$ were increased to 2.4 eq and $ZrCp_2Cl_2$ to 2.4 eq in an attempt to increase the *E/Z* ratio, but to no avail. To ensure that no excess hydride source was present in solution, 0.1 eq less of LiAlH(Ot-Bu)$_3$ was used, and LiAlH(Ot-Bu)$_3$ was added dropwise at 0˚C; this did result in a lower amount of (**35**) to around 6%, and an overall 61% yield of the inseparable compounds. The 2:1 mixture of isomers was carried on in hopes that future steps would allow either: i) conversion of the *Z*- to the *E*-isomer, or ii) separation of isomers through column chromatography or HPLC.

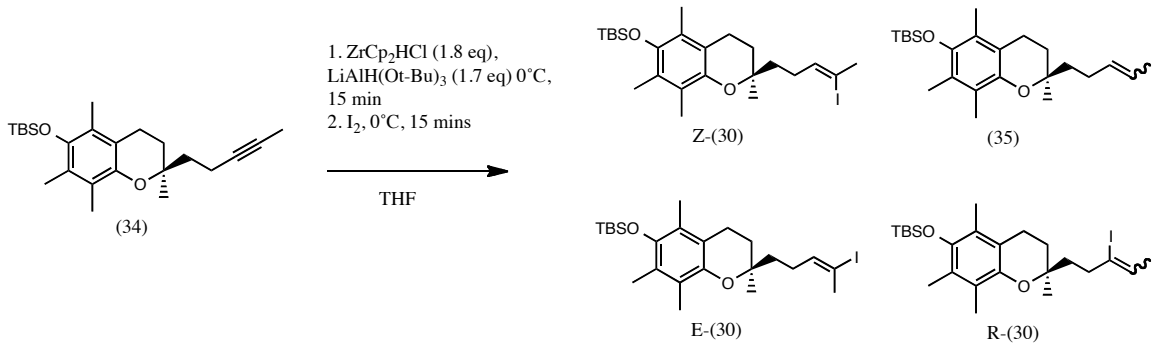

Scheme 11. *In situ* synthesis of Schwartz reagent during the reaction produced a mixture of three compounds, viewed as a single spot on TLC.

2.6. Stille Coupling of Compounds (25) and (5)

The next step in the synthesis was a Stille coupling of (**36**) and (**5**) (**Scheme 12**). The Stille reaction is a cross-coupling reaction between organic electrophiles and organostannes.[106,107] This reaction constitutes a versatile way to form C-C bonds between stannanes and halides.[107] The first examples of coupling were witnessed by Eaborn[108] and Kosugi-Migita[109] in 1976-77 (which actually preceded Stille), but the valuable mechanistic studies and synthetic work accomplished by Stille merit that the reaction be in his name. Multiple conditions were attempted for this reaction (**Table 2**). The optimum yield obtained was 70%. It was also at this stage, where the regioisomer, could be separated from the geometric isomers (**36**) via column chromatography.

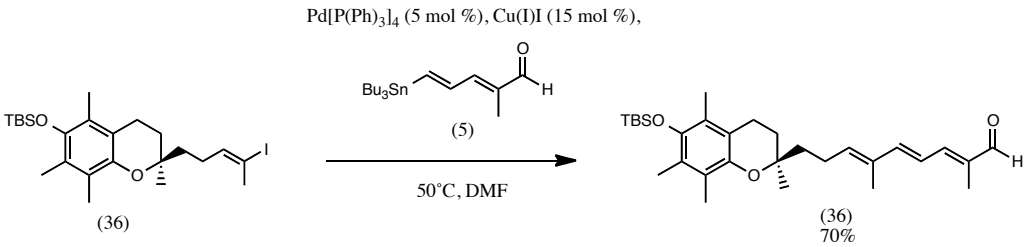

Scheme 12. Optimized Stille coupling conditons between vinyl halide (26) and (5).

The use of copper (I) salts have been widely used as co-catalysts in Stille couplings because of their beneficial effects of increasing yields. It has been proposed that copper salts act as free neutral ligand scavengers, which otherwise would cause autoretardation of the rate-determining associative transmetalation.[106,110]

Table 2. Various Stille reaction conditions with the corresponding yields in the synthesis of (**32**)

Reaction #	Reagents	Time	Temperature	Yield
1	Bis(triphenylphosphine) palladium (II) dichloride (6 mol%) Et_3N 1.4 eq (5) 1.45 eq (36) 1 eq DMF	22 hrs	40˚C	32%
2	Tetrakis triphenyphosphine Pd (0) 5 mol % CsF 2 eq Cu(I)I 10 mol % (5) 1.4 eq (36) 1 eq DMF	3 hrs	45˚C	23%
3	Tetrakis triphenyphosphine Pd (0) 5 mol % Cu(I)I 0.8 eq (5) 1.33 eq (36) 1 eq DMF	15 hrs	50˚C	53%
4	Tetrakis triphenyphosphine Pd (0) 6 mol % Cu(I)I 1.5 eq (5) 1.4 eq (36) 1 eq DMF	4 hrs	50˚C	33%
5	Tetrakis triphenyphosphine Pd (0) 5 mol % Cu(I)I 15 mol % (5) 1.45 eq (36) 1 eq DMF	19 hrs	50˚C	70%

In an attempt to separate the different triene products, we tried using silver nitrate impregnated TLC plates. Unfortunately, in most cases, separation of geometric isomers on silica gel is either very difficult, or not possible. One of the methods which has been successful in achieving this separation uses silver nitrate impregnated silica. The term "argentation" is used to describe the phenomenon whereby silver ions form complexes with *cis* double bonds, to a greater extent than the *trans*. In these cases, the separation of *cis*/*trans* isomers depends on how well the π-electrons in the alkene isomers interact with the silver ions. This interaction is dependent on the number, geometry, an position of the olefins.[111]

Examples of argentation in separating mixtures have been recently demonstrated by Kramer.[112] *Trans*-monounsaturated, *cis*-monounsaturated, and *cis*-/*trans*-conjugated diene fatty acids were separated on 5% impregnated silver nitrate TLC plates. The plates were washed with a 50:50 methanol/chloroform mixture, activated at 110˚C for 1 hour, impregnated with the 5% silver nitrate solution in acetonitrile, and activated again.[112] In my attempt, TLC plates were impregnated with a 10% silver nitrate solution (H_2O), activated in the oven for 1 hour at 100˚C and after sample spotting and developing the plate, were viewed under UV. No separation of *cis*-/*trans*- isomers was observed.

The mixture of *cis*-/*trans*-(**36**) was carried on through the final Wittig reaction (**Scheme 13**). Similarly to the rest of the phytyl tail, a *trans*-geometry was required. The stereochemistry of the Wittig reaction for olefination of aldehydes is reliant on the type of phosphonium salt used and the exact reaction conditions employed. Non-stabilized ylides will typically generate (*Z)*-alkenes, whereas the

corresponding stabilized ylides produce (*E)*-olefins (**Figure 27**). These outcomes are the case regardless of the type of substituents on the phosphorous.[113]

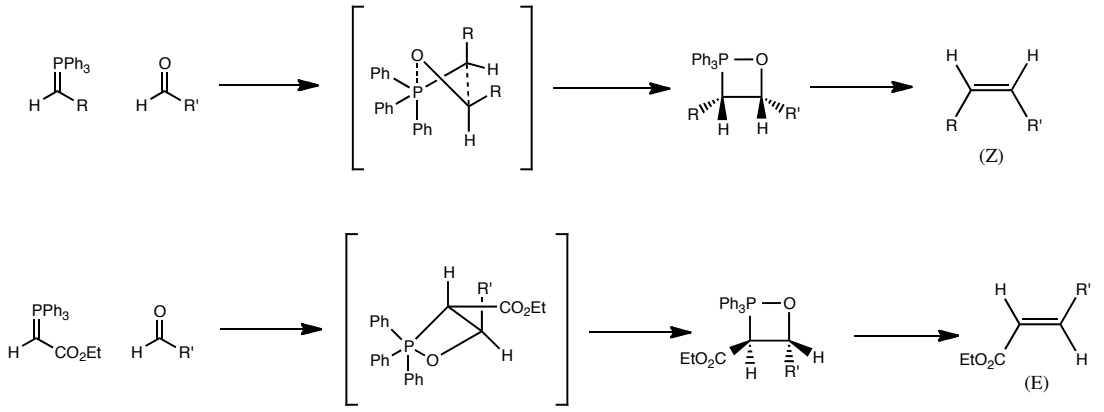

Figure 27. Top: Non-stabilized ylides favour (Z)-olefins, whereas stabilized ylides favour (E)-olefins (bottom).

With a non-stabilized ylide, the 1,3-interactions are reduced by 'puckering' of the four-membered ring. As a result, there is a smaller 1,2-interactions (gauche) between the R substituent of the ylide, and the R' of the aldehyde. Additionally, there is less eclipsing strain between the R substituent and the phenyl substituents on the phosphorous; favoring the (*Z*)-configuration.[114]

In the case of the stabilized ylide, there is an increase in the P-O bonding in the later transition state, which favours a planar four-centered geometry. Because phosphorous is almost a trigonal bipyramidal geometry, there is less 1,3-interactions, and 1,2-interactions are the controlling factor. For the *trans* process, the thermodynamic advantage is present in the product-like transition state, and the (*E*)-configuration predominates.[113,114]

As recorded in 1988, the olefination of non-bulky aldehydes with allylic tributylphosphonium ylides resulted in products with high *E*-selectivity.[115]

However, in these reactions the steric effects of the aldehyde and ylide have vital effects on the outcome of the geometry. With tributylphosphonium ylides, *E*-olefins were predominately the product when *n*-BuLi was present in the reaction mixture. Additionally, the use of lithium salt was required for better yields. When *t*-BuOK was used, yields diminished. The reactions with tributylphosphonium ylides favor the more stable planar transition state, owing to the large decrease in 1,3-interactions between the phosphorous ligands and R_2.[115]

In Wang's synthesis of αT6, the same phosphonium salt was used on an almost identical intermediate. The recorded yield of that reaction was 88%. However, when the reaction was attempted on my intermediate, only a 26% yield of (**38**) was observed (**Scheme 13**). Confused as to why the drastic decrease in yield, further investigation into Wang's procedure discovered the actual yield was 45% (not 88%). Wang's products appeared to be an 11:1 *E:Z* inseparable mixture (in favor of the *E*-isomer). Unfortunately, because of the 2:1 mixture of geometric isomers of the precursor (**30**), and limited amount of material in hand, the geometry of the Wittig reaction appeared to be *trans*, but the *cis* product may have been present in trace amounts in overlapping peaks in the H-NMR, and as a result the geometric purity was not able to be determined.

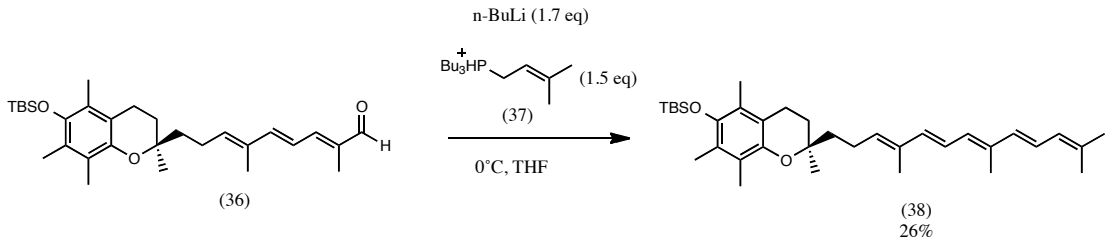

Scheme 13. Wittig reaction between (36) and phosphonium salt (37) produced TBSO- αT6 in a 26% yield.

2.7. Final Attempts at Correcting the C3'/C4' Geometry

2.7.1 Takai Olefination

As we were unable to overcome the selectivity in the *trans*/*cis* geometry at the C3′ position on the phytyl tail, an additional approach was suggested. It's known that the methyl groups on the phytyl tail are unnecessary for binding to αTTP.[7,116] With this knowledge, the omission of the methyl group on the C4′ position would allow additional reactions to be attempted that were previously incompatible (**Figure 28**), one of which was the Takai olefination of aldehydes.

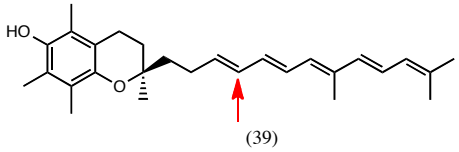

Figure 28. Removal of the methyl group at C4' position would allow for a different pathway in attempts of obtaining (E)-geometry across that bond. The omission of the methyl group would not affect the binding to αTTP.

The Takai olefination describes a reaction where an aldehyde is converted to an alkene.[117] This reaction was reported in a 1986 publication, where benzaldehyde and an organochromium complex was created from a haloform and an excess of chromium (II) chloride; producing a vinyl halide with (*E*)-selectivity (**Figure 29**).[117]

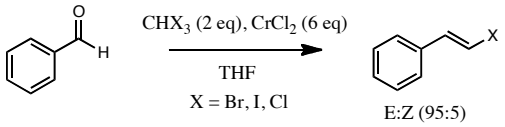

Figure 29. Typical reaction conditions used in the Takai Olefination.

Shown in **Figure 30** is the mechanism proposed by Takai. Chromium (II) chloride is oxidized to chromium (III) after substitution of two of the iodine atoms. The resulting geminal carbodianion acts as a nucleophile, reacting with the aldehyde in a 1,2- addition. After addition, an *anti*-elimination of both chromium (III) groups produces the vinyl halide product.[118]

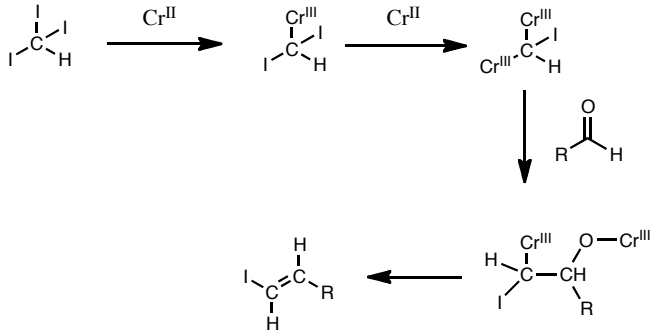

Figure 30. The reaction mechanism proposed by Takai. Chromium (II) is oxidized to chromium (III) after substitution of both iodine atoms. The geminal carbodianion acts as a nucleophile on the aldehyde. Following elimination of both chromium-bearing groups, the vinyl halide is formed.

The Takai olefination was performed on the Trolox-aldehyde (**19**) obtained from the Lemieux-Johnson oxidation. Iodoform (2 eq) and $CrCl_2$ (6 eq) were mixed together in a glove box (to ensure no prior oxidation of chromium took place). THF was added and the solution was allowed to stir at 0˚C whereupon aldehyde (**21**) was added slowly drop-wise. After 2 hours there was a complete conversion of starting material. After purification, it was found that the reaction had produced a vinylic halide (**40**) in a 69% yield, but the selectivity was only a 2.4:1 mixture in favor of the *trans* (**Scheme 14**).

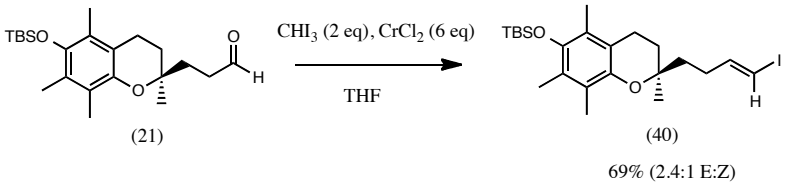

Scheme 14. Reaction conditions used for the Takai olefination.

2.7.2 Potassium Azodicarboxylate (PAD) Reduction

As the Takai selectivity was unsatisfactory, a final attempt to remedy this problem was attempted. Decarboxylation of potassium azodicarboxylate (PAD) (**41**) produces diimide ($H_2N{=}NH_2$). Diimide reductions of alkenes and alkynes occur in a syn addition of dihydrogen.[119] There are numerous examples in the literature where the diimide selectively reduces less substituted double bonds.[119–123] However, there were no examples of PAD selectively reducing one geometric isomer over another. It was hoped that the steric hinderance of the iodine atom and alkenyl carbon, in the *trans*-isomer, would be enough to have PAD selectively reduce the cis-isomer (**40**) (**Scheme 15**). If this were to be the case, addition of pyridine to the iodoalkane (**42**) product would produce a quaternary salt that could be removed from the reaction mixture. Similarly, if un-separated, only the vinylic iodine (**40**) would react in the subsequent Stille coupling, leaving the reduced iodoalkane (**42**) unreacted.

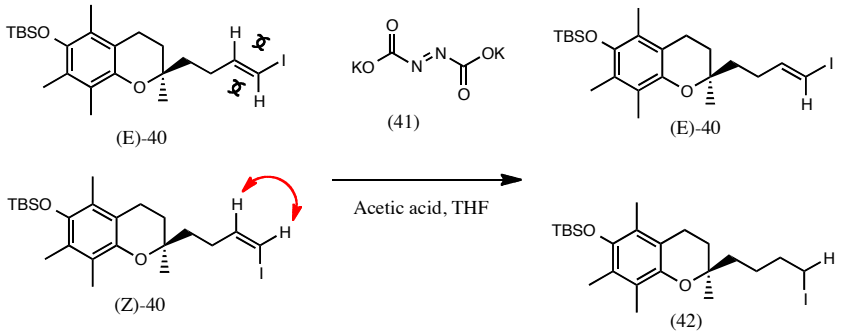

Scheme 15. Thought process for using PAD as a reductant on the olefin. In the *trans*-scenario (top), the steric hinderance was hoped to be enough to prevent PAD from reducing it. However, with the *cis*-geometry, PAD would have easy access to the olefin, reducing it selectively, or at least first. However, this was not the case. Both *cis* and *trans* reduced equally with no discrimination.

Unfortunately, there was no selective reduction of the *cis*-isomer, as seen by the ^{1}H-NMR (with the allylic proton of the trans-isomer integrated for 1, to show the ratio before and after PAD reduction of the *cis*) (**Figure 31**), (**Figure 32**), and (**Figure 33**). There was an overall 30% reduction to the iodoalkane (**42**), but with no discrimination between the *cis*/*trans* isomers. The non-selective reduction may be a result of the *trans*-olefin not being sterically hindered. Further research showed di-substituted trans-olefins can be reduced by PAD, whereas trisubstituted are very sluggish.[124]

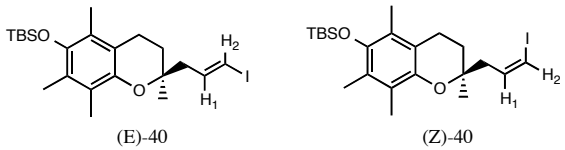

Figure 31. Highlighting H_1 and H_2 in both the cis and trans- olefins. See Figure 29 and 30 for ^{1}HNMR analysis before and after PAD reduction.

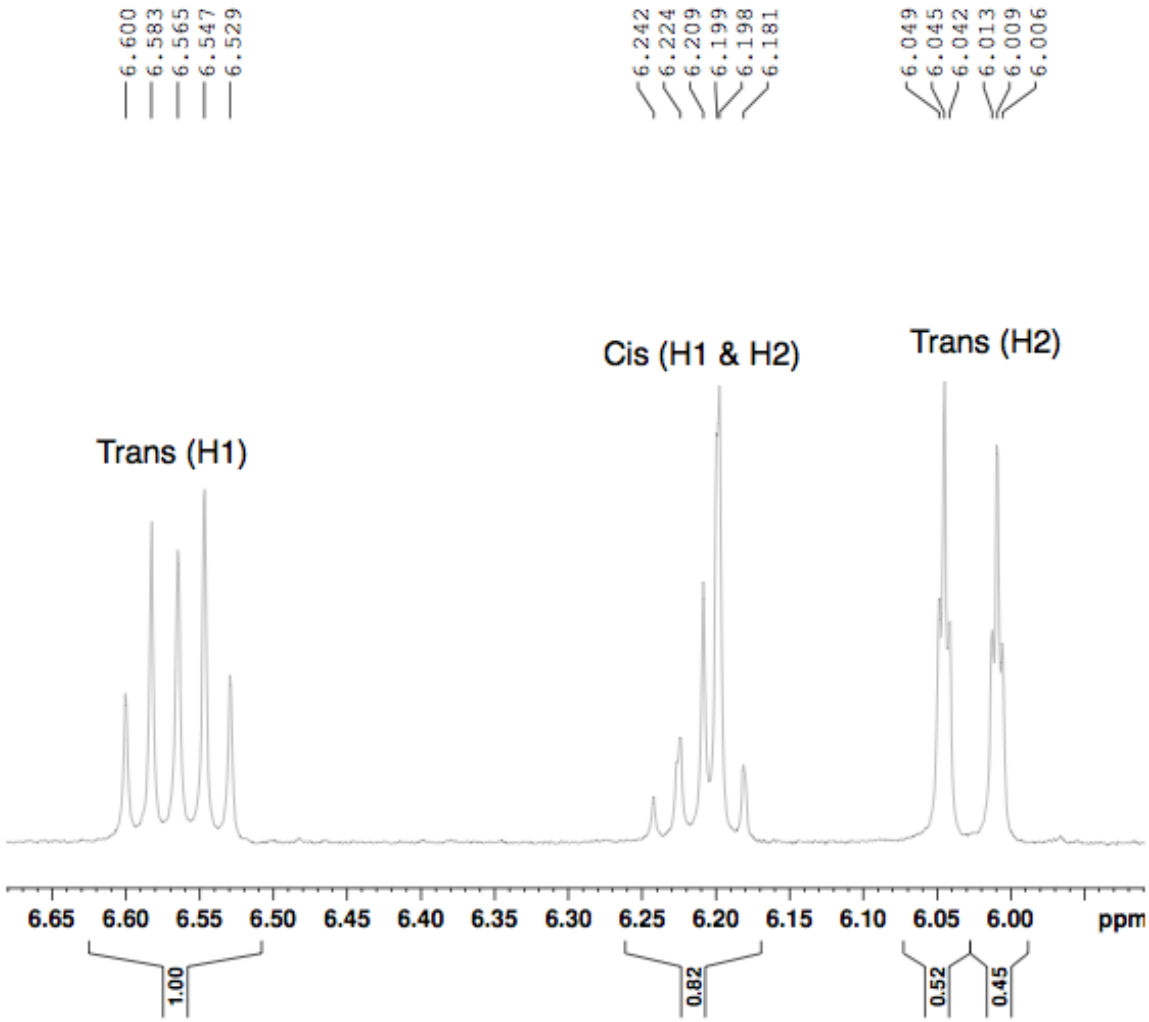

Figure 32. [1]HNMR of an inseparable mixture of (*E*) and (*Z*)-40 before PAD reduction

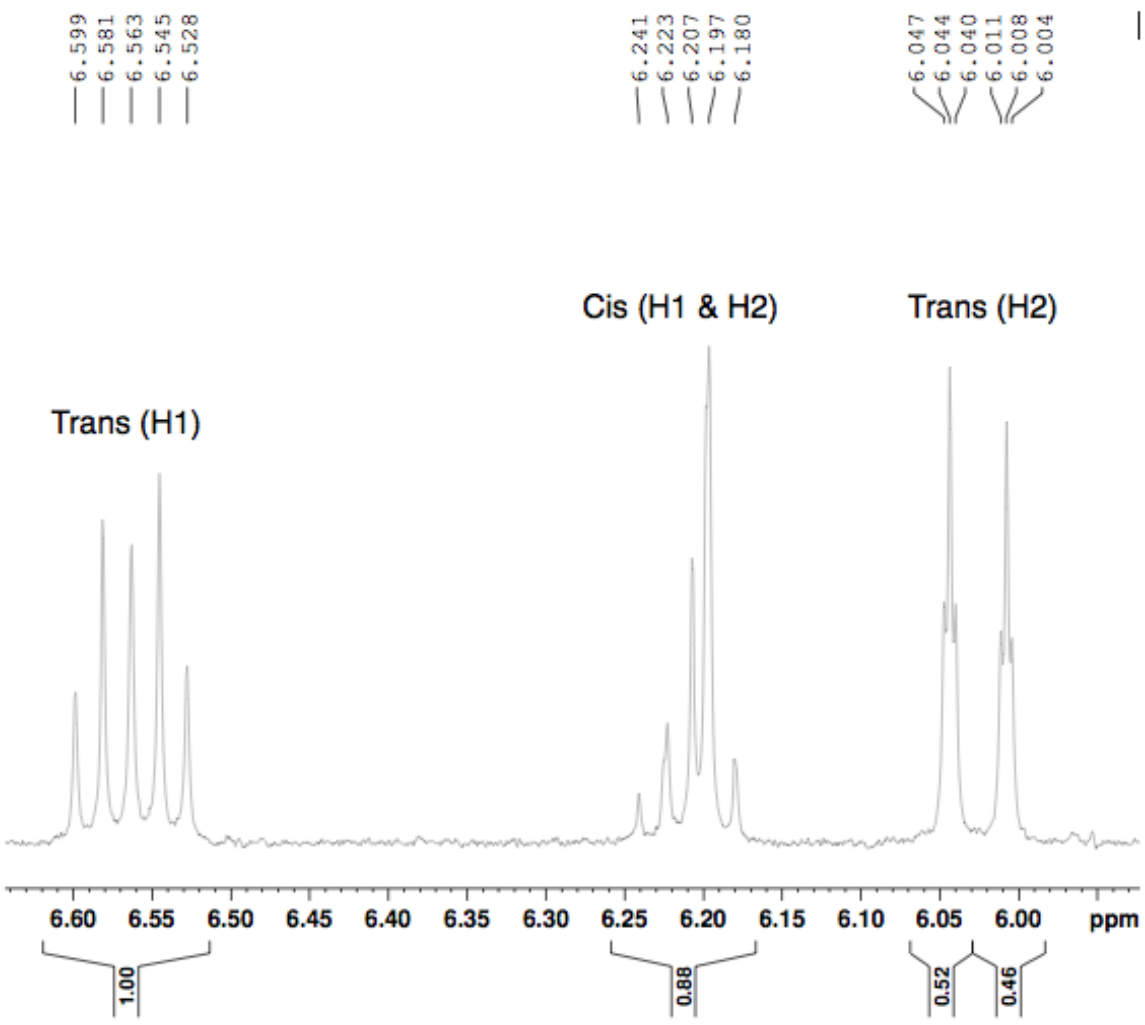

Figure 33. [1]HNMR of an inseparable mixture of (*E*) and (*Z*)-40 after PAD reduction

Additional suggestions were proposed. Unfortunately, many would generate the wrong geometry (*Z*-isomer). One suggestion was the reduction of a propargylic alcohol, as used by Corey in his juvenille hormone synthesis (**Figure 34**).[125] Even though juvenile hormones are all *trans*-isomers in nature, the LAH reduction and quenching of the propargylic alcohol results in *cis*-addition of the iodine. Only upon cuprate exchange with an ethyl substituent does the olefin switch to *trans*.[125]

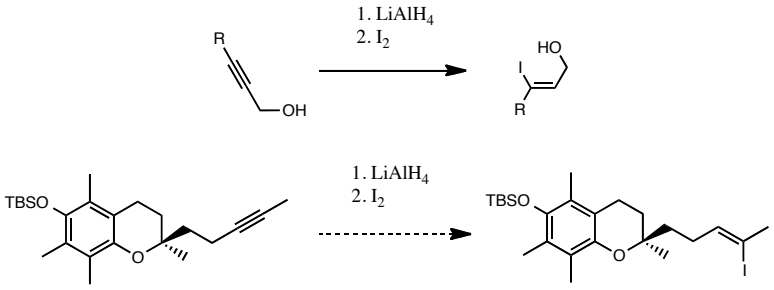

Figure 34. Corey's method of producing (Z)-specific olefins from propargylic alcohols. Only after substitution of iodine, is the trans-geometry instilled.

None-the-less, TBSO-αT5 (**38**) was produced as an unknown mixture of geometrical isomers. The batch of TBSO-αT5 (6 mg) is currently being stored at -78˚C. The final step is deprotection of the TBSO-group using TBAF. TBSO-αT5 has a maximum absorption at 338 nm and has an absorption coefficient of 33,070 M^{-1} cm^{1} in ethanol (**Figure 35**).

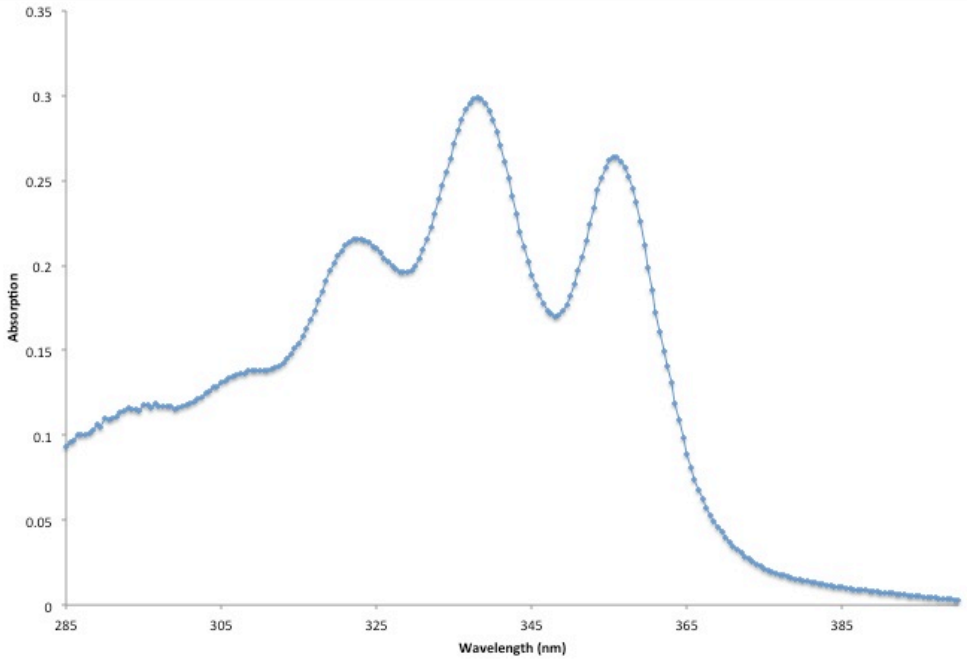

Figure 35. UV-Vis absorption of TBSO-αT5 in ethanol (concentration 9.07 μM).

2.9. Stability of αT5

Conjugated polyenes such as lycopene are known to be susceptible to high temperatures, air oxidation, and light.[126] To confirm the success of the design of αT5 the oxidative stability of this compound and αT6 should be compared. Similar to αT6, TBSO-αT5 is very sensitive to acidic conditions. This was seen on two accounts, when in contact with non-deactivated silica, a bottom spot is observed. Similarly, when in contact with deuterated chloroform that hasn't been deactivated, degradation is also seen. During isomerization experiments with catalytic (4 mol %) of I_2, it was found that TBSO-αT5 will degrade in under 30 minutes when exposed to sunlight. No oxidative studies were performed by bubbling oxygen into a solution containing αT5, as it is almost certain to degrade the compound. Promising results were seen after TBSO-αT5 was stored in the -78˚C freezer, under N_2 for a month, and TLC indicated almost all the compound remained intact.

3. Conclusions and Future Work

Additional attempts at correcting the C3' geometry will be attempted after the defense (**Figure 36**). The route of primary interest is the hydrostannylation of an alkyne.[127–129] For example, one article demonstrated the utility of hydrostannylation of an internal alkyne.[129] In Asano's article, conversion of an internal methyl alkyne to the corresponding vinyl iodide under standard conditions failed; giving poor yields. These conditions included radical-mediated hydrostannylation/iodination, palladium-catalyzed hydrostannylation/iodination, and hydrozirconation/ iodination. However, using Semmelhacks conditions (*n*-Bu_3SnH, $Pd(OAc)_2$ and PCy_3 in hexane) furnished the corresponding (*E*)-vinyl stannane (58% yield), which would then go on to react with iodine (84% yield).

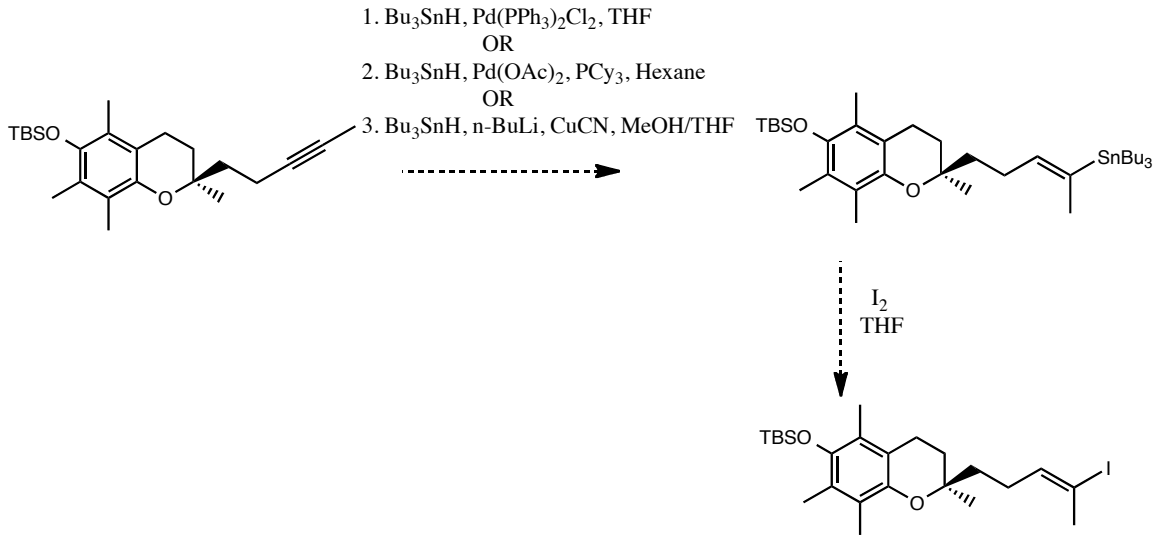

Figure 36. Future attempts at establishing correct (*E*)-geometry across the C3' bond using hydrostannylation methods

The synthesis of TBSO-αT5 (**38**), a fluorescent analogue of α-tocopherol, has been successfully completed (albeit in a 2:1 *E:Z* mixture of the C3' bond). Compound (**38**) Has a maximum absorption at 338 nm. The fluorescence emission is expected to be ≈ 500 nm; as a result, should not interfere with endogenous protein fluorophores such as tryptophan. The stability of this compound seems to exceed that of αT6, if stored in the dark, under N_2, at -78˚C. When bioassays are pursued, the new molecule will most likely not show similar affinity to αTTP as natural αT because of the increased rigidity of the phytyl tail. However, the lack of conjugation on the phytyl tail in connection to the chromanol ring may increase affinity in comparison to αT6 which has a $K_d = 540 \pm 35$ nM.[69] However, this analogue maintains a high structural similarity to α-tocopherol in comparison to many previously synthesized α-tocopherol fluorophores.

Just as αT6 retained much of αT similarity, and was susceptible to oxidative stress resulting in loss of fluorescence, we suspect αT5 to also be susceptible. The absorption of αT6 decreased at 368 nm, evidence to the consumption of the compound. α-Tocopentaenol should also show a decrease in fluorescence when exposed to peroxidative stress. Atkinson's group will perform the binding assay of αT5 to αTTP to determine the dissociation constant of this derivative. However, for the fluorescence assays, αT5 will have to be sent off to our collaborator, Dr. Danny Manor, in the near future.

4. Experimental

All reagents were purchased from Sigma-Aldrich Chemical Co., Oakville, Ontario. All glassware was dried in an oven of 100˚C overnight or flame-dried. Cooling baths were prepared with acetone/dry ice for -78˚C, and ice/water for 0˚C. Air or moisture sensitive reactions were performed under N_2. THF was distilled with sodium/benzophenone immediately before use; benzene was distilled over sodium metal; dichloromethane was distilled over CaH_2; methanol was distilled from Mg/iodine. *n*-Butyllithium and LDA were titrated with *N*-benzylbenzamide to a blue endpoint, immediately before use. Reagent grade solvents were used for extractions. Distilled water was used for any aqueous work-ups.

Analytical thin-layer chromatography (TLC) was performed on Merck 0.25 mm pre-coated silica gel 60 Å F-254 aluminum plates and visualized under UV light, or stained in I_2, or Hanessian stain solution. Column chromatography was carried out on silica gel (200-300 mesh) purchased from Aldrich.

^{1}H-NMR and ^{13}C-NMR spectra were measured on a Bruker Advance DPX-400 or -300 digital FT-NMR spectrometer in $CDCl_3$ with residual chloroform as internal reference (7.281 ppm for ^{1}H and 77.0 ppm for ^{13}C) unless otherwise noted. Chemical shifts are reported as δ values (ppm) and coupling constants (*J*) are reported in Hertz (Hz). The following abbreviations are used: s (singlet), d (doublet), t (triplet), q (quartet), m (multiplet) and br (broad). Mass spectra (MS) were recorded on a Carlo Erba/Kratos GC/MS Concept 1S double focusing mass spectrometer interfaced to a Kratos DART aquistion system and a Sun SPARC workstation.Samples were introduced through a direct inlet system. Ions are

generated using electron impact (EI), Fast Atom Bombardment (FAB) or Electrospray Ionization (ESI) and are reported in *m/z* values. Melting points (mp) recorded on recrystallized solids and solidified material.

4.1. Synthesis of 1-(2,4-dinitrophenyl)-3-methylpyridin-1-ium chloride (2)

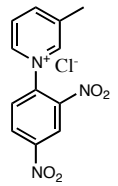

3-methyl pyridine (1.72 mL, 17.7 mmol) was added to 17 mL of acetone and stirred while 2,4-dinitro-chlorobenzene (3.56 g, 17.5 mmol) of was added in a single portion. The mixture was heated at reflux for 30 h. The solvent was removed *in vacuo*. The resulting off-white solid was washed and filtered multiple times with hexane to yield a tan/white powdery solid (4.88 g, 94%). Mp 165-166˚C (recrystallized in EtOH:hexane).

^{1}H-NMR (DMSO, 400 MHz) = δ 9.33 (s, 1H, =CH), 9.25 (d, *J*= 6.3 Hz, 1H, =CH), 9.13 (d, *J*= 2.7 Hz, 1H, =CH), 8.99 (dd, *J*= 8.7 Hz, 1H, =CH), 8.80 (d, *J*= 8.1 Hz, 1H, =CH), 8.40 (d, *J*= 8.7 Hz, 1H =CH), 8.34 (dd, *J*= 6.3 Hz, 1H, =CH), 2.60 (s, 3H, CH_3)

^{13}C-NMR (DMSO) = δ 149.59, 145.8, 145.6, 143.8, 143.5, 139.3, 139.1, 132.4, 130.7, 127.7, 122.0, 18.4

m/z (ESI+)= 261.0 (6.3%), 260.0 (M+H, 100%)

4.2. Synthesis of (2*E*,4*E*)-5-(dimethylamino)-2-methylpenta-2,4-dienal (3)

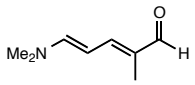

Compound (**2**) (1.93 g, 6.5 mmol) of was dissolved in 25 mL of refluxing EtOH while 2.1 mL (16.3 mmol, 2.5 eq) of dimethyl amine was added to the mixture (dropwise). The mixture was heated for 1 h 15 min, whereupon the solvent was removed *in vacuo*. Aqueous 2M NaOH was added and the mixture turned dark purple. This solution was extracted 3x with DCM (20 ml). Organic extracts were combined and yielded a dark purple oil after evaporation. Column chromatography with EtOAc yielded a light yellow solid. After recrystallization (hexane), yellow crystals were obtained (622 mg, 72%). Mp 73-74˚C (hexane).

R_f= 0.45 EtOAc

^{1}H-NMR ($CDCl_3$, 400 MHz)= δ 9.18 (s, 1H, CHO), 6.86 (d, *J*= 11.6 Hz, 1H, =CH), 6.77 (d, *J*= 12.4 Hz, 1H, =CH), 5.26 (t, *J*= 12.2 Hz, 1H, =CH), 2.97 (s, 6H, $2CH_3$), 1.78 (s, 3H, CH_3)

^{13}C-NMR ($CDCl_3$, 400 MHz) = 192.70, 153.49, 151.32, 126.09, 94.96, 9.09

m/z (ESI+)= 141.0 (12.0%), 140.0 (M+H, 100%)

4.3. Synthesis of (2*E*,4*E*)-5-(dibutylamino)-2-methylpenta-2,4-dienal (4)

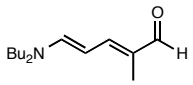

Compound (**2**) (1.0 g, 3.4 mmol) was dissolved in 15 mL of refluxing EtOH while dibutylamine (1.4 mL, 8.2 mmol, 2.4 eq) was added to the mixture (dropwise). The mixture was heated for 1 h 45 min, where the color had turned bright red. The solvent was removed *in vacuo*. Aqueous 4M NaOH (15 ml) was added and the solution turned dark purple. This solution was extracted 3x with DCM (20 ml). Organic extracts were combined and provided a dark purple oil after evaporation. Column chromatography with 7.5:1 hexane:EtOAc yielded a yellow/orange oil (415 mg, 55%).

R_f= 0.48 (3:2 hexane:EtOAc)

^{1}H-NMR ($CDCl_3$, 400 MHz) = δ 9.16 (s, 1H, CHO), 6.84 (d, *J*= 11.6 Hz, 1H, =CH), 6.75 (d, *J*= 12.8 Hz, 1H, =CH), 5.28 (t, *J*= 12.2 Hz, 1H, =CH), 3.18 (t, 4H, $2CH_2$), 1.76 (s, 3H, CH_3), 1.56 (t, 4H, $2CH_2$), 1.33 (t, 4H, $2CH_2$), 0.95 (t, 6H, $2CH_3$)

^{13}C-NMR ($CDCl_3$, 400 MHz)= δ 192.18, 153.56, 150.11, 125.64, 94.50, 51.95, 29.95, 20.02, 13.61, 9.02

m/z (ESI+)= 225.2 (14.2%), 224.1 (M+H, 100%)

4.4. Synthesis of (2*E*,4*E*)-2-methyl-5-(tributylstannyl)penta-2,4-dienal (5)

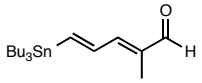

In a 25 mL RBF was placed 0.32 mL of LDA (1.2 M, 0.38 mmol, 1.2 eq) under N_2 atmosphere. At -20˚C, 0.35 mL (0.35 mmol, 1.1 eq) of tributyltin hydride was added dropwise and stirred for 40 mins. After this time, (**3**) (45 mg, 0.32 mmol) in THF was added dropwise at -20˚C. The solution was allowed to stir for an additional hour and a half. Acetyl chloride was then added all at once, still at -20˚C and stirred for an additional 15 mins. Saturated $NaHCO_3$(3 mL) was added and stirred for 15 min. The solution was extracted with DCM (3x 10 ml), dried with $NaSO_4$, filtrated and concentrated *in vacuo*. Column chromatography with 30:1 hexane:DCM yielded a pale yellow oil (48 mg, 42%).

R_f= 0.51 9:1 hexane:ether

^{1}H-NMR ($CDCl_3$, 400 MHz) = δ 9.47 (s, 1H, CHO), 7.03 (m, 2H, 2CH), 6.77 (d, *J*= 9.2 Hz, 1H, CH), 1.90 (s, 3H, CH_3), 1.54 (m, 6H, $3CH_2$), 1.32 (m, 6H, $3CH_2$), 1.00 (m, 6H, $3CH_2$), 0.92 (t, *J*= 7.2 Hz, 9H, $3CH_3$)

^{13}C-NMR ($CDCl_3$, 400 MHz)= δ 195.73, 150.21, 149.63, 141.39, 135.85, 29.17, 29.06, 29.00, 28.96, 27.51, 27.24, 26.96, 13.67, 9.74, 9.50

m/z (ESI+)= 409.1 (M+H Na^+, 100%), 408.2 (42.9%), 407.1 (57.1%), 406.1 (35.7%), 405.1 (42.9%)

4.5. Synthesis of Racemic methyl 6-hydroxy-2,5,7,8-tetramethylchroman-2-carboxylate (8)

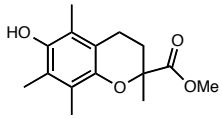

Methyl methacrylate (3.3 g, 33.3 mmol, 5 eq), formaldehyde (1.1 g, 36.7 mmol, 5.6 eq), and trimethylhydroquinone (1 g, 6.6 mmol) were placed in a 10 mL glass vessel and transferred to the microwave reactor (CEM Corp. 201A14, 20 MHz clock, CPU019613). The mixture was allowed to stir for 15 mins at 180˚C (P= 150W). After completion, the product was washed successively with methanol and vacuum filtrated, and recrystallized in MeOH to yield beige/white powder (1.3 g, 82%). Mp 134-136˚C (MeOH).

R_f= 0.27 DCM

^{1}H-NMR ($CDCl_3$, 300 MHz) = δ 3.69 (s, 3H, CH_3CO_2), 2.52- 2.66 (m, 2H, CH_2), 2.18-2.21 (d, 6H, $ArCH_3$), 2.09 (s, 3H, $ArCH_3$), 1.83- 1.93 (m, 2H, CH_2), 1.62 (s, 3H, CH_3)

^{13}C-NMR ($CDCl_3$, 300 MHz) = δ 174.47, 145.53, 121.21, 118.36, 116.89, 52.34, 30.61, 25.42, 20.96, 12.21, 11.81, 11.23

m/z (EI) = 264 (M+, 77%), 205 (100%), 164 (75%)

4.6. Synthesis of (*S*)-methyl 6-hydroxy-2,5,7,8-tetramethylchroman-2-carboxylate (8)

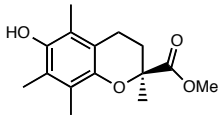

α-Trolox® (2.39 g, 9.5 mmol) and *p*-toluenesulphonic acid (480 mg, 2.7 mmol, 0.3 eq) was dissolved in 60:10 mL of MeOH:DCM . The reaction mixture was stirred under reflux for 20 h. The mixture was extracted with EtOAc, washed with $NaHCO_3$ (2x) and then H_2O (1x). The combined organic layers were dried over $NaSO_4$, filtered, and concentrated *in vacuo*. The product was washed with hexane and recrystallized in MeOH to yield beige/white powder (2.28 g, 92%). Mp 134-136˚C (MeOH).

R_f= 0.21 DCM

^{1}H-NMR ($CDCl_3$, 400 MHz) = δ 3.69 (s, 3H, OCH_3), 2.65 (m, 2H, CH_2), 2.47 (m, 1H,CH_2), 2.20 (s, 3H, CH_3), 2.18 (s, 3H, CH_3), 2.08 (s, 3H, CH_3), 1.91 (m, 1H, CH_2), 1.62 (s, 3H, CH_3)

^{13}C-NMR ($CDCl_3$, 400 MHz) = δ 174.47, 145.53, 121.21, 118.36, 116.89, 52.34, 30.61, 25.42, 20.95, 12.20, 11.81, 11.24

m/z (EI) = 264 (M+, 77%), 205 (100%), 164 (75%)

4.7. Synthesis of (*S*)-methyl 6-((*tert*-butyldimethylsilyl)oxy)-2,5,7,8-tetramethylchroman-2-carboxylate (9)

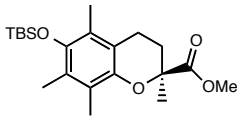

To a solution of compound (**8**) (1.49 g, 5.6 mmol) in anhydrous DMF (15 ml) was added imidazole (1.60 g, 23.1 mmol, 4.1 eq) and TBDMS chloride (1.3 g, 8.6 mmol, 1.5 eq). The mixture was heated to 85˚C and stirred under N_2 for 20 h. After water was added, the mixture was extracted with EtOAc (3 x 25 ml). The combined organic layers were washed with water and brine, dried over $NaSO_4$, and concentrated. Purification on SiO_2 (DCM/hexane: 5:1) afforded a light orange/yellow oil (2.02 g, 94%).

R_f= 0.54 (DCM:hexane = 3:1)

^{1}H-NMR ($CDCl_3$, 400 MHz) = δ 3.68 (s, 3H, -OCH_3), 2.61-2.43 (m, 3H, 2CH_2), 2.17 (s, 3H, ArCH_3), 2.13 (s, 3H, ArCH_3), 2.04 (s, 3H, ArCH_3), 1.89 (m, 1H, 2CH_2), 1.62 (s, 3H, CH_3), 1.06 (s, 9H, 3CH_3), 0.13 (s, 6H, 2CH_3)

^{13}C-NMR ($CDCl_3$, 400 MHz) = δ 174.55, 144.81, 122.70, 117.05, 52.27, 30.56, 26.09, 25.38, 21.05, 18.62, 14.32, 13.37, 11.89, -3.30, -3.36

m/z= EI 378 (M+ 8.9%), 189 (24.8%), 147 (100%)

4.8. Synthesis of (*S*)-6-((*tert*-butyldimethylsilyl)oxy)-2,5,7,8-tetramethylchroman-2-carbaldehyde (10)

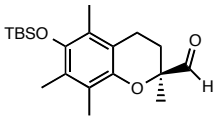

A solution of (**9**) (1.80 g, 4.7 mmol) in dry toluene was cooled to -78˚C in a dry ice/acetone bath. DIBAL (1M, 8.55 ml, 8.5 mmol, 1.8 eq) was added via syringe over a period of 10 min. After 2 h, the reaction was quenched with 25 mL of MeOH, followed by 25 mL of H_2O. A 25 mL portion of 2M HCl was added, and the solution was extracted with ether (4x). Purification with 3:1 hexane:DCM yielded a colorless oil that crystallized to hard, white crystals (1.39 g, 83%). Mp 72-73˚C (MeOH).

R_f= 0.82 DCM

^{1}H-NMR ($CDCl_3$, 400 MHz) = δ 9.65 (s, 1H, CHO), 2.53 (m, 2H, CH_2), 2.32 (m, 1H, CH_2) 2.26 (s, 3H, $ArCH_3$), 2.19 (s, 3H, $ArCH_3$), 2.14 (s, 3H, $ArCH_3$), 1.86 (m, 1H, CH_2), 1.41 (s, 3H, CH_3), 1.07 (s, 9H, $3CH_3$), 0.14 (s, 6H, $2CH_3$)

^{13}C-NMR ($CDCl_3$, 400 MHz) = δ 204.81, 145.56, 145.15, 126.47, 123.86, 122.83, 117.61, 80.26, 27.93, 26.08, 21.59, 20.48, 18.60, 14.34, 13.36,12.04, -3.31

m/z (EI)= 348 (M+, 42.2%), 319 (33%), 277 (100%), 73 (56.3%)

4.9. Synthesis of (*S*,*E*)-ethyl 3-(6-((*tert*-butyldimethylsilyl)oxy)-2,5,7,8-tetramethylchroman-2-yl)acrylate (14)

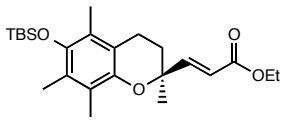

Phosphonium salt (**13**) (0.135 g, 0.31 mmol, 1.3 eq) of was stirred in 0.7 mL of dry THF. *n*-BuLi (1.9M, 0.19 ml, 1.5 eq) was added dropwise at 0˚C, warmed to room temperature, and allowed to stir for an additional 1 h 30 min. After this time (**10**) (84 mg, 0.24 mmol) was added dropwise at room temperature, and allowed to stir for 44 h, until all starting material was consumed. NH_4Cl was added to the mixture. The solution was extracted with DCM (3x), dried with $NaSO_4$, filtered, and concentrated *in vacuo*. Column chromatography with 10:1 hexane:EtOAc yielded (**18**) as a clear oil (45 mg) , and (**14**) (15 mg) as a clear oil.

R_f= 0.77 (3:1 hexane:EtOAc)

^{1}H-NMR ($CDCl_3$, 400 MHz)= δ 6.95 (d, *J*= 15.6 Hz, 1H, CH), 5.89 (d, *J*= 15.6 Hz, 1H, CH), 4.17 (q, *J*= 1.2 Hz, 2H, CH_2), 2.61 (m, 1H, CH_2), 2.43 (m, 1H, CH_2), 2.17 (s, 3H, $ArCH_3$), 2.14 (s, 3H, $ArCH_3$), 2.05 (s, 3H, $ArCH_3$), 2.00 (m, 1H, CH_2), 1.90 (m, 1H, CH_2), 1.46 (s, 3H, CH_3), 1.29 (t, 3H, CH_3), 1.07 (s, 9H, $3CH_3$), 0.14 (s, 6H, $2CH_3$)

^{13}C-NMR ($CDCl_3$, 400 MHz) = 166.7, 151.3, 145.4, 144.5, 126.3, 123.6, 122.4, 119.9, 117.2, 74.9, 60.4, 26.5, 21.0, 18.6, 14.3, 13.4, 12.0, -3.3

m/z (ESI+)= 419.4 (M+H, 28.0%), 441.2 (Na^+, 100%), 442.2 (5.2%)

4.10. Modified synthesis of (*S*,*E*)-ethyl 3-(6-((*tert*-butyldimethylsilyl)oxy)-2,5,7,8-tetramethylchroman-2-yl)acrylate (14)

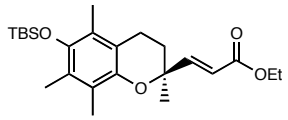

To a solution of phosphonium salt (**13**) (753 mg, 1.8 mmol, 1.3 eq) suspended in DMSO (2 mL), was added drop-wise *n*-buLi (1.1 mL, 2M, 1.3 eq) at room temperature. This pale yellow solution was stirred for an additional hour. At room temperature, (**10**) (462 mg, 1.3 mmol) in dry THF was added at a fast drop-wise pace. This solution was stirred an additional 5 h 30 min. The reaction was quenched with NH_4Cl (5 ml) and extracted with ether (3x 15 ml). Column chromatography with 10:1 hexane:EtOAc yielded (**14**) as a clear oil (461 mg, 84%).

R_f= 0.77 (3:1 hexane:EtOAc)

^{1}H-NMR ($CDCl_3$, 400 MHz)= δ 6.95 (d, *J*= 15.6 Hz, 1H, CH), 5.89 (d, *J*= 15.6 Hz, 1H, CH), 4.17 (q, *J*= 1.2 Hz, 2H, CH_2), 2.61 (m, 1H, CH_2), 2.43 (m, 1H, CH_2), 2.17 (s, 3H, $ArCH_3$), 2.14 (s, 3H, $ArCH_3$), 2.05 (s, 3H, $ArCH_3$), 2.00 (m, 1H, CH_2), 1.90 (m, 1H, CH_2), 1.46 (s, 3H, CH_3), 1.29 (t, 3H, CH_3), 1.07 (s, 9H, $3CH_3$), 0.14 (s, 6H, $2CH_3$)

^{13}C-NMR ($CDCl_3$, 400 MHz)= 166.7, 151.3, 145.4, 144.5, 126.3, 123.6, 122.4, 119.9, 117.2, 74.9, 60.4, 26.5, 21.0, 18.6, 14.3, 13.4, 12.0, -3.3

m/z (ESI+)= 419.4 (M+H, 28.0%), 441.2 (Na^+, 100%), 442.2 (5.2%)

Combustion:

Element: C

Theory: 68.86; Found: 71.04

Element: H

Theory: 9.15; Found: 9.49

4.11. Synthesis of *tert*-butyldimethyl(((*R*)-2,5,7,8-tetramethyl-2-((3*E*,7*E*)-4,8,12-trimethyltrideca-3,7,11-trien-1-yl)chroman-6-yl)oxy)silane (20)

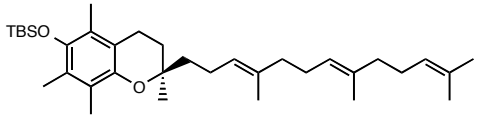

To a flask containing α-tocotrienol (344 mg, 8.4 mmol) was added TBSCl (189 mg, 12.5 mmol, 1.5 eq) and imidazole (234 mg, 34.3 mmol, 4.1 eq). The mixture was dissolved in 3.5 ml of dry DMF and allowed to stir at 85˚C for 24 h. After this time, the mixture was allowed to cool to room temperature and diluted with water (10 ml) and extracted with diethyl ether (5 x 10 mL). The combined organic layers were dried with Na_2SO_4. After filtration, the residue was concentrated under reduced pressure. Purification by chromatography (90:2 hexanes:EtOAc) provided (**20**) as a yellow, orange oil (415 mg, 92%).

R_f = 0.71 (DCM/Hexane 3:1)

^{1}H-NMR ($CDCl_3$, 400 MHz)= δ 5.19 (m, 3H, CH), 2.58 (t, 2H, CH2), 2.14 (s, 3H, Ar-CH_3), 2.12 (s, 3H, Ar-CH_3), 2.11 (S, 3H, Ar-CH_3), 2.01 (m, 4H, 2CH_2), 1.85 (m, 2H, CH_2), 1.71 (s, 3H, CH_3), 1.61 (s, 3H, CH_3), 1.57 (s, 3H, CH_3), 1.07 (s, 9H, 3CH_3), 0.14 (s, 6H, 2CH_3).

^{13}C-NMR ($CDCl_3$, 400 MHz)= 145.8, 144.1, 134.7, 129.9, 125.8, 124.5, 124.4, 124.2, 123.2, 122.7, 117.4, 74.3, 39.7, 39.5, 31.6, 26.8, 26.6, 26.1, 25.7, 23.8, 22.2, 20.9, 18.6, 17.6, 16.0, 15.8, 14.3, 13.4, 11.8, -3.4

m/z (EI)= 538 (M^+, 100%), 279 (26.4%), 223 (11.1%), 73 (53.9%)

4.12. Synthesis of (*S*)-3-(6-((*tert*-butyldimethylsilyl)oxy)-2,5,7,8-tetramethylchroman-2-yl)propanal (21)

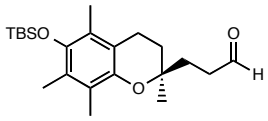

To a solution of (**27**) (56 mg, 1.0 mmol) in THF:H_2O (3.5:1 mixture, 1.5 mL) was added: 2,6- lutidine (0.07 mL, 6.2 mmol, 6 eq), $NaIO_4$ (242 mg, 11.4 mmol, 11 eq), OsO_4 (2.5 wt % in 2-methyl-2-propanol, 0.06 mL, 4 mol %). The reaction was stirred for 48 h at 40˚C at which time the mixture had turned a black/yellow color. H_2O (5 mL) and saturated sodium sulfite (10 mL) were added and extracted with DCM (3 x 10 mL). The combined organic layers were washed with brine and dried with Na_2SO_4. After filtration, the residue was concentrated under reduced pressure. Purification by column chromatography yielded (**21**) as a clear oil, which crystallized in the refrigerator as white crystals. Recrystallization in EtOH (20 mg, 50%). Mp 65-66˚C.

R_f= 0.63 4:1 hexane:EtOAc

^{1}H-NMR ($CDCl_3$, 400 MHz)= δ 9.82 (s, 1H, CHO), 2.64 (q, J= 8Hz, 4H, CH_2), 2.12 (s, 3H, $ArCH_3$), 2.07 (s, 6H $2ArCH_3$), 2.00 (m, 1H, CH_2) 1.88 (m, 3H, CH_2), 1.24 (s, 3H, CH_3), 1.07 (s, 9H, $3CH_3$), 0.14 (s, 6H, $2CH_3$)

^{13}C-NMR ($CDCl_3$, 400 MHz)= δ 202.66, 145.37, 144.44, 126.13, 123.68, 122.7, 117.16, 73.39, 38.63, 31.91, 31.75, 26.10, 23.50, 20.74, 18.61, 14.33, 13.41, 12.00, -3.30.

m/z (EI)= 378.25 (12.0%), 377.25 (33.5%), 376.23 (M+, 100%), 259.09 (84.5%)

Combustion:

Element: C

Theory: 70.16; Found: 70.20

Element: H

Theory: 9.63; Found: 9.69

4.13. Synthesis of (*R*,*E*)-*tert*-butyl((2-(4-iodopent-3-en-1-yl)-2,5,7,8-tetramethylchroman-6-yl)oxy)dimethylsilane (30)

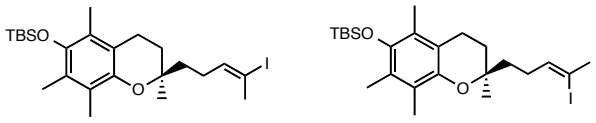

(a) 7 : (b) 1

Alkyne (**30**) (92 mg, 0.17 mmol) and Schwartz reagent (178 mg, 0.48 mmol, 2.8 eq) were dissolved in dry THF (0.5 mL). The solution was stirred under N_2 at 60˚C for 3 h. The reaction was cooled to -10˚C and stirred for 5 min before a solution of I_2 (60 mg, 0.24 mmol, 1.4 eq) in THF (1 mL) was added dropwise. The reaction turned a dark purple colour. After an additional 20 min of stirring at -10˚C, the reaction

mixture was diluted with sat. $Na_2S_2O_3$ and stirred for 10 min. The reaction was extracted with EtOAc (3x 10 ml). The organic layers were collected, dried with Na_2SO_4, filtered and the mixture was concentrated *in vacuo*. Column chromatography with 20:1 hexane:DCM yielded a 7:1 E:Z mixture of product, which solidified after chromatography to a white solid (40 mg, 25%). Mp 58-59˚C (last contacted solvents: hexane/EtOAc)

R_f= 0.63 (5:3 hexane:DCM)

^{1}H-NMR ($CDCl_3$, 400 MHz)= δ 6.20 (dt, *J*=7.2 Hz, 0.9H, CH)[a,b], 5.85 (m, 0.06H, CH)[35], 2.59 (t, *J*= 6.8 Hz, 2H, CH_2)[a,b,35], 2.37 (s, 2.3H, CH_3)[a], 2.20 (q, *J*= 7.6 Hz, 2H, CH_2)[a,b,35], 2.12 (s, 2.7H, $ArCH_3$)[a,35], 2.11 (s, 0.3H, $ArCH_3$)[b], 2.10 (s, 3H, $ArCH_3$)[a,b,35], 2.08 (s, 3H, $ArCH_3$)[a,b,35], 1.77 (m, 3H, CH_2)[a,b,35], 1.62 (d, 0.2H, CH_3)[35], 1.59 (m, 1H, CH_2)[a,b,35], 1.58 (s, 0.3H, CH_3)[b], 1.28 (s, 0.5H, CH_3)[b,35], 1.25 (s, 2.5H, CH_3)[a], 1.07 (s, 9H, $3CH_3$)[a,b,35], 0.14 (s, 6H, $2CH_3$)[a,b,35]

^{13}C-NMR ($CDCl_3$, 400 MHz)= δ 144.29[a], 141.19[a], 135.22[b], 126.02[a], 123.63[a], 122.65[a], 117.35[b], 117.28[a], 102.95[b], 93.52[a], 73.79[a], 38.58[b], 38.34[a], 33.08[b], 31.81[a], 27.26[a], 26.12[a], 25.00[a], 23.68[a], 20.80[a], 18.62[a], 15.89[a], 14.34[a], 13.41[a], 11.98[a], -3.30[a], -3.34[a]

m/z (EI)= 517.16 (3.9%), 516.17 (6.1%), 515.17 (25.2%), 514.17 (M+, 100%), 73.06 (34.4%)

4.14. Synthesis of (*R*,*E/Z*)-*tert*-butyl((2-(4-iodopent-3-en-1-yl)-2,5,7,8-tetramethylchroman-6-yl)oxy)dimethylsilane (30)

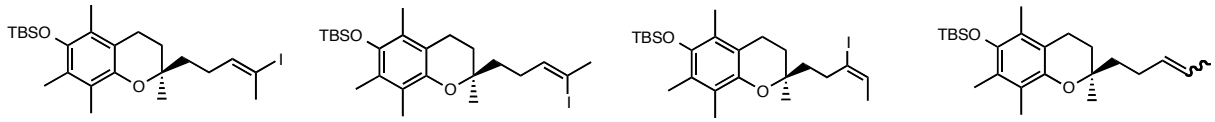

2 : 1

(a) (b) (c) (35)

Compound (**34**) (84 mg, 0.22 mmol) and $ZrCp_2Cl_2$ (116 mg, 0.39 mmol, 1.8 eq) were dissolved in dry THF (0.4 mL). The solution was placed in an ice bath and LiAlH(Ot-Bu)$_3$ (1M, 0.36 ml, 0.38 mmol, 1.7 eq) was added at a fast drop-wise rate. The solution turned dark red and was brought to room temperature after addition. After 15 min, the solution (now being an orange/red color) was placed back in an ice bath and I_2 (90 mg, 0.35 mmol, 1.6 eq) was added drop-wise to the solution. The reaction mixture was allowed to stir at 0˚C for an additional 15 min. After this time, 1M HCl (1 ml) and saturated $Na_2S_2O_3$ (1 mL) were added and extracted with EtOAc (3x 15 ml). Column chromatography with 20:1 hexane: DCM yielded an inseparable 2:1 *E:Z* mixture of (**30a**)and (**30b**) (70 mg), ≈6% (**c**) and ≈10% (**35**) as a clear oil. See appendix for 2D analysis.

R_f= 0.63 (5:3 hexane:DCM)

^{1}H-NMR ($CDCl_3$, 400 MHz)= δ 6.21 (m, 0.8H, CH)^{a,b}, 5.42 (m, 0.2H, 2CH)^{c,35}, 2.59 (t, 2H, CH_2)^{a,b,35,c}, 2.36 (s, 1.6H, CH_3)^a, 2.21 (q, 1.4H, $2CH_2$)^{a,35}, 2.12 (s, 2.8H, $ArCH_3$)^{a,35,c}, 2.12 (s, 1.2H, $ArCH_3$)^{b,35,c}, 2.11 (s, 2H, $ArCH_3$)^{a,b}, 2.10 (s, 3H, $ArCH_3$)^{a,b,35,c}, 1.79 (m, 3.5H, $2CH_2$)^{a,35,c}, 1.62 (d, 0.5H, CH_3)^{35,c}, 1.59 (q, 0.6, CH_2), 1.59 (s, 0.8H, CH_3)^b, 1.59 (m, 0.5H, CH_2)^b, 1.28 (s, 1.3H, CH_3)^{b,35,c}, 1.26 (s, 1.6H, CH_3)^a, 1.07 (s, 9H, $3CH_3$)^{a,b,35,c}, 0.14 (s, 6H, $2CH_3$)^{a,b,35,c}

^{13}C-NMR ($CDCl_3$, 400 MHz)= δ 144.29[a], 141.19[a], 135.22[b], 126.02[a], 123.63[a], 122.65[a], 117.35[b], 117.28[a], 102.95[b], 93.52[a], 73.79, 39.23[35], 38.58[b], 38.34[a], 33.08[b], 31.81[a], 27.26[a], 26.12[a], 25.00[a], 23.68[a], 20.80[a], 18.62[a], 15.89[a], 14.34[a], 13.41[a], 11.98[a], -3.30[a], -3.34[a]

m/z (EI)= 517.16 (3.9%), 516.17 (6.1%), 515.17 (25.2%), 514.17 (M+, 100%), 73.06 (34.4%)

4.15. Synthesis of diethyl (1-iodoethyl)phosphonate (32)

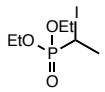

n-BuLi (1.75 M, 8.1 mL, 14.2 mmol, 2.3 eq) was added to dry THF (12 mL) and cooled to -78˚C. A solution of i-Pr_2NH (2.1 mL, 14.8 mmol) in THF (12 mL) was slowly added via syringe. After 15 min of stirring, diethyl ethylphosphonate in THF (12 mL) was added, maintaining the temperature at -78˚C. Stirring was continued for 15 min at -78˚C, after which time dry TMSCl (0.86 mL, 6.8 mmol, 1.1 eq) was added. The solution was allowed to stir for 5 min at -78˚C and then transferred to an ice bath to stir at 0˚C for 10 min. This solution was cooled back down to -78˚C. I_2 (1.72 g, 6.8 mmol, 1.1 eq) in THF (12 mL) was slowly added (over 10 min), after which time the orange/yellow solution was placed in an ice bath to stir for an additional 15 min. At 0˚C, a 1M solution of EtOLi/EtOH (12 mL) was added and after 30 min the reaction mixture was rapidly poured into a stirring solution consisting of 2M HCl (15 mL), DCM (15 mL) and crushed ice. The solution was extracted with

DCM (3x). The organic layers were combined, dried over $NaSO_4$, filtrated, and concentrated *in vacuo*. Distillation at 70˚C yielded a clear oil (777 mg, 44%).

^{1}H-NMR ($CDCl_3$, 400 MHz)= δ 4.17 (p, 4H, CH_2), 3.86 (dq, 1H CHI), 2.00 (dd, 3H, CH_3), 1.35 (dt, 6H, $2CH_3$)

^{13}C-NMR ($CDCl_3$, 400 MHz)= δ 63.59, 21.91, 16.45, 8.20, 6.65

^{31}P-NMR ($CDCl_3$, 400 MHz)= δ +22.64 (s)

m/z (EI)= 291.97 (M+, 12.0%), 165.05 (38.9%), 137.07 (45.1%), 108.99 (100%), 80.95 (43.8%).

4.16. Synthesis of (*R*)-*tert*-butyl((2-(4,4-dibromobut-3-en-1-yl)-2,5,7,8-tetramethylchroman-6-yl)oxy)dimethylsilane (33)

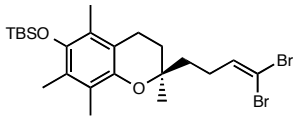

Carbon tetrabromide (301 mg, 0.91 mmol) was dissolved in dry DCM (0.9 mL) at -10˚C. PPh_3 (480mg, 1.8 mmol) (in 0.9mL dry DCM) was added drop-wise and stirred for 30 min. During addition of PPh_3, the clear solution turned bright yellow/orange in color. Drop-wise addition of (**21**) (171mg, 0.45 mmol) in dry DCM (1 mL) at -5˚C was allowed to stir for an additional 45 min. After this time, hexane was added at -5˚C and stirred for 15 min. During this time phosphonium oxide had precipitated out of solution. The mixture was washed with hexane, vacuum filtrated, and the filtrate

was concentrated *in vacuo*. Column chromatography with hexane → 9:1 hexane:EtOAc yielded clear oil which crystallized overnight to a white solid (191 mg, 79%). Mp 57-59˚C (last contacted solvent, hexane:EtOAc).

R_f= 0.35 (3.5% EtOAc in Hexane)

^{1}H-NMR ($CDCl_3$, 400 MHz)= δ 6.45 (t, J=7.2, 1H, =CH), 2.60 (t, 2H, CH_2) 2.89 (m, 2H, CH_2), 2.12 (s, 3H, $ArCH_3$), 2.11 (s, 3H, $ArCH_3$), 2.08 (s, 3H, $ArCH_3$), 1.80 (m, 3H, CH_2), 1.64 (m, 1H, CH_2), 1.28 (s, 3H, CH_3), 1.07 (s, 9H, $3CH_3$), 0.15 (s, 6H, $2CH_3$)

^{13}C-NMR ($CDCl_3$, 400 MHz)= δ 145.55, 144.35, 138.74, 88.70, 73.72, 37.08, 31.75, 27.67, 26.12, 23.65, 22.66, 20.78, 18.62, 14.34, 14.12, 13.40, 12.03, -3.30

m/z (ESI+)= ESI+ 557.0 (50.1%), 555.0 (100%), 535.0 (35.3%), 533.0 (M+H, 70.0%)

Combustion:

Element: C

Theory: 51.88; Found: 52.65

Element: H

Theory: 6.82; Found: 6.83

4.17. Synthesis of (*R*)-*tert*-butyldimethyl((2,5,7,8-tetramethyl-2-(pent-3-yn-1-yl)chroman-6-yl)oxy)silane (34)

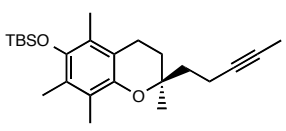

Dibromoolefin (**33**) (186 mg, 0.35 mmol) in dry THF (0.6 mL) was cooled to -78˚C and treated with *n*-BuLi (2M, 0.39mL, 0.79 mmol, 2.2 eq). This red/purple solution was stirred at -78˚C for 30 min before being warmed to 0˚C. After 45 min at 0˚C, the reaction turned a pale yellow/orange color. The solution was cooled back to -78˚C and MeI (0.1 mL, 1.5 mmol, 4.1 eq) was added dropwise. The mixture was warmed slowly from -78˚C to room temperature over 19 h, at which time the reaction had turned a darker orange color. The solution was diluted with aqueous NH_4Cl and extracted with EtOAc (3x). The combined organic layers were dried (anhydrous $NaSO_4$), filtered and concentrated *in vacuo*. The crude product was purified by flash chromatography with 20% EtOAc (in hexane) to yield a clear oil (126 mg, 92%).

R_f= 0.40 5:3 hexane:DCM

^{1}H-NMR ($CDCl_3$, 400 MHz)= δ 2.59 (t, *J*=6.4 Hz, 2H, CH_2), 2.31 (m, 2H, CH_2) 2.11 (s, 3H, $ArCH_3$) 2.08 (s, 3H, $ArCH_3$) 2.07 (s, 3H, $ArCH_3$), 1.82 (m, 4H, $2CH_2$), 1.79 (s, 3H, CH_3), 1.25 (s, 3H, CH_3), 1.07 (s, 9H, $3CH_3$), 0.14 (s, 6H, $2CH_3$)

^{13}CNMR ($CDCl_3$, 400 MHz)= δ 145.58, 144.25, 125.98, 123.58, 122.73, 117.25, 79.52, 75.24, 73.60, 38.88, 31.61, 26.11, 23.59, 20.75, 18.61, 14.32, 13.39, 12.99, 11.92, 3.46, -3.31

m/z (ESI+)= 387.2 (M+H, 100%), 388.3 (36.4%), 389.2 (8.7%)

Combustion:

Element: C

Theory: 74.55; Found: 74.85

Element: H

Theory: 9.91; Found 10.02

4.18. Synthesis of (2*E*,4*E*,6*E*)-9-((*R*)-6-((*tert*-butyldimethylsilyl)oxy)-2,5,7,8-tetramethylchroman-2-yl)-2,6-dimethylnona-2,4,6-trienal (36)

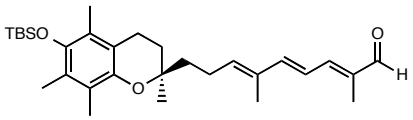

(a)

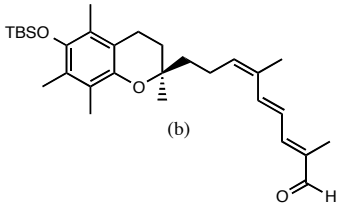

(b)

To an inseparable mixture of **30a** and **30b** (110 mg, 0.22 mmol), in dry DMF, was added tetrakis(triphenylphosphine)palladium(0) (12.4 mg, 5 mol%) and Cu(I)I (6.3 mg, 15 mol %) under an N_2 atmosphere at room temperature. To this solution was added (5) (123 mg, 0.29 mmol, 1.45 eq) dropwise. The reaction mixture soon turned yellow/black. This reaction mixture was allowed to stir at 50˚C for 19 h. After this time, H_2O (10 ml) was added and extracted with DCM (5x 15 ml). Column chromatography with 60:1 hexane:EtOAc (in 4% TEA) yielded (**32**) as a pale yellow oil (still a 2.2:1 E:Z mixture) (74 mg, 71%).

R_f= 0.54 (7:1.2 hexane:EtOAc)

^{1}H-NMR ($CDCl_3$, 400 MHz)= δ 9.48 (s, 0.65H, CHO)^a, 9.44 (s, 0.3H, CHO)^b, 6.90 (d, *J*= 10 Hz, 1H, CH)^{a,b}, 6.66 (d, *J*= 0.65H, CH)^a, 6.58 (d, 0.65H, CH)^a, 6.56 (m, 0.45H, CH)^b, 5.84 (m, 1H, CH)^{a,b}, 2.62 (t, 2H, CH_2)^{a,b}, 2.41 (t, 1H, CH_2)^b, 2.15 (s, 0.85H, CH_3)^b, 2.15

(s, 2.5H, $ArCH_3$)[a], 2.12 (s, 2.5H, $ArCH_3$)[a], 2.08 (s, 3H, $ArCH_3$)[a,b], 1.90 (s, 2.4H, CH_3)[a], 1.83 (s, 2.5, CH_3)[a], 1.81 (s, 0.85, CH_3)[b], 1.77 (m, 2H, CH_2)[a,b], 1.36 (s, 0.9H CH_3)[b], 1.29 (s, 2.4H, CH_3)[a], 1.07 (s, 9H, $3CH_3$)[a,b], 0.14 (s, 6H, $2CH_3$)[a,b]

^{13}C-NMR ($CDCl_3$, 400 MHz)= δ 194.78[a], 194.72[b], 149.88[a], 149.76[b], 146.66[a], 145.66[a], 145.55[b], 144.36[a], 144.28[b], 139.83[a], 139.77[b], 138.07[a], 136.55[a], 136.50[b], 134.11[a], 134.06[b], 126.08[a], 126.03[b], 123.70[a], 123.65[b], 122.67[a], 122.56[b], 121.04[a], 120.50[b], 117.32[a], 177.25[b], 73.99[a], 38.72[a], 38.23[b], 31.94[a], 31.80[b], 29.72[a], 29.38[b], 26.11[a], 23.74[a], 23.74[b], 23.53[a], 23.17[b], 20.84[a], 20.46[b], 18.62[a], 14.13[a], 14.13[b], 13.42[a], 12.16[a], 12.05[b], 11.99[a], 9.55[a], -3.31[a]

m/z (ESI+)= 483.3 (M+H, 89.5%) 505.3 (Na^+, 100%)

Combustion:

Element: C

Theory: 74.64; Found: 68.90

Element: H

Theory: 9.60; Found: 8.85

Degradation most likely a result of the sample being held up in customs for a month.

4.19. Synthesis of tributyl(3-methylbut-2-en-1-yl)phosphorane (37)

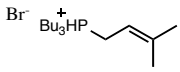

A mixture of tributyl phosphine (2 mL, 17.2 mmol) and 4-bromo-2-methyl-2-butene (4.25 mL, 17.2 mmol) in toluene (30 mL) was heated at reflux for 6 h. The reaction

mixture was concentrated *in vacuo*, and hexane (50 mL) was added to the solution and heated at reflux for an additional hour. The solution was allowed to cool to room temperature, filtered, and dried under vacuum to yield white/pale yellow crystals (5.15 g, 89%). Mp 62-64˚C (last contacted solvent→ hexane)

R_f= 0.6 (EtOAc:MeOH= 9:1)

^{1}H-NMR ($CDCl_3$, 400 MHz)= δ 5.04 (m, 1H, CH), 3.44 (q, 2H, CH_2), 2.46 (m, 6H, $2CH_3$), 1.82 (d, 6H, PCH_2), 1.55 (m, 12H, $6CH_2$), 0.99 (t, 9H, $3CH_3$)

^{13}C-NMR ($CDCl_3$, 400 MHz)= δ 109.08, 108.96, 24.01, 23.81, 23.75, 23.68, 19.19, 18.57, 13.41

m/z (EI)= 271 (M-Br, 100%)

4.20. Synthesis of *tert*-butyldimethyl(((*R*)-2,5,7,8-tetramethyl-2-((3*E*,5*E*,7*E*,9*E*)-4,8,12-trimethyltrideca-3,5,7,9,11-pentaen-1-yl)chroman-6-yl)oxy)silane (38)

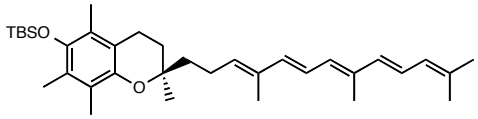

To a solution of phosphonium salt (**37**) (80.3 mg, 0.23 mmol, 1.5 eq) in dry THF (1.5 ml) was added *n*-BuLi (0.14 ml, 2M, 1.7 eq) at 0˚C. The resulting pale yellow solution was stirred 30 min under N_2. Aldehyde (**36**) (73.5 mg, 0.15 mmol) in THF (1.5 ml) was added dropwise to the stirring solution at -78˚C. The mixture was allowed to warm up to room temperature while stirring overnight. Water was added, followed by extraction with ethyl ether (4 x 15 ml). The combined organic extracts were

dried over $NaSO_4$, and concentrated. Purification on column chromatography (70:1 hexane: EtOAc) with 5% TEA afforded (**38**) as a yellow oil (20 mg, 26%).

R_f= 0.57 (50:1 Hex:EtOAc on 4% TEA deactivated TLC plates)

^{1}H-NMR ($CDCl_3$, 400 MHz)= δ 6.47 (dt, *J*= 14.8 Hz, 1.8H, =CH), 6.29 (s, 0.5H, =CH), 6.20 (m, 2.5H, =CH), 5.95 (d, *J*= 11.2 Hz, 0.7H, =CH), 5.83 (m, 0.3H, =CH), 5.56 (m, 1H, =CH), 2.59 (m, 2H, CH_2), 2.46 (m, 0.5H, CH_2), 2.34 (q, 1H, CH_2), 2.19 (s, 6H, $2CH_3$), 2.12 (s, 1H, $ArCH_3$), 2.12 (s, 2H, $ArCH_3$), 2.11 (s, 2H, $ArCH_3$), 2.07 (s, 3H $ArCH_3$), 2.05 (s, 0.5H, $ArCH_3$), 1.95 (s, 1H, CH_3), 1.86 (s, 0.5H, CH_3), 1.83 (s, 6H, $2CH_3$), 1.80 (s, 3H, CH_3), 1.72 (m, 3H, $2CH_2$), 1.61 (m, 1.5H, $2CH_2$), 1.36 (s, 1H, CH_3), 1.28 (s, 4H, $2CH_3$), 1.07 (s, 9H, $3CH_3$), 0.14 (s, 6H, $2CH_3$)

^{13}C-NMR ($CDCl_3$, 400 MHz)= δ 145.76, 144.19, 137.64, 135.28, 135.03, 134.92, 134.43, 133.52, 131.21, 126.01, 125.94, 124.20, 123.58, 122.94, 122.69, 117.39, 74.17, 46.20, 39.08, 31.64, 29.71, 26.11, 24.72, 23.77, 22.84, 20.60, 17.96, 14.33, 12.80, 11.96, 11.44, -3.31

m/z= Similar to that of the αT6, we witnessed degradation when attempting to perform ESI+ and a clean mass spectra was not obtainable.

4.21. Synthesis of (*R*,*E*)-*tert*-butyl((2-(4-iodobut-3-en-1-yl)-2,5,7,8-tetramethylchroman-6-yl)oxy)dimethylsilane (40)

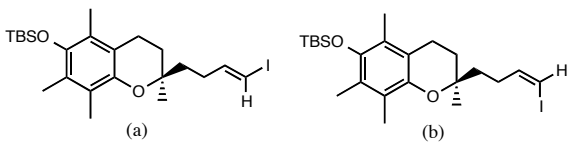

Iodoform (170 mg, 0.43 mmol, 2 eq) was placed in a 2-necked RBF. The RBF was transferred to the glove-box, where anhydrous $CrCl_2$ (185 mg, 1.5 mmol, 6 eq) was added. After removal from the glove-box, dry THF (2 mL) was added and the solution was allowed to stir at 0˚C for 20 min. To this red/brown colored solution, was added of (**21**) (80 mg, 0.21 mmol) in THF (1 mL), dropwise at 0˚C. The solution was allowed to stir for 2 h at 0˚C. After which time, the mixture was poured into H_2O (15 mL) and extracted with EtOAc (3x 15 ml). The combined organic extracts were dried over $NaSO_4$, and concentrated. Column chromatography in 60:1 hexane:EtOAc to 10:1, yielded 2.4:1 mixture of (**a**):(**b**) as a clear oil (73 mg, 69%).

R_f= 0.65 (50:1 hexane: EtOAc)

^{1}H-NMR ($CDCl_3$, 400 MHz)= δ 6.57 (dt, 0.5H, CH)^a, 6.20 (m, 0.5H, 2CH)^b, 6.04 (t, J= 1.2 Hz, 0.5H, CH)^a, 6.01 (t, J= 1.2Hz, 0.5H, CH)^a, 2.60 (t, 2H, CH_2)^{a,b}, 2.32 (q, 0.5H, CH_2)^b, 2.24 (q, 1.5H, CH_2)^a, 2.12 (s, 3H, $ArCH_3$)^{a,b}, 2.09 (s, 3H, $ArCH_3$)^{a,b}, 2.07 (s, 3H, $ArCH_3$)^{a,b}, 1.85 (m, 3H, $2CH_2$)^{a,b}, 1.64 (m, 1H, $2CH_2$)^{a,b}, 1.31 (s, 1H, CH_3)^b, 1.25 (s, 2H, CH_3)^a, 1.07 (s, 9H, $3CH_3$)^{a,b}, 0.14 (s, 6H, $2CH_3$)^{a,b}

^{13}C-NMR ($CDCl_3$, 400 MHz)= δ 146.6^a, 145.6^b, 144.3^a, 141.3^a, 126.0^a, 123.6^a, 122.8^a, 122.7^b, 117.3^b, 117.2^a, 82.4^b, 74.4^a, 73.9^b, 73.7^a, 38.0^a, 37.3^b, 31.8^a, 31.7^b, 30.4^a, 29.5^b, 26.1^a, 23.8^b, 23.7^a, 20.9^b, 20.8^a, 18.6^a, 14.3^a, 13.4^a, 12.1^a, 12.0^a, -3.3^a

m/z (ESI+)= 501.1 (M+H, 100%), 502.1 (30%), 503.2 (23%), 504.2 (7%)

4.22. Synthesis of *tert*-butyl(((2*S*)-2-(3-iodobutyl)-2,5,7,8-tetramethylchroman-6-yl)oxy)dimethylsilane (41)

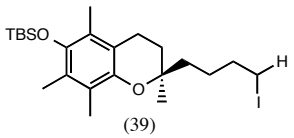

(39)

To a solution of (**40**) (73 mg of a 2.4:1 mixture of E:Z. Approximately, only 24 mg being *Z*-isomer, so calculations were based off this number) (24 mg, 0.05 mmol), and potassium azodicarboxylate (50 mg, 0.25 mmol, 5.2 eq) in dry THF:isopropanol (1:1) was added acetic acid (0.03 ml, 0.52 mmol, 10.4 eq) dropwise at room temperature, under N_2. This solution was allowed to stir an additional 23 h. After which time, the reaction was poured into water, and extracted with DCM (3x 10 ml). Column chromatography with 10:1 hexane:EtOAc yielded (**41**) (21 mg), and recovered (**40**) (47 mg). The ratio of *cis*:*trans* (**40**) remained the same- no selective reduction of *trans*-geometry.

R_f= 0.63 (50:1 hexane:EtOAc)

^{1}H-NMR ($CDCl_3$, 400 MHz)= δ 3.22 (t, 2H, CH_2I), 2.91 (t, 2H, CH_2), 2.12 (s, 3H, $ArCH_3$), 2.10 (s, 3H, $ArCH_3$), 2.07 (s, 3H, $ArCH_3$), 1.85 (m, 4H, $2CH_2$), 1.65 (m, 4H, $2CH_2$), 1.26 (s, 3H, CH_3), 1.07 (s, 9H, $3CH_3$), 0.14 (s, 6H, $2CH_3$)

^{13}C-NMR ($CDCl_3$, 400 MHz)= δ 145.72, 144.18, 125.97, 123.58, 122.70, 117.37, 74.18, 38.27, 33.81, 31.61, 29.71, 26.11, 23.79, 20.85, 18.62, 14.34, 13.41, 12.01, 7.12, -3.33

m/z (ESI+)= 505.2 (8%), 504.2 (32%), 503.2 (M+H, 100%)

5. References

1. Evans, H. M., Bishop, K. S. On the existence of a hitherto unrecognized dietary factor essential for reproduction. *Science* **56,** 650–1 (1922).

2. Wolf, G. The Discovery of the Antioxidant Function of Vitamin E: the contribution of Henry A. Mattill. *J. Nutr.* **135,** 363–366 (2005).

3. Jiang, Q., Christen, S., Shigenaga, M. K., Ames, B. N. gamma-tocopherol, the major form of vitamin E in the US diet, deserves more attention. *Am. J. Clin. Nutr.* **74,** 714–22 (2001).

4. Traber, M. G., Arai, H. Molecular mechanisms of vitamin E transport. *Annu. Rev. Nutr.* **19,** 343–55 (1999).

5. Wang, X., Quinn, P. J. Vitamin E and its function in membranes. *Prog. Lipid Res.* **38,** 309–336 (1999).

6. Brigelius-Flohe, R., Traber, M. G. Vitamin E: function and metabolism. *Faseb J* **13,** 1145–1155 (1999).

7. Nava, P. Cecchini, M., Chirico, S., Atkinson, J. Preparation of fluorescent tocopherols for use in protein binding and localization with the alpha-tocopherol transfer protein. *Bioorg. Med. Chem.* **14,** 3721–36 (2006).

8. Atkinson, J. K., Nava, P., Frahm, G., Curtis, V., Manor, D. Fluorescent tocopherols as probes of intervesicular transfer catalyzed by the α-tocopherol transfer protein. *Ann. N. Y. Acad. Sci.* **1031,** 324–327 (2004).

9. Blatt, D. H., Leonard, S. W., Traber, M. G. Vitamin E kinetics and the function of

tocopherol regulatory proteins. *Nutrition* **17,** 799–805 (2001).

10. McLaughlin, P. J., Weihrauch, J. L. Vitamin E content of foods. *J. Am. Diet. Assoc.* **75,** 647–65 (1979).

11. Wagner, K.H., Kamal-Eldin, A., Elmadfa, I. Gamma-tocopherol--an underestimated vitamin? *Ann. Nutr. Metab.* **48,** 169–88 (2004).

12. Germolec, D. R., McCary, C., Abdala-Valencia, H., Berdnikovs, S., Cook-Mills, J. M. Supplemental and highly elevated tocopherol doses differentially regulate allergic inflammation: reversibility of α-tocopherol and γ-tocopherol's effects. *J. Immunol.* **186,** 3674–85 (2011).

13. Clément, M., Bourre, J. M. Graded dietary levels of RRR-γ-tocopherol induce a marked increase in the concentrations of α- and γ-tocopherol in nervous tissues, heart, liver and muscle of vitamin-E-deficient rats. *Biochim. Biophys. Acta - Gen. Subj.* **1334,** 173–181 (1997).

14. Rasool, A. H. G., Yuen, K. H., Yusoff, K., Wong, A. R., Rahman, A. R. a. Dose dependent elevation of plasma tocotrienol levels and its effect on arterial compliance, plasma total antioxidant status, and lipid profile in healthy humans supplemented with tocotrienol rich vitamin E. *J. Nutr. Sci. Vitaminol. (Tokyo).* **52,** 473–478 (2006).

15. Butterfield, D. A., Castegna, A., Drake, J., Scapagnini, G., Calabrese, V. Vitamin E and neurodegenerative disorders associated with oxidative stress. *Nutr. Neurosci.* **5,** 229–239 (2002).

16. Bieri, J., Evarts, P. Gamma activity vitamin tocopherol: metabolism, and

significance in human E nutrition. *Am. J. Clin. Nutr.* **27,** 980–986 (1974).

17. Lim, Y., Traber, M. G. Alpha-tocopherol transfer protein (alpha-TTP): Insights from Alpha-Tocopherol Transfer Protein Knockout Mice. *Nutr. Res. Pract.* **1,** 247–53 (2007).

18. Simon, E. The metabolism of vitamin E. II. Purification and characterization of urinary metabolites of alpha-tocopherol. *J Biol Chem* **221,** 807–817 (1956).

19. Brigelius-Flohé, R. Kelly, FJ., Salonen, JT., Neuzil, J., Zingg, JM., Azzi, A. The European perspective on vitamin E: Current knowledge and future research. *American Journal of Clinical Nutrition* **76,** 703–716 (2002).

20. Shultz, M., Leist, M., Petrzika, M., Gassmann, B., Brigelius-Flohe, R. Novel urinary metabolite of alpha tocopherol, 2,5,7,8-tetramethyl-2(2'-carboxyethyl)-6-hydroxychroman, as an indicator of an adequate vitamin E supply? *Am. J. Clin. Nutr.* **62,** 1527–1534 (1995).

21. Wu, J. H., Croft, K. D. Vitamin E metabolism. *Molecular Aspects of Medicine* **28,** 437–452 (2007).

22. Parker, R. S., Sontag, T. J., Swanson, J. E. Cytochrome P4503A-dependent metabolism of tocopherols and inhibition by sesamin. *Biochem. Biophys. Res. Commun.* **277,** 531–4 (2000).

23. Preedy, V., Watson, R. . *The Encyclopedia of Vitamin E*. (CABI, 2007).

24. Schuelke, M. Elsner, A., Finckh, B., Kohlschutter, A., Hubner, C., Brigelius-Flohé, R. Urinary alpha-tocopherol metabolites in alpha-tocopherol transfer protein-deficient patients. *J. Lipid Res.* **41,** 1543–51 (2000).

25. Hentati, A., Deng, HX., Hung, WY., Nayer, M., Ahmed, MS., He, X., Tim, R., Stumpf, DA., Siddique, T. Human alpha-tocopherol transfer protein: gene structure and mutations in familial vitamin E deficiency. *Ann. Neurol.* **39,** 295–300 (1996).

26. Alex, G., Oliver, M. R., Collins, K. J. Ataxia with isolated vitamin E deficiency: A clinical, biochemical and genetic diagnosis. *J. Paediatr. Child Health* **36,** 515–516 (2000).

27. Meier, R., Tomizaki, T., Schulze-Briese, C., Baumann, U., Stocker, A. The molecular basis of vitamin E retention: Structure of human α-tocopherol transfer protein. *J. Mol. Biol.* **331,** 725–734 (2003).

28. Panagabko, C., Morley, S., Hernandez, M., Cassolato, P., Gordon, H., Parsons, R., Manor, D., Atkinson, J. Ligand specificity in the CRAL-TRIO protein family. *Biochemistry* **42,** 6467–6474 (2003).

29. Otzen, D. E., Rheinnecker, M., Fersht, R. Structural factors contributing to the hydrophobic effect: the partly exposed hydrophobic minicore in chymotrypsin inhibitor 2. *Biochemistry* **34,** 13051–8 (1995).

30. Traber, M. G., Atkinson, J. Vitamin E, antioxidant and nothing more. *Free Radic. Biol. Med.* **43,** 4–15 (2007).

31. Leonard, S. W., Terasawa, Y., Farese, R. V., Traber, M. G. Incorporation of deuterated RRR- or all-rac-α-tocopherol in plasma and tissues of α-tocopherol transfer protein-null mice. *Am. J. Clin. Nutr.* **75,** 555–560 (2002).

32. Litwack, G. *Vitamin E: Vitamins and Hormones*. (Academic Press, 2007).

33. Huang, H.-Y., Appel, L., Croft K., Miller, E., Moria, T., Puddey, I. Effects of vitamin C and vitamin E on in vivo lipid peroxidation: results of a randomized controlled trial. *Am. J. Clin. Nutr.* **76,** 549–555 (2002).

34. Schneider, C. An update on products and mechanisms of lipid peroxidation. *Molecular Nutrition and Food Research* **53,** 315–321 (2009).

35. Wagner, B. A., Buettner, G. R., Burns, C. P. Vitamin E slows the rate of free radical-mediated lipid peroxidation in cells. *Archives of Biochemistry and Biophysics* **334,** 261–267 (1996).

36. Niki, E., Yoshida, Y., Saito, Y., Noguchi, N. Lipid peroxidation: mechanisms, inhibition, and biological effects. *Biochemical and Biophysical Research Communications* **338,** 668–676 (2005).

37. Buettner, G. R. The pecking order of free radicals and antioxidants: lipid peroxidation, α-tocopherol, and ascorbate. *Archives of biochemistry and biophysics* **300,** 535–543 (1993).

38. Nimse, S. B., Pal, D. Free radicals, natural antioxidants, and their reaction mechanisms. *RSC Adv.* **5,** 27986–28006 (2015).

39. Shahidi, F., Zhong, Y. Novel antioxidants in food quality preservation and health promotion. *Eur. J. Lipid Sci. Technol.* **112,** 930–940 (2010).

40. Ginter, E., Simko, V., Panakova, V. Antioxidants in health and disease. *Bratislava Medical Journal.* **115,** 603–606 (2014).

41. Birben, E., Sahiner, U. M., Sackesen, C., Erzurum, S., Kalayci, O. Oxidative stress and antioxidant defense. *World Allergy Organ. J.* **5,** 9–19 (2012).

42. Yin, H., Xu, L., Porter, N. Free radical lipid peroxidation: mechanisms and analysis. *Chem. Rev.* **111,** 5944–5972 (2011).

43. Hogg, N., Kalyanaraman, B. Nitric oxide and lipid peroxidation. *Biochim. Biophys. Acta - Bioenerg.* **1411,** 378–384 (1999).

44. Sevanian, A., Hochstein, P. Mechanisms and consequences of lipid peroxidation in biological systems. *Ann. Rev. Nutr.* **5,** 365–390 (1985).

45. Blanksby, S. J., Ellison, G. B. Bond dissociation energies of organic molecules. *Acc Chem Res* **36,** 255–263 (2003).

46. Wagner, B., Buettner, G. R., Burns, C. P. Free radical-mediated lipid peroxidation in cells: oxidizability is a function of cell lipid bis-allylic hydrogen content. *Biochemistry* **33,** 4449–4453 (1994).

47. Pratt, D. A., Mills, J. H., Porter, N. A. Theoretical calculations of carbon-oxygen bond dissociation enthalpies of peroxyl radicals formed in the autoxidation of lipids. *J. Am. Chem. Soc.* **125,** 5801–5810 (2003).

48. Pratt, D. A., Tallman, K. A., Porter, N. A. Free radical oxidation of polyunsaturated lipids: New mechanistic insights and the development of peroxyl radical clocks. *Acc. Chem. Res.* **44,** 458–467 (2011).

49. Wang, X., Quinn, P. J. The location and function of vitamin E in membranes (review). *Mol. Membr. Biol.* **17,** 143–156 (2000).

50. Lemoyne, M., Van Gossum, A., Kurian, R., Jeejeebhoy, K. N. Plasma vitamin E and selenium and breath pentane in home parenteral nutrition patients. *Am. J. Clin. Nutr.* **48,** 1310–5 (1988).

51. Foti, M. C., Daquino, C., Mackie, I. D., DiLabio, G. A., Ingold, K. U. Reaction of phenols with the 2,2-diphenyl-1-picrylhydrazyl radical. Kinetics and DFT calculations applied to determine ArO-H bond dissociation enthalpies and reaction mechanism. *J. Org. Chem.* **73,** 9270–9282 (2008).

52. Bowry, V., Ingold, K. The unexpected role of vitamin E (alpha-tocopherol) in the peroxidation of human low-density lipoprotein. *Acc Chem Res* **32,** 27–34 (1999).

53. Upston, J. M., Terentis, A., Stocker, R. Tocopherol-mediated peroxidation of lipoproteins: implications for vitamin E as a potential antiatherogenic supplement. *FASEB J.* **13,** 977–94 (1999).

54. Packer, J. E., Slater, T. F., Willson, R. L. Direct observation of a free radical interaction between vitamin E and vitamin C. *Nature* **278,** 737–738 (1979).

55. Niki, E., Saito, T., Kawakami, A., Kamiya, Y. Inhibition of oxidation of methyl linoleate in solution by vitamin E and vitamin C. *J. Biol. Chem.* **259,** 4177–4182 (1984).

56. Mukai, K., Nishimura, M., Kikuchi, S. Stopped-flow investigation of the reaction of vitamin C with tocopheroxyl radical in aqueous Triton X-100 micellar solutions. The structure-activity relationship of the regeneration reaction of tocopherol by vitamin C. *J. Biol. Chem.* **266,** 274–278 (1991).

57. Burton, G. W., Doba, T., Gabe, E., Hughes, L., Lee, F.L., Prasad, L., Ingold, K.U. Autoxidation of biological molecules . 4 . maximizing the antioxidant activity of phenols. *J. Am. Chem. Soc.* **107,** 7053–7065 (1985).

58. Burton, G. W., Joyce, A., Ingold, K. U. Is vitamin E the only lipid-soluble, chain-breaking antioxidant in human blood plasma and erythrocyte membranes? *Arch. Biochem. Biophys.* **221,** 281–290 (1983).

59. Burton, G. W., Ingold, K. U. Autoxidation of biological molecules. 1. Antioxidant activity of vitamin E and related chain-breaking phenolic antioxidants in vitro. *J. Am. Chem. Soc.* **103,** 6472–6477 (1981).

60. Morley, S. Cross, V., Cecchini, M., Nava, P., Atkinson, J., Manor, D. Utility of a fluorescent vitamin E analogue as a probe for tocopherol transfer protein activity. *Biochemistry* **45,** 1075–1081 (2006).

61. Clegg, R. M. Fluorescence resonance energy transfer. *Curr. Opin. Biotechnol.* **6,** 103–110 (1995).

62. Morley, S. Cecchini, M., Zhang, W., Virgulti, A., Noy, N., Atkinson, J., Manor, D. Mechanisms of ligand transfer by the hepatic tocopherol transfer protein. *J. Biol. Chem.* **283,** 17797–17804 (2008).

63. West, R., Panagabko, C., Atkinson, J. Synthesis and characterization of BODIPY-α-tocopherol: A fluorescent form of vitamin E. *J. Org. Chem.* **75,** 2883–2892 (2010).

64. Chattopadhyay, A., London, E. Parallax method for direct measurement of membrane penetration depth utilizing fluorescence quenching by spin-labeled phospholipids. *Biochemistry* **26,** 39–45 (1987).

65. Ulrich, G., Ziessel, R., Harriman, A. The chemistry of fluorescent bodipy dyes: Versatility unsurpassed. *Angewandte Chemie - International Edition* **47,** 1184–

1201 (2008).

66. Drummen, G. P. C., Van Liebergen, L. C. M., Op den Kamp, J. A. F., Post, J. A. C11-BODIPY581/591, an oxidation-sensitive fluorescent lipid peroxidation probe: (Micro)spectroscopic characterization and validation of methodology. *Free Radic. Biol. Med.* **33,** 473–490 (2002).

67. Ghelfi, M., Ulatowski, L., Manor, D., Atkinson, J. Synthesis and characterization of a fluorescent probe for α-tocopherol suitable for fluorescence microscopy. *Bioorg. Med. Chem.* **24,** 2754–2761 (2016).

68. Palozza, P. Piccioni, E., Avanzi, L., Vertuani, S., Calviello, G., Manfredini, S. Design, synthesis, and antioxidant activity of FeAOX-6, a novel agent deriving from a molecular combination of the chromanyl and polyisoprenyl moieties. *Free Radic. Biol. Med.* **33,** 1724–1735 (2002).

69. Wang, Y., Panagabko, C., Atkinson, J. Synthesis of α-tocohexaenol (α-T6) a fluorescent, oxidatively sensitive polyene analogue of a-tocopherol. *Bioorganic Med. Chem.* **18,** 777–786 (2010).

70. Mehta, A. Ultraviolet-visible (uv-vis) spectroscopy- woodward-fieser rules to calculate wavelength of maximum absorption (lambda-max) of polyenes. Postet on May 13, 2013 in Analytical Chemistry, Notes.

71. Zincke, T., Heuser, G., Moller, W. Ueber Dinitrophenylpyridiniumchlorid und dessen Umwandlungsproducte. *Justus Liebigs Ann. Chem.* **2-3,** 296–335 (1903).

72. Becher, J., Finsen, L., Winckelmann, L. Derivatives and reactions of

glutaconaldehyde—XIII: Regiospecific ring opening of 3-substituted pyridines. *Tetrahedron.* **37**, 2375-2378 (1981).

73. Michels, T. D., Rhee, J. U., Vanderwal, C. D. Synthesis of delta-tributylstannyl-alpha, beta, gamma, delta-unsaturated aldehydes from pyridines. *Org. Lett.* **10,** 4787–4790 (2008).

74. Katritzky, A., Meth-Cohn, O., Rees, C. *comprehensive organic functional group transformations.* (Elseiver LTD., 1995).

75. Zhu, L., Mootoo, D. R. Synthesis of Nonadjacently Linked Tetrahydrofurans: An lodoetherification and Olefin Metathesis Approach. *Org. Lett.* **5,** 3475–3478 (2003).

76. Zhu, L., Mootoo, D. R. Synthesis of nonadjacently linked tetrahydrofurans: an iodoetherification and olefin metathesis approach. *Org. Lett.* **5,** 3475–3478 (2003).

77. Musolino, M. G., De Maio, P., Donato, A., Pietropaolo, R. Hydrogenation versus isomerization in α,β-unsaturated alcohols reactions over Pd/TiO2 catalysts. *J. Mol. Catal. A Chem.* **208,** 219–224 (2004).

78. EP1710239 A1. 6–7 (2006). European Patent, Mitsubishi Gas Chemical Company, Process for producing chroman compound

79. Waltherl, W., Vetter, W., Netscher, T. (S)- Trolox™ methyl ether: a powerful derivatizing reagent for the GC determination of the enantiomers of aliphatic alcohols. *Chimia (Aarau).* **45,** 121–123 (1991).

80. Ohnmacht, S., West, R., Simionescu, R., Atkinson, J. Assignment of the 1H and

13C NMR of tocotrienols. *Magn. Reson. Chem.* **46,** 287–294 (2008).

81. Ley, S. V. Ramarao, C., Lee, A., Ostergaard, N., Smith, S., Shirley, I. Microencapsulation of osmium tetroxide in polyurea. *Org. Lett.* **5,** 185–187 (2003).

82. Nicolaou, K. C., Adsool, V. A., Hale, C. R. H. An expedient procedure for the oxidative cleavage of olefinic bonds with $PhI(OAc)_2$, NMO, and Catalytic OsO_4. *Org. Lett.* **12,** 1552–1555 (2010).

83. Yang, D., Zhang, C. Ruthenium-catalyzed oxidative cleavage of olefins to aldehydes. *J. Org. Chem.* **66,** 4814–4818 (2001).

84. Miller, K. M., Huang, W.-S., Jamison, T. F. Catalytic asymmetric reductive coupling of alkynes and aldehydes: enantioselective synthesis of allylic alcohols and alpha-hydroxy ketones. *J. Am. Chem. Soc.* **125,** 3442–3 (2003).

85. Pappo, R., Allen, D. S., Lemieux, R. U., Johnson, W. S. Osmium tetroxide-catalyzed periodate oxidation of olefinic bonds. *J. Am. Chem. Soc.* **21,** 478–479 (1956).

86. Yu, W., Mei, Y., Kang, Y., Hua, Z., Jin, Z. Improved procedure for the oxidative cleavage of olefins by OsO_4-$NaIO_4$. *Org. Lett.* **6,** 3217–3219 (2004).

87. Criegee, R. Mechanism of Ozonolysis. *Angew. Chem. Int. Ed.* **14,** 745–752 (1975).

88. Wayne F., C., Larson, R. Products of ozonolysis of aromatic compounds in aqueous solution containing nitrite ion. *Ozone Sci. Eng.* **17,** 627–634 (2012).

89. Chen, J., Wang, T., Zhao, K. Preparation and use of 1-iodoalkyl ylides. *Tetrahedron Lett.* **35,** 2827–2828 (1994).

90. Horner, L., Hoffmann, H., Wippel, H. G. Phosphinoxyde als Olefinierungsreagenzien. *Chem. Ber.* **91,** 61–63 (1958).

91. Wadsworth, W. S., Emmons, W. D. The utility of phosphonate carbanions in olefin synthesis. *J. Am. Chem. Soc.* **83,** 1733–1738 (1961).

92. Lim, H. N., Parker, K. A. Total synthesis of the potent androgen receptor antagonist (-)-arabilin: A strategic, biomimetic [1,7]-hydrogen shift. *J. Am. Chem. Soc.* **133,** 20149–20151 (2011).

93. Iorga, B., Eymery, F., Savignac, P. Controlled monohalogenation of phosphonates. Part II. Preparation of pure diethyl α-monohalogenated alkylphosphonates. *Synthesis (Stuttg).* 576–580 (2000). doi:10.1055/s-2000-6375

94. Schlosser, M., Christmann, K. F. Trans-selective olefin syntheses. *Angew. Chem. Int. Ed. Engl.* **5,** 126 (1966).

95. Hodgson, D. M., Arif, T. Convergent and stereoselective synthesis of trisubstituted E-alkenyl bromides and iodides via β-oxido phosphonium ylides. *J. Am. Chem. Soc.* **130,** 16500–16501 (2008).

96. Corey, E. J., Fuchs, P. L. Synthetic method for conversion of formyl groups into ethynyl groups (RCHO --> RC --> CH or RC --> CR1). *Tetrahedron Lett.* 3769–3772 (1972).

97. Hart, D. W., Schwartz, J. Hydrozirconation. Organic synthesis via

organozirconium intermediates. Synthesis and rearrangement of alkylzirconium (IV) complexes and their reaction with. *J. Am. Chem. Soc.* **199,** 95–96 (1974).

98. Wailes, P. C., Weigold, H. Hydrido complexes of zirconium I. Preparation. *J. Organomet. Chem.* **24,** 405–411 (1970).

99. Wipf, P., Kendall, C. Hydrozirconation and its applications. *Top. Organomet. Chem.* **8,** 1–25 (2004).

100. Endo, J., Koga, N., Morokuma, K. Theoretical study on hydrozirconation. *Organometallics* **12,** 2777 (1993).

101. Schwartz, J., Labinger, J. Hydrozirconation: A new transition metal reagent for organic synthesis. *Angew. Chemie Int. Ed. English* **15,** 333–340 (1976).

102. Zhao, Y., Snieckus, V. A practical in situ generation of the schwartz reagent. reduction of tertiary amides to aldehydes and hydrozirconation. *Org. Lett.* **16,** 390–393 (2014).

103. Lipshutz, B. H., Keil, R., EIIsworth, E. L. A new method for the in situ generation of $Cp_2Zr(H)Cl$ (Schwartz' Reagent). *Tetrahedron Lett.* **31,** 7257–7260 (1990).

104. Negishi, E., Miller, J. A., Yoshida, T. Reaction of alkenes and dienes with t-butylmagnesium halides and zirconocene dihalides. A convenient procedure for hydrozirconation and a novel t-butylzirconation of conjugated alkenes. *Tetrahedron Lett.* **25,** 3407–3410 (1984).

105. Huang, Z., Negishi, E. I. A convenient and genuine equivalent to $HZrCp_2Cl$

generated in situ from $ZrCp_2Cl_2$-DIBAL-H. *Org. Lett.* **8,** 3675–3678 (2006).

106. Cordovilla, C., Bartolomé, C., Martínez-Ilarduya, J. M., Espinet, P. The Stille reaction, 38 years later. *ACS Catalysis* **5,** 3040–3053 (2015).

107. Stille, J. K. The palladium-catalyzed cross-coupling reactions of organotin reagents with organic electrophiles. *Angew. Chemie* **25,** 508–524 (1986).

108. Azarian, D., Dua, S. S., Eaborn, C., Walton, D. R. M. Reactions of organic halides with R3 MMR3 compounds (M = Si, Ge, Sn) in the presence of tetrakis(triarylphosphine)palladium. *J. Organomet. Chem.* **117,** (1976).

109. Kosugi, M., Sasazawa, K., Shimizu, Y., Migita, T. Reactions of allyltin compounds Iii. Allylation of aromatic halides With allyltributyltin in the presence of tetrakis(triphenylphosphine)palladium(O). *Chem. Lett.* 301–302 (1977).

110. Mee, S. P. H., Lee, V., Baldwin, J. E. Stille coupling made easier - The synergic effect of copper(I) salts and the fluoride ion. *Angew. Chemie - Int. Ed.* **43,** 1132–1136 (2004).

111. Akoh, C. C., Min, D. B. *Food Lipids: Chemistry, Nutrition, and Biotechnology*. (Marcel Dekker, Inc, 2002).

112. Kramer, J., Cruz-Hernandez, C., Deng, Z., Zhou, J., Jahreis, G., Dugan, M. Analysis of conjugated linoleic acid and trans 18 : 1 isomers in synthetic and animal products. *Am. J. Clin. Nutr.* **79,** 1137S–1145S (2004).

113. Vedejs, E., Marth, C. F. Mechanism of the Wittig reaction: the role of substituents at phosphorus. *Sect. Title Organomet. Organometalloidal Compd.*

110, 3948–3958 (1988).

114. Vedejs, E., Marth, C. F. Mechanism of Wittig reaction: evidence against betaine intermediates. *J. Am. Chem. Soc.* **112,** 3905–3909 (1990).

115. Foundation, N. S., Tamura, R., Saegusa, K., Kakihana, M., Academy, D. Stereoselective E and Z- olefin formation by Wittig olefination of aldehydes with allylic phosphorus ylides. *J. Org. Chem* **728,** 2723–2728 (1988).

116. Ingold, K. U., Burton, G. W., Foster, D. O., Hughes, L. Is methyl-branching in α-tocopherol's 'tail' important for its in vivo activity? Rat curative myopathy bioassay measurements of the vitamin E activity of three 2RS-n-alkyl-2,5,7,8-tetramethyl-6-hydroxychromans. *Free Radic. Biol. Med.* **9,** 205–210 (1990).

117. Takai, K., Nitta, K., Utimoto, K. Simple and selective method for aldehydes (RCHO) to (E)-haloalkenes (RCH:CHX) conversion by means of a haloform-chromous chloride system. *J. Am. Chem. Soc.* **108,** 7408–7410 (1986).

118. Kürti, L., Czakó, B. *Strategic applications of named reactions in organic synthesis: background and detailed mechanisms*. *Reactions* (2005).

119. Spears, L. G., Hutchinson, J. S. Classical dynamics of trans-diimide: Intramolecular vibrational relaxation involving an active torsion. *J. Chem. Phys.* **88,** 240 (1988).

120. Buszek, K. R., Brown, N. Improved method for the diimide reduction of multiple bonds on solid-supported substrates. *J. Org. Chem.* **72,** 3125–3128 (2007).

121. Tamelen, E., Dewey, R. S., Timmons, R. J. The reduction of olefins by means of

azodicarboxylic acid in situ. *J. Am. Chem. Soc.* **83,** 3725–3726 (1961).

122. Hünig, S., Müller, H.-R., Thier, W. Reduktionen mit diimid. *Tetrahedron Lett.* **2,** 353–357 (1961).

123. Makosza, M., Jagusztyn-Grochowska, M., Ludwikow, M., Jawdosiuk, M. Reactions of organic anions-L. Reactions of phenylacetonitrile derivatives with aromatic nitrocompounds in basic media. *Tetrahedron* **30,** 3723–3735 (1974).

124. Zaidlewicz, M., Wolan, A., Budny, M. *Comprehensive Organic Synthesis: Reduction*; *hydrometallation of C=C and C≡C bonds*. 877-963. (Elseiver LTD., 1991).

125. Corey, E. J. Stereospecific chemical synthesis of juvenile hormones Stereospecific chemical synthesis. *Bull. la société Entomol. suisse* **44,** 87–96 (1971).

126. Shi, J., Le Maguer, M. *Lycopene in tomatoes: chemical and physical properties affected by food processing. Critical reviews in biotechnology* **20,** (2000).

127. Yan, R., Bian, C., Yu, X. Total synthesis of herbimycin A. *Org. Lett.* **16,** 3280–3283 (2014).

128. Zurwerra, D., Gertsch, J., Altmann, K. H. Synthesis of (-)-dactylolide and 13-desmethylene-(-)-dactylolide and their effects on tubulin. *Org. Lett.* **12,** 2302–2305 (2010).

129. Asano, M., Inoue, M., Katoh, T. Enantioselective synthesis of the tricyclic core

of GKK1032, novel antibiotic anti-tumor agents, by employing an intramolecular Diels-Alder cycloaddition strategy. *Synlett* **1,** 1539–1542 (2005).

VITA

Andrew D. Hildering was born in St. Thomas, Ontario on March 12, 1992. He graduated from London District Christian Secondary School in June 2010. Proceeding high school, he attended the University of Toronto from September 2010- April 2011 for a degree in biochemistry. In 2011, he transferred to Brock University. In 2015, he obtained a double major in chemistry and biology and in 2016 he completed his MSc in organic chemistry.

Appendix

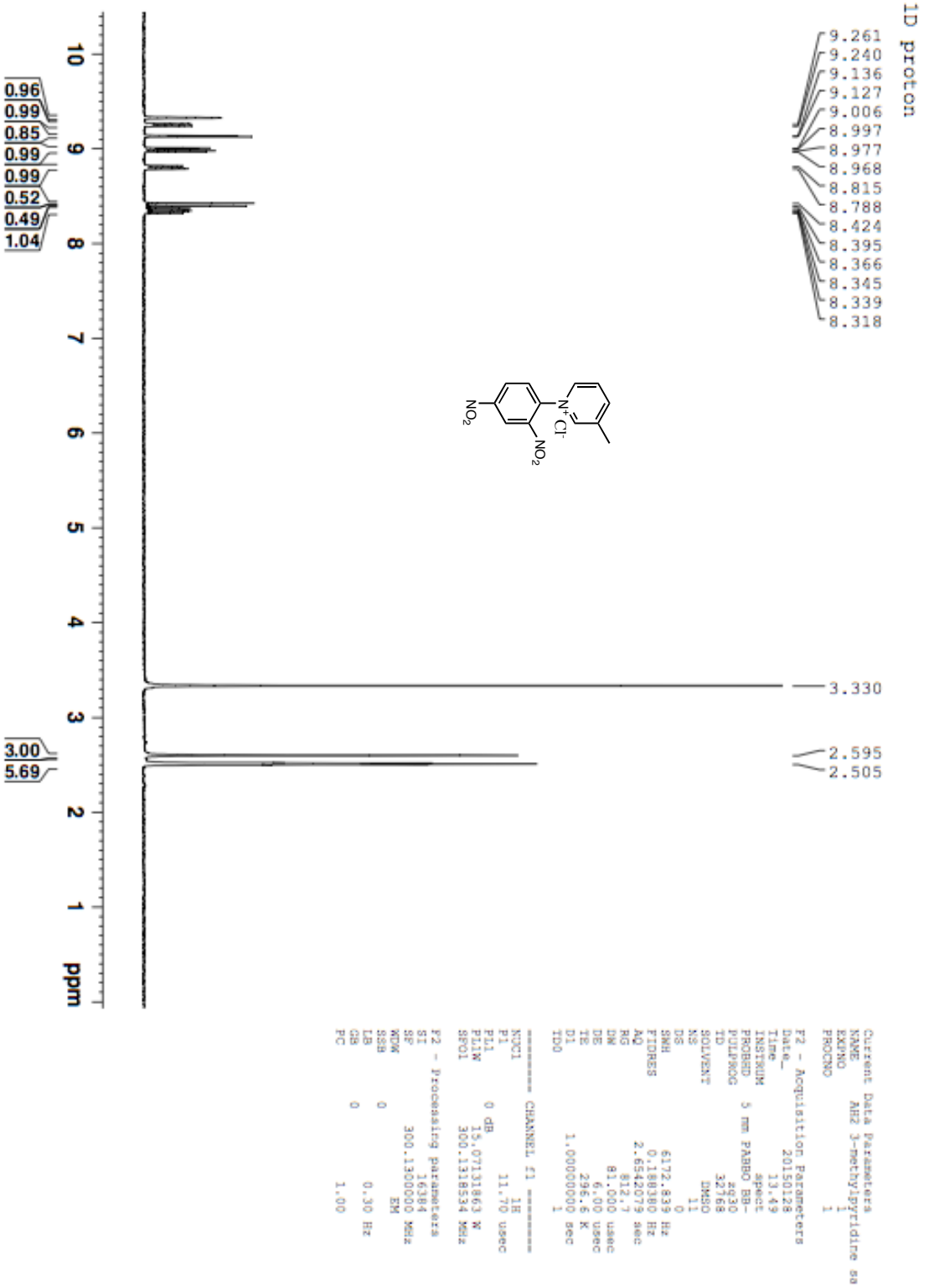
1D proton
9.261
9.240
9.136
9.127
9.006
8.997
8.977
8.968
8.815
8.788
8.424
8.395
8.366
8.345
8.339
8.318
3.330
2.595
2.505
0.96
0.99
0.85
0.99
0.99
0.52
0.49
1.04
3.00
5.69
ppm

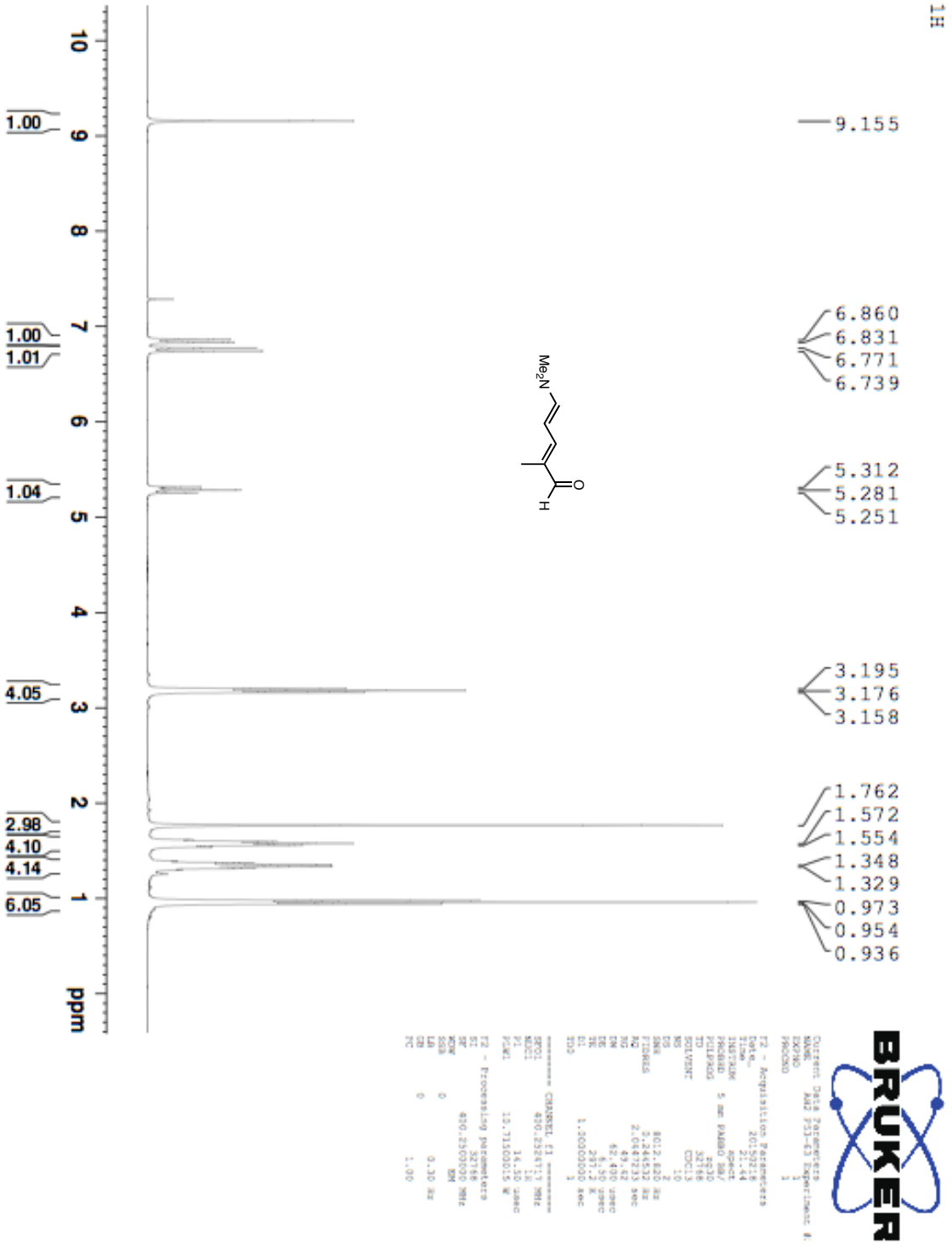
1H
9.155
6.860
6.831
6.771
6.739
5.312
5.281
5.251
3.195
3.176
3.158
1.762
1.572
1.554
1.348
1.329
0.973
0.954
0.936
1.00
1.00
1.01
1.04
4.05
2.98
4.10
4.14
6.05
ppm
Me2N
O
H
BRUKER

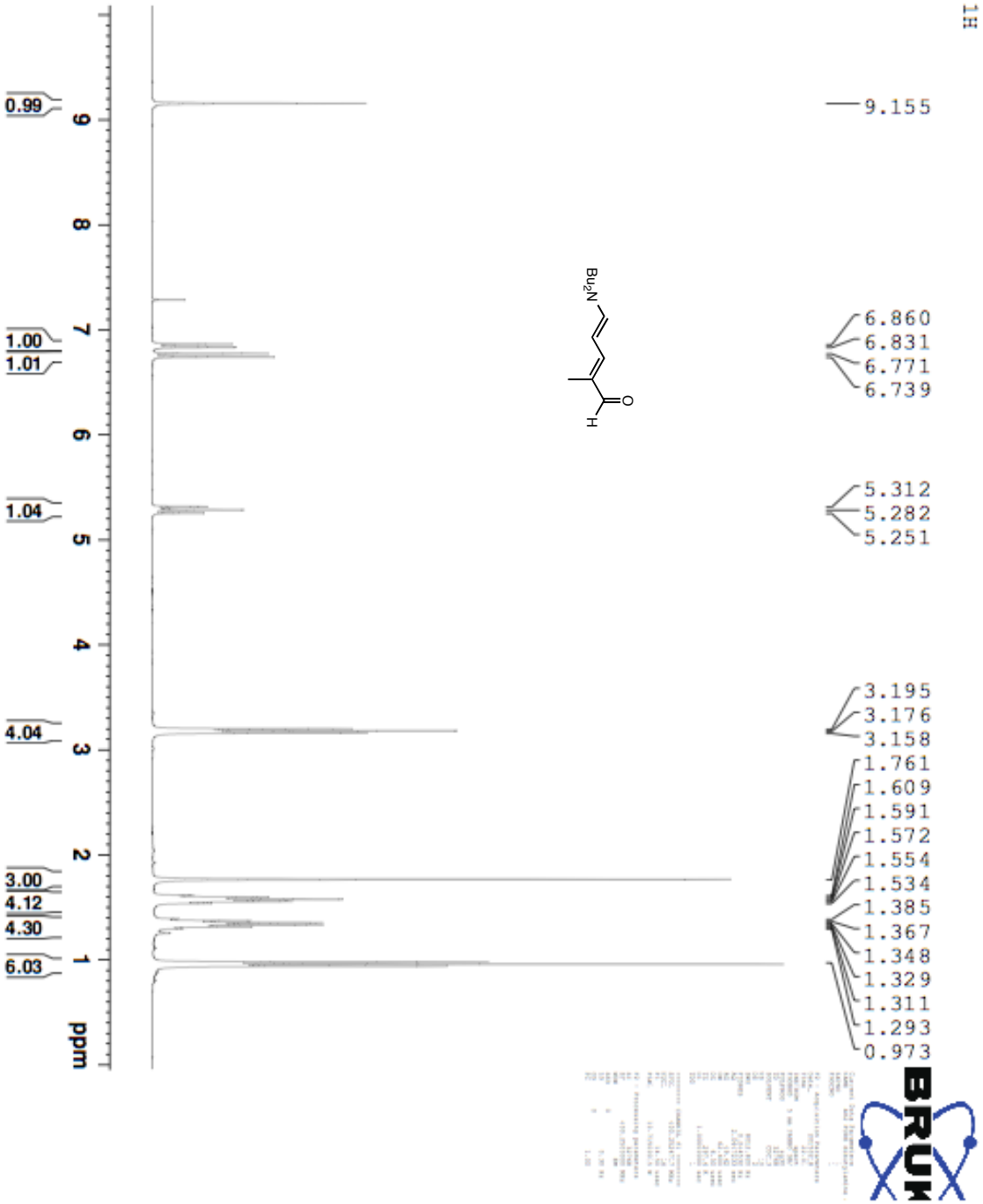
1H
9.155
6.860
6.831
6.771
6.739
5.312
5.282
5.251
3.195
3.176
3.158
1.761
1.609
1.591
1.572
1.554
1.534
1.385
1.367
1.348
1.329
1.311
1.293
0.973
0.99
1.00
1.01
1.04
4.04
3.00
4.12
4.30
6.03
ppm
Bu2N
O
H
BRUK

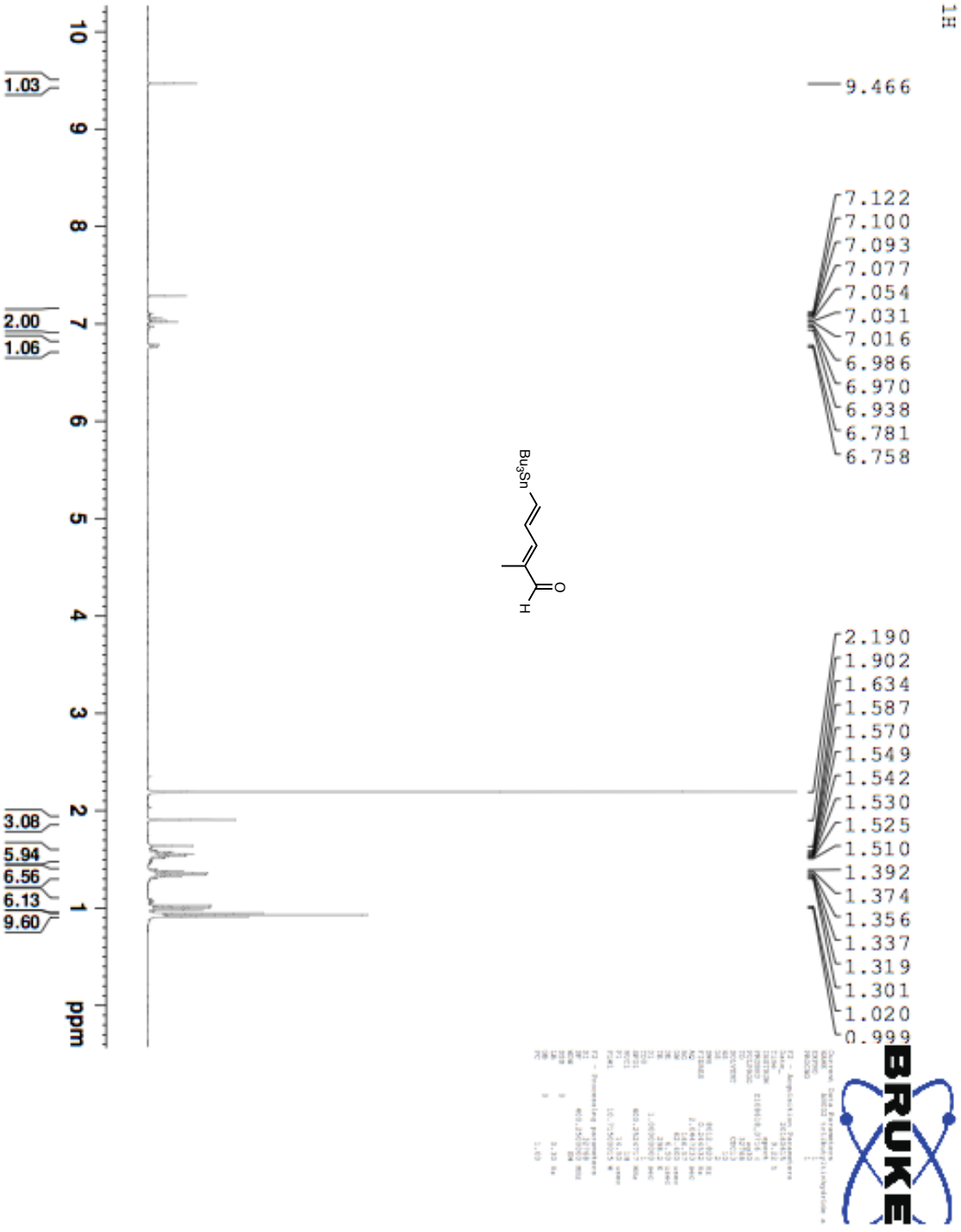
1H
9.466
7.122
7.100
7.093
7.077
7.054
7.031
7.016
6.986
6.970
6.938
6.781
6.758
2.190
1.902
1.634
1.587
1.570
1.549
1.542
1.530
1.525
1.510
1.392
1.374
1.356
1.337
1.319
1.301
1.020
0.999
1.03
2.00
1.06
3.08
5.94
6.56
6.13
9.60
ppm
Bu3Sn
O
H
BRUKER

1H

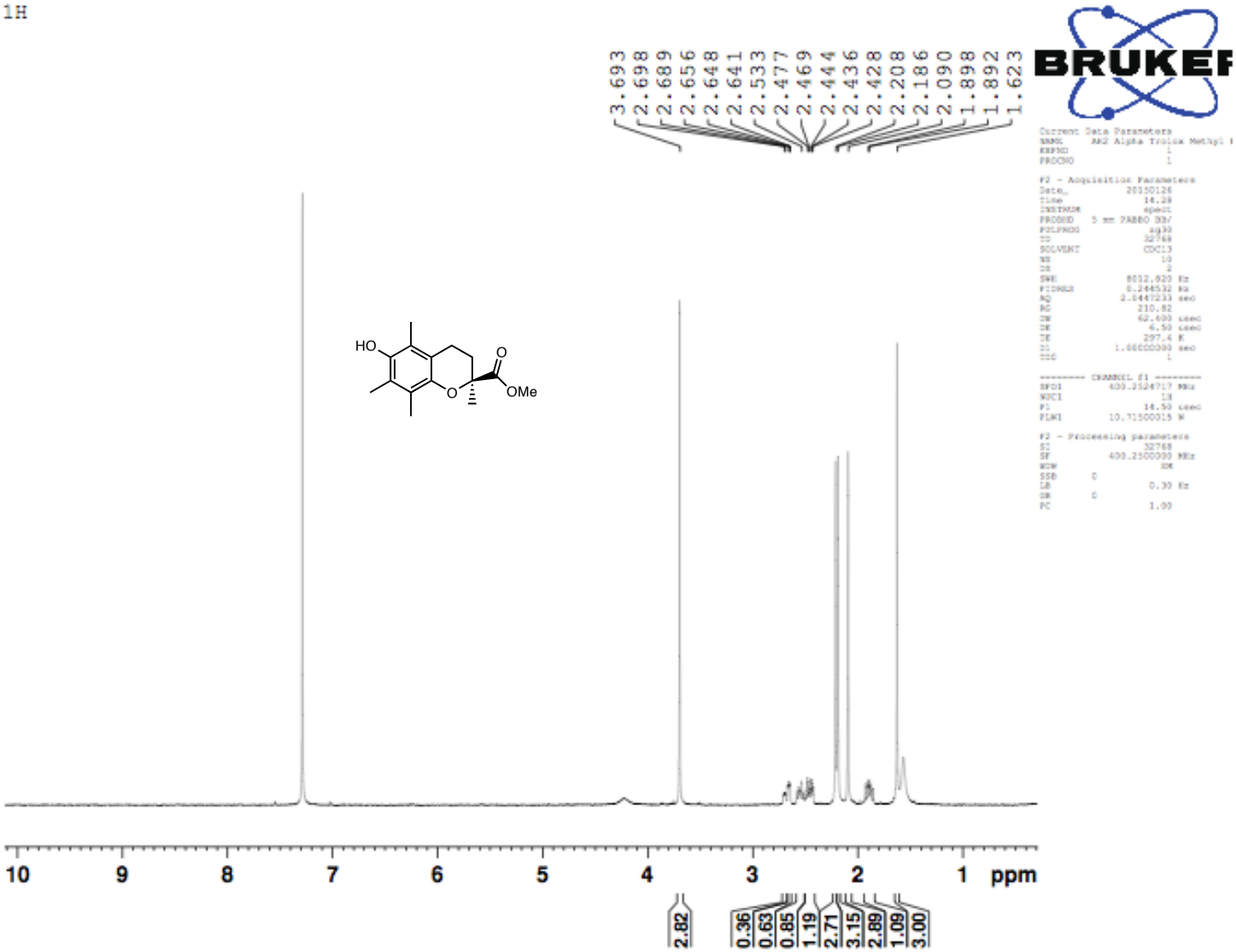
3.693
2.698
2.689
2.656
2.648
2.641
2.533
2.477
2.469
2.444
2.436
2.428
2.208
2.186
2.090
1.898
1.892
1.623
BRUKER
HO
O
O
OMe
10
9
8
7
6
5
4
3
2
1
ppm
2.82
0.36
0.63
0.85
1.19
2.71
3.15
2.89
1.09
3.00

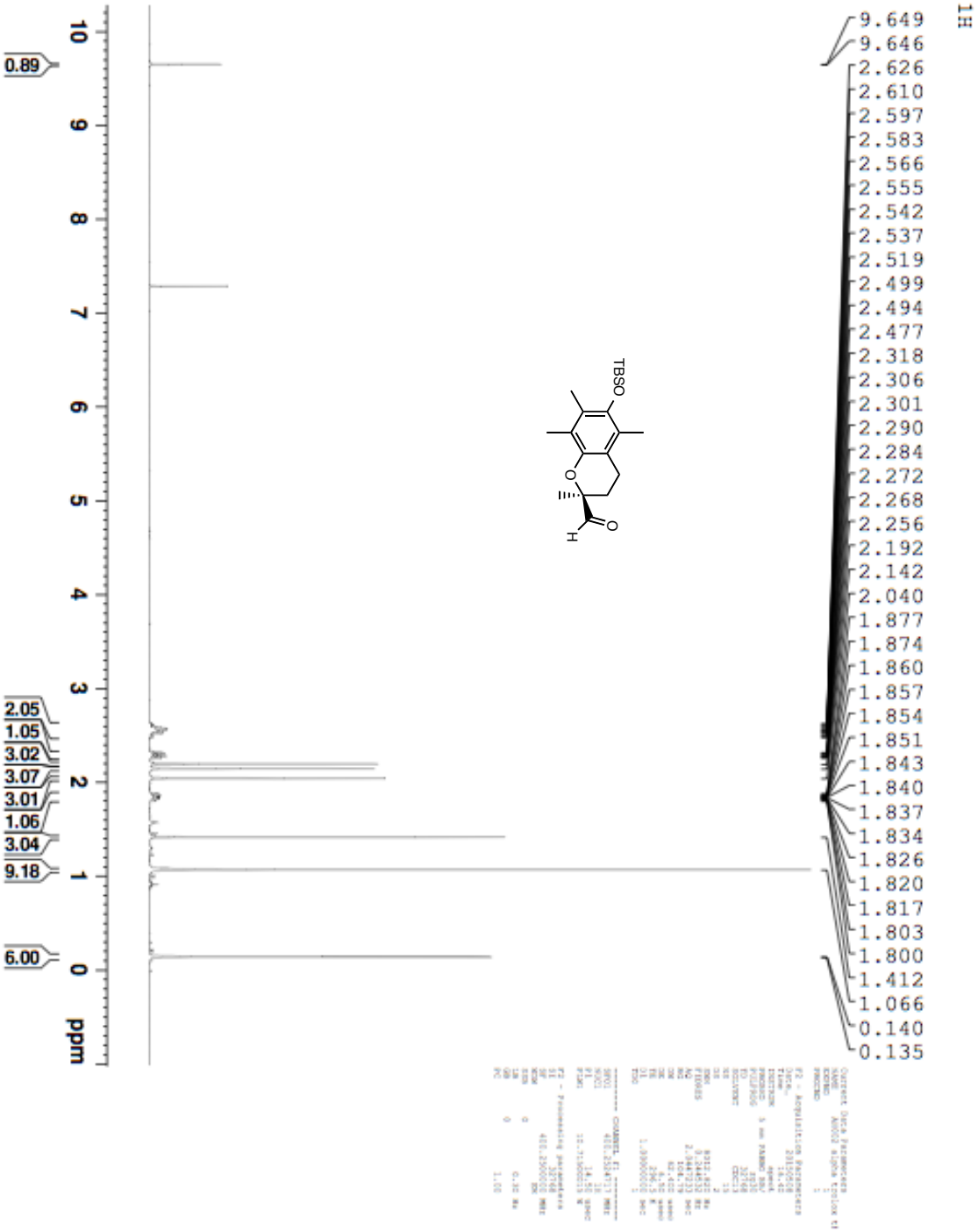
1H
9.649
9.646
2.626
2.610
2.597
2.583
2.566
2.555
2.542
2.537
2.519
2.499
2.494
2.477
2.318
2.306
2.301
2.290
2.284
2.272
2.268
2.256
2.192
2.142
2.040
1.877
1.874
1.860
1.857
1.854
1.851
1.843
1.840
1.837
1.834
1.826
1.820
1.817
1.803
1.800
1.412
1.066
0.140
0.135
TBSO
O
O
H
0.89
2.05
1.05
3.02
3.07
3.01
1.06
3.04
9.18
6.00
10
9
8
7
6
5
4
3
2
1
0
ppm

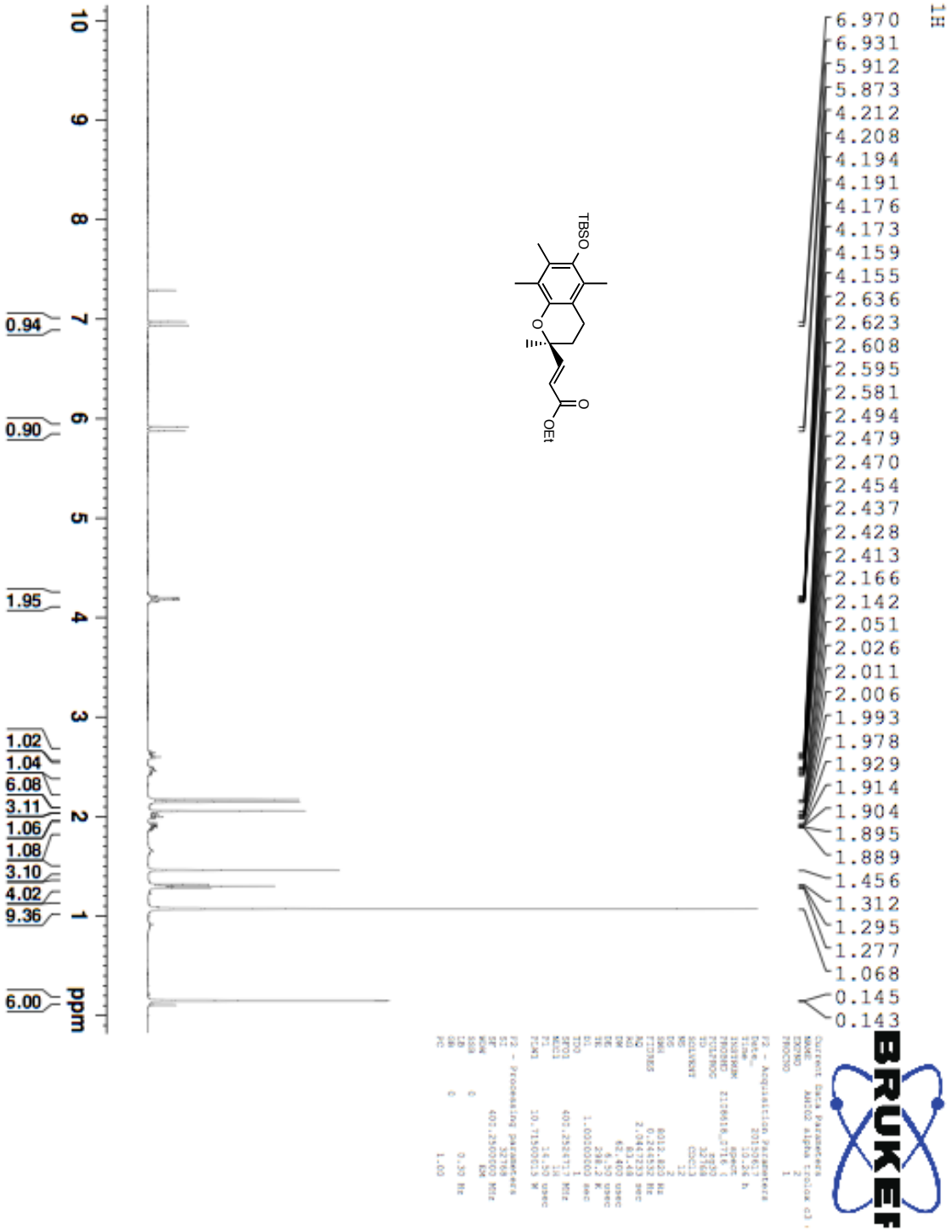
1H
6.970
6.931
5.912
5.873
4.212
4.208
4.194
4.191
4.176
4.173
4.159
4.155
2.636
2.623
2.608
2.595
2.581
2.494
2.479
2.470
2.454
2.437
2.428
2.413
2.166
2.142
2.051
2.026
2.011
2.006
1.993
1.978
1.929
1.914
1.904
1.895
1.889
1.456
1.312
1.295
1.277
1.068
0.145
0.143
TBSO
O
OEt
0.94
0.90
1.95
1.02
1.04
6.08
3.11
1.06
1.08
3.10
4.02
9.36
6.00
10
9
8
7
6
5
4
3
2
1
ppm
BRUKER

1H

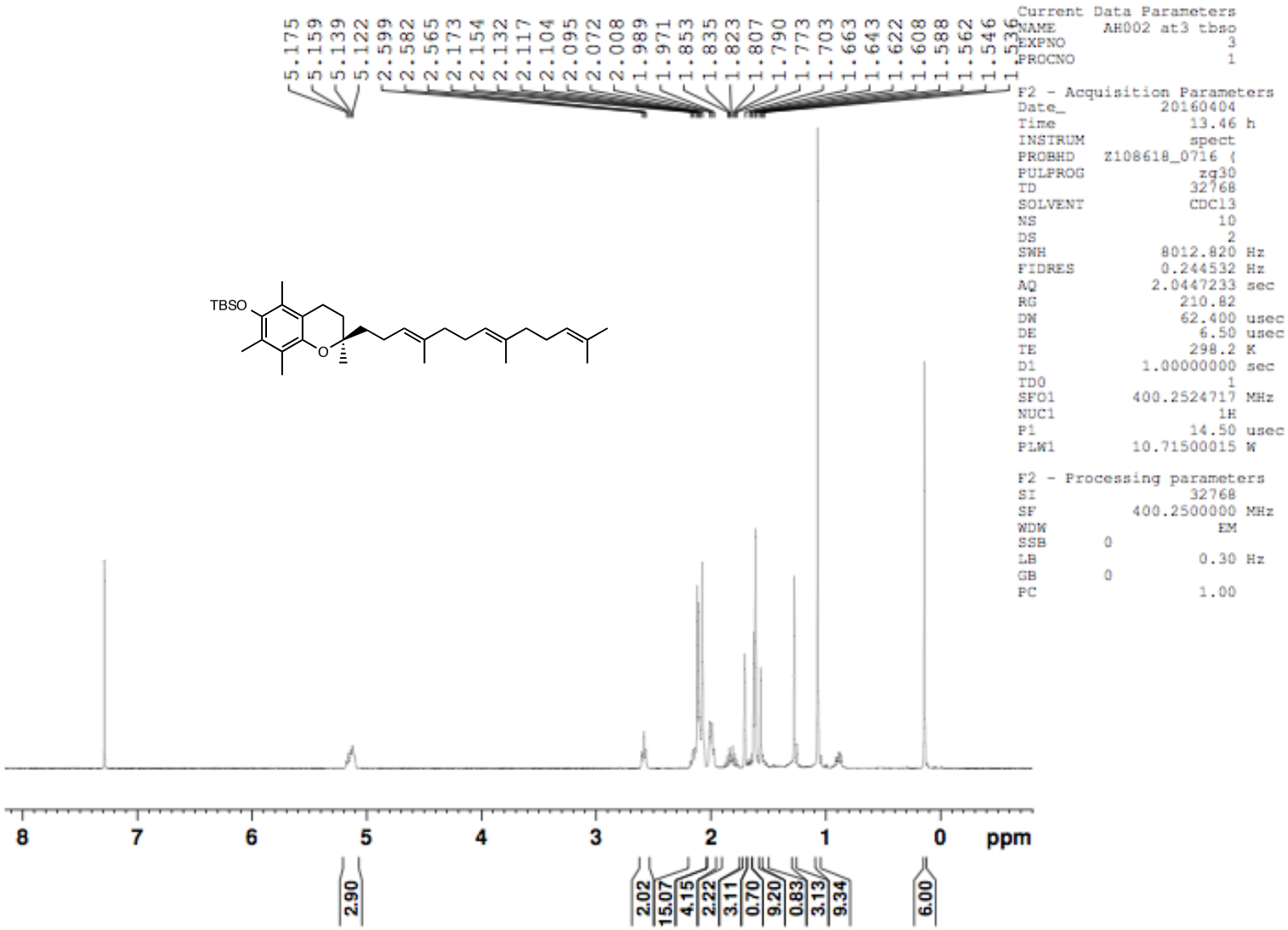


```
Current Data Parameters
NAME      AH002 at3 tbso
EXPNO                  3
PROCNO                 1

F2 - Acquisition Parameters
Date_           20160404
Time              13.46 h
INSTRUM            spect
PROBHD    Z108618_0716 (
PULPROG             zg30
TD                 32768
SOLVENT            CDCl3
NS                    10
DS                     2
SWH             8012.820 Hz
FIDRES          0.244532 Hz
AQ              2.0447233 sec
RG                210.82
DW                62.400 usec
DE                 6.50 usec
TE                298.2 K
D1             1.00000000 sec
TD0                    1
SFO1          400.2524717 MHz
NUC1                  1H
P1                14.50 usec
PLW1          10.71500015 W

F2 - Processing parameters
SI                 32768
SF            400.2500000 MHz
WDW                   EM
SSB       0
LB                0.30 Hz
GB        0
PC                1.00
```

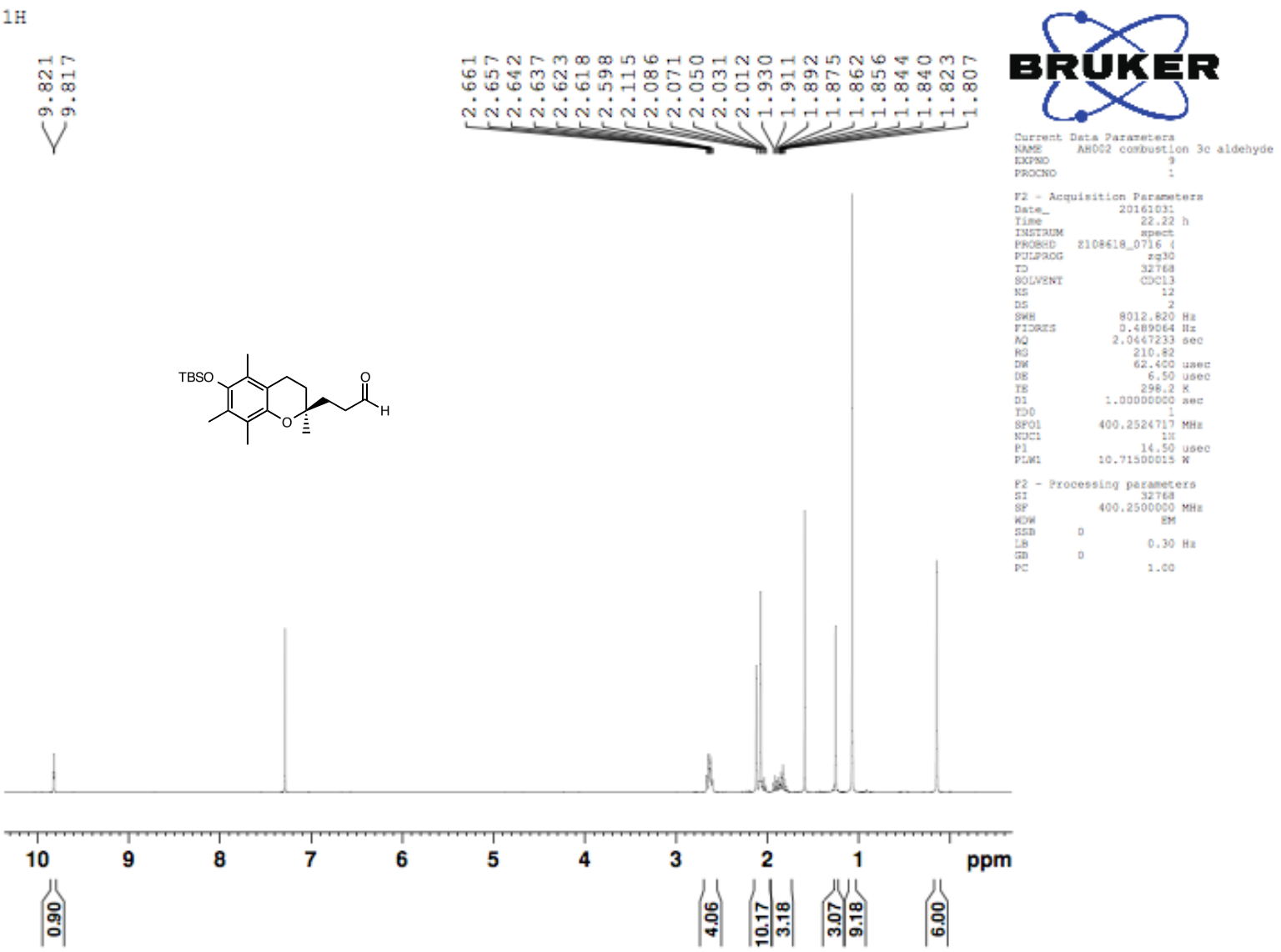
1H
9.821
9.817
2.661
2.657
2.642
2.637
2.623
2.618
2.598
2.115
2.086
2.071
2.050
2.031
2.012
1.930
1.911
1.892
1.875
1.862
1.856
1.844
1.840
1.823
1.807
BRUKER
Current Data Parameters
NAME AH002 combustion 3c aldehyde
EXPNO 9
PROCNO 1
F2 - Acquisition Parameters
Date_ 20161031
Time 22.22 h
INSTRUM spect
PROBHD Z108618_0716 (
PULPROG zg30
TD 32768
SOLVENT CDCl3
NS 12
DS 2
SWH 8012.820 Hz
FIDRES 0.489064 Hz
AQ 2.0447233 sec
RG 210.82
DW 62.400 usec
DE 6.50 usec
TE 298.2 K
D1 1.00000000 sec
TD0 1
SFO1 400.2524717 MHz
NUC1 1H
P1 14.50 usec
PLW1 10.71500015 W
F2 - Processing parameters
SI 32768
SF 400.2500000 MHz
WDW EM
SSB 0
LB 0.30 Hz
GB 0
PC 1.00
TBSO
O
H
O
10
9
8
7
6
5
4
3
2
1
ppm
0.90
4.06
10.17
3.18
3.07
9.18
6.00

1D proton

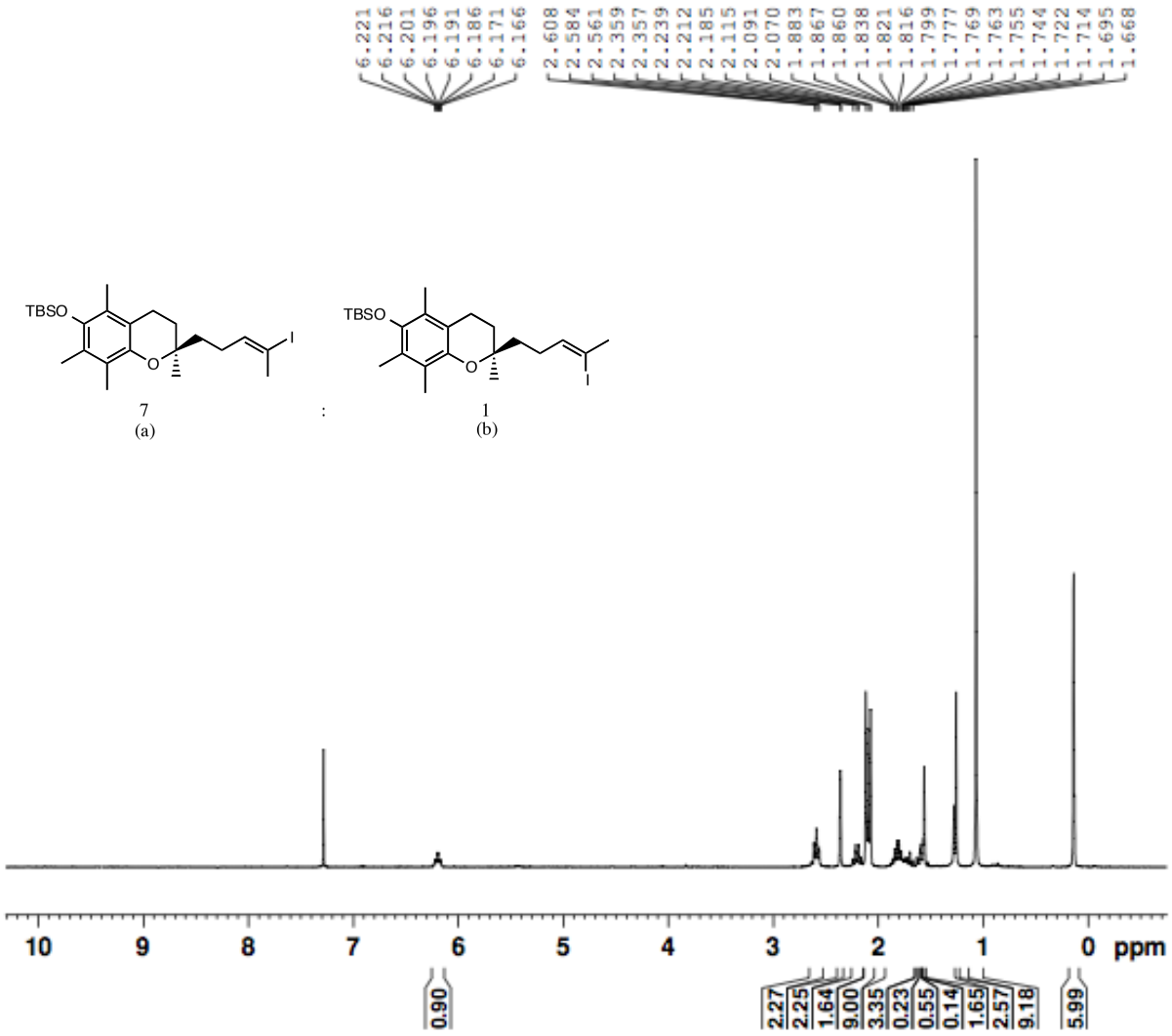

7 : 1

(a) (b)

```
Current Data Parameters
NAME      AK002 8mg vinylic iod!
EXPNO                  3
PROCNO                 1

F2 - Acquisition Parameters
Date_            20160124
Time                11.08
INSTRUM             spect
PROBHD    5 mm PABBO BB-
PULPROG             zg30
TD                 32768
SOLVENT            CDCl3
NS                    16
DS                     0
SWH              6172.839 Hz
FIDRES           0.188380 Hz
AQ               2.6542079 sec
RG                   512
DW                81.000 usec
DE                 6.00 usec
TE                298.2 K
D1             1.00000000 sec
TD0                    1

======== CHANNEL f1 ========
NUC1                  1H
P1                 11.70 usec
PL1       0 dB
PL1W        15.07131863 W
SFO1       300.1318534 MHz

F2 - Processing parameters
SI                 16384
SF            300.1300000 MHz
WDW                   EM
SSB       0
LB                 0.30 Hz
GB        0
PC                 1.00
```

2D-COSY

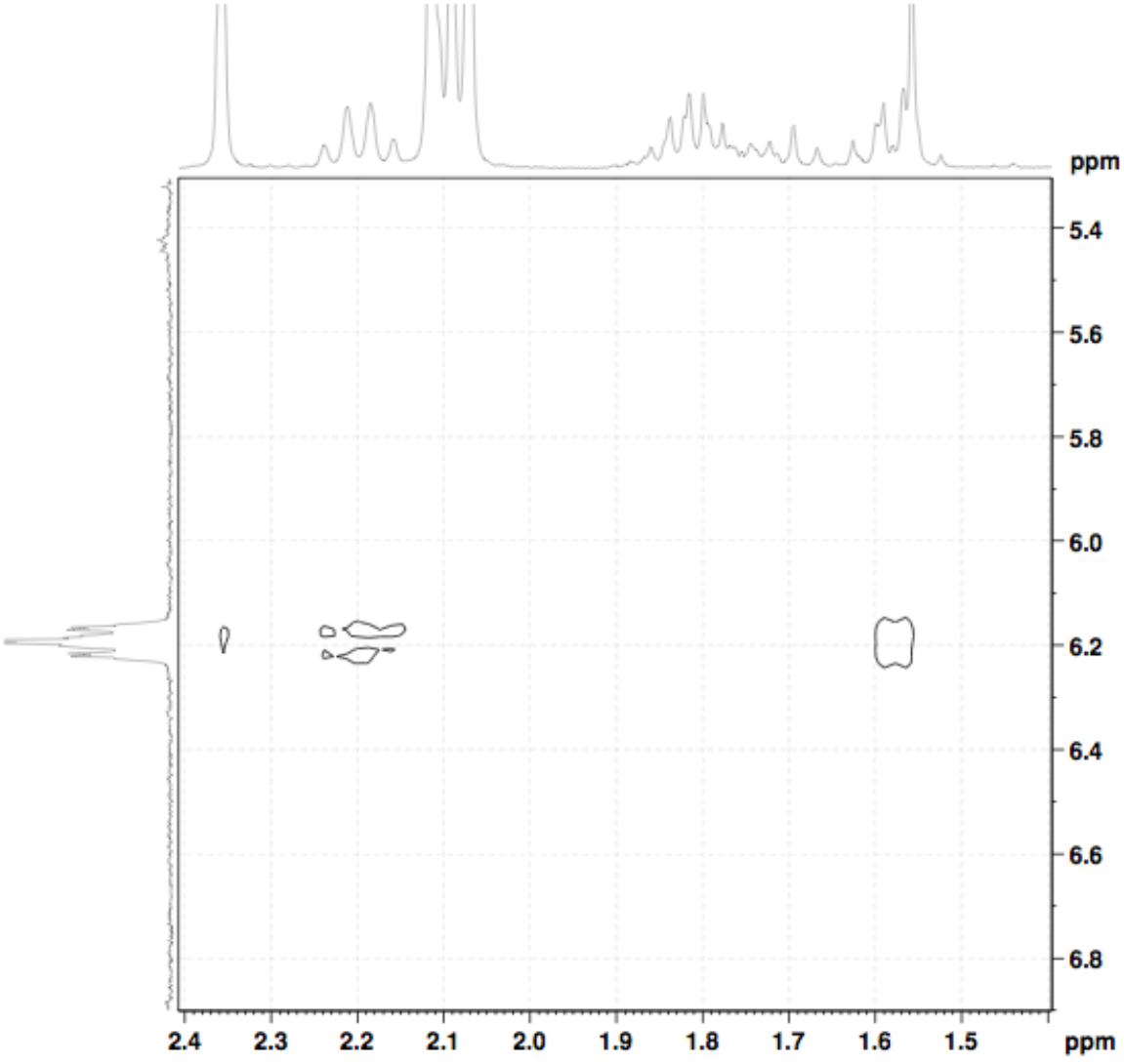
ppm
5.4
5.6
5.8
6.0
6.2
6.4
6.6
6.8
2.4
2.3
2.2
2.1
2.0
1.9
1.8
1.7
1.6
1.5
ppm

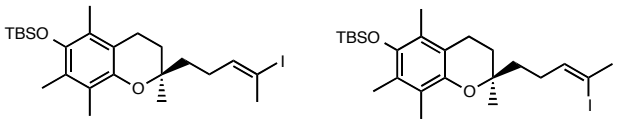
TBSO
O
I
TBSO
O
I

2 (a) : 1 (b)

2D-HMBC

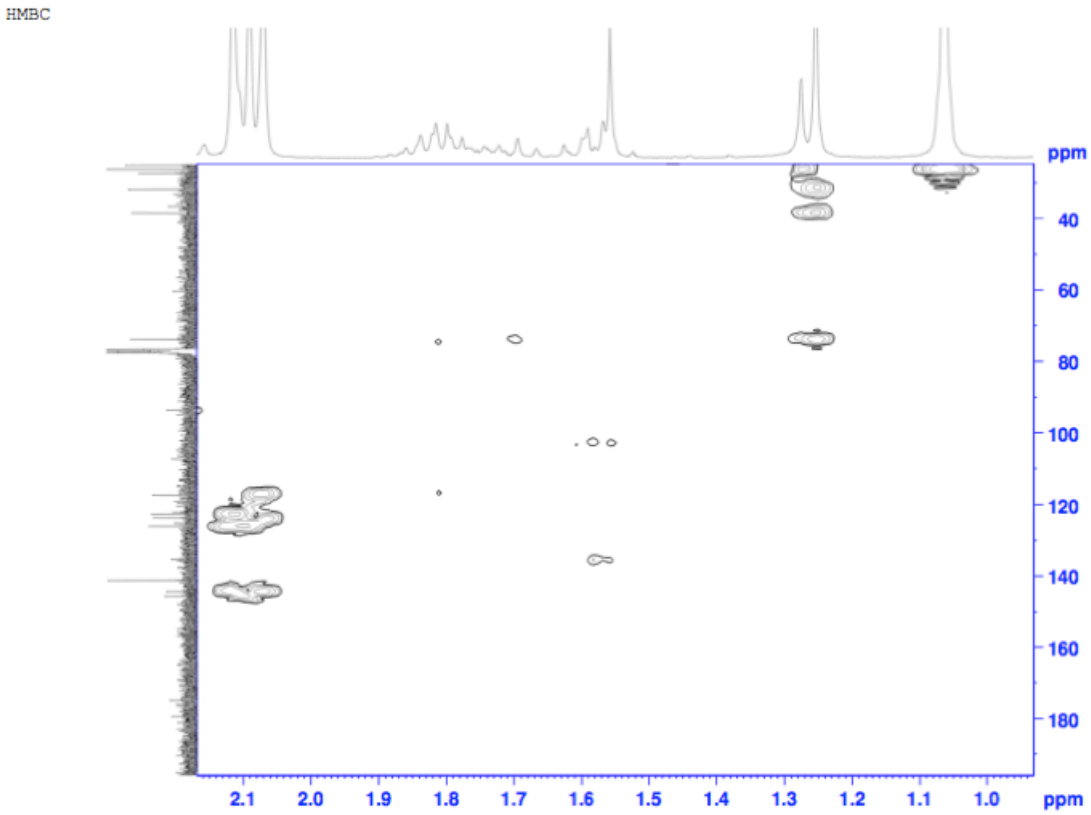
HMBC
ppm
40
60
80
100
120
140
160
180
2.1
2.0
1.9
1.8
1.7
1.6
1.5
1.4
1.3
1.2
1.1
1.0
ppm

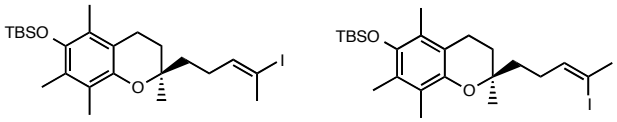
TBSO
O
I
TBSO
O
I

2 (a) : 1 (b)

H-13C HSQC

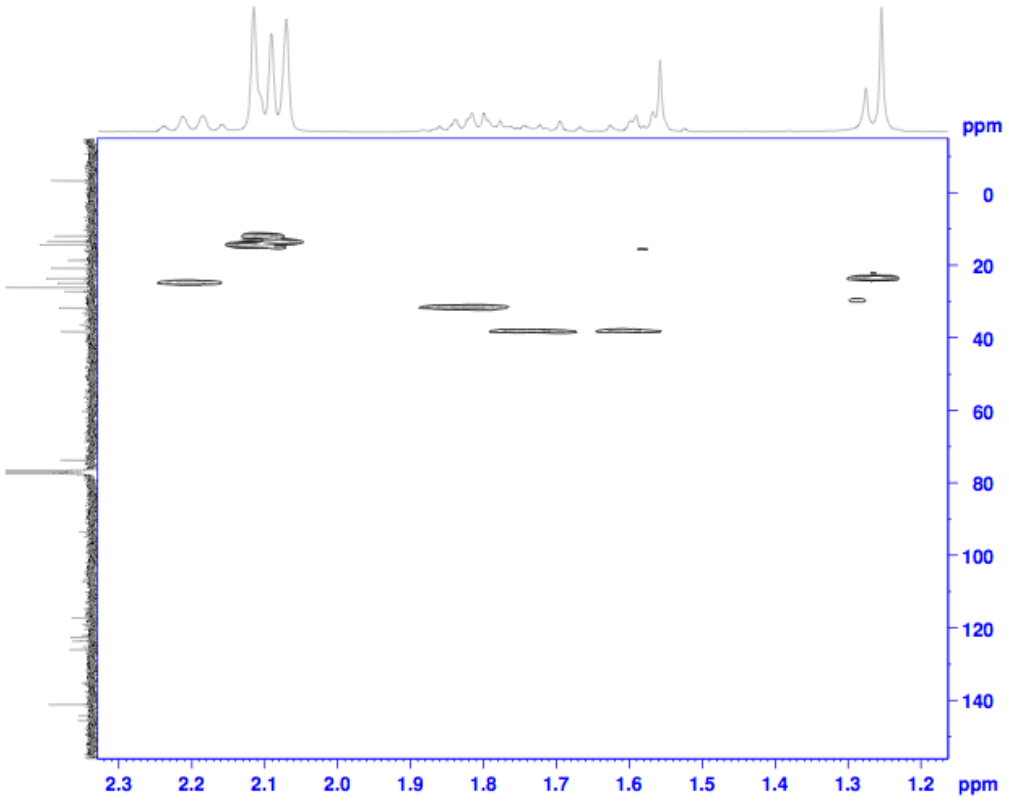

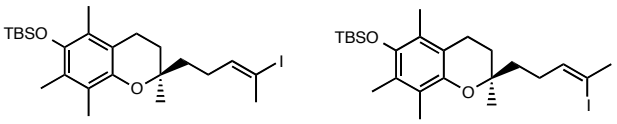

2 : 1

(a) (b)

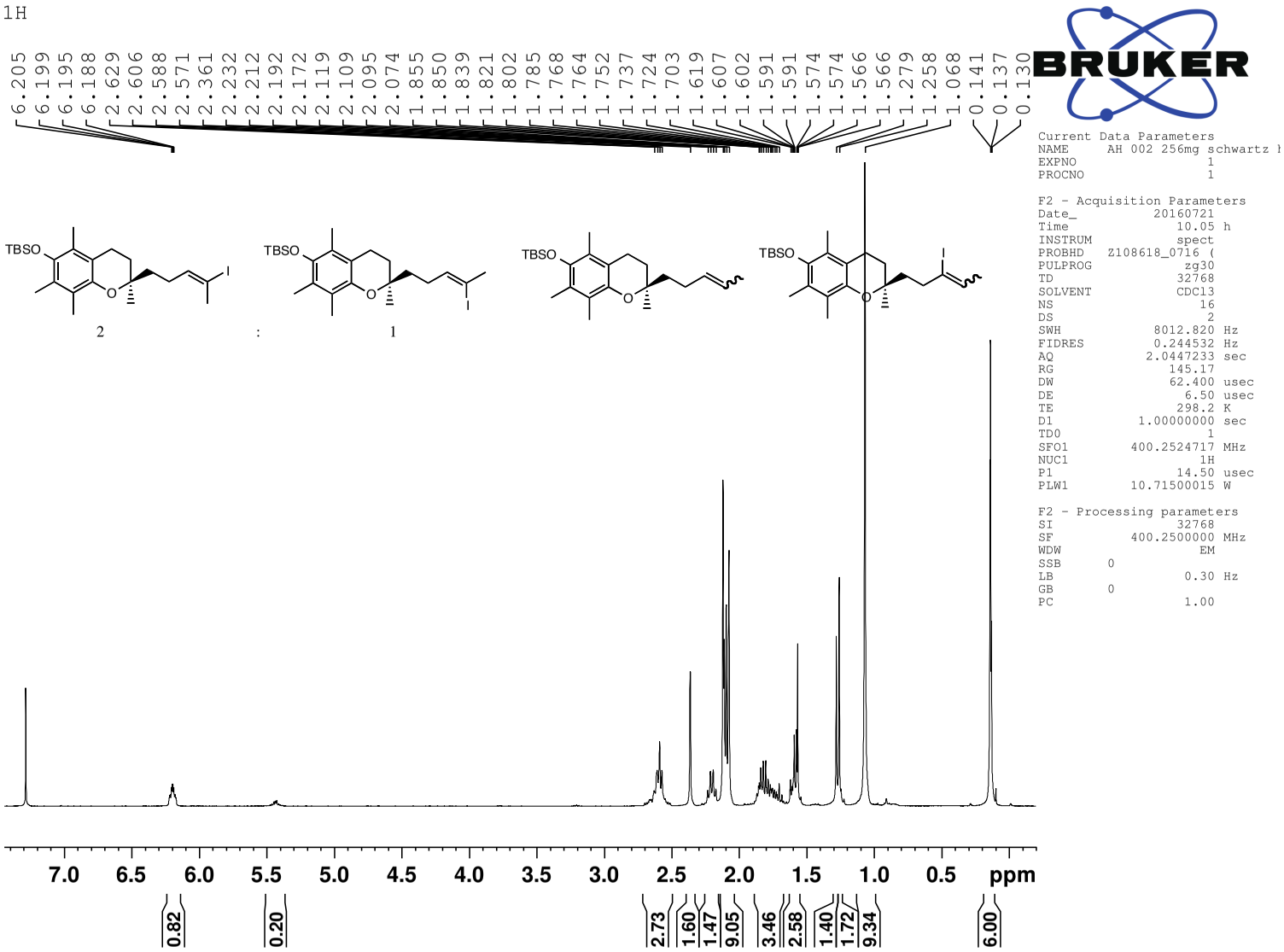

BRUKER

```
Current Data Parameters
NAME      AH 002 256mg schwartz h
EXPNO                   1
PROCNO                  1

F2 - Acquisition Parameters
Date_           20160721
Time              10.05 h
INSTRUM             spect
PROBHD   Z108618_0716 (
PULPROG             zg30
TD                 32768
SOLVENT             CDCl3
NS                    16
DS                     2
SWH              8012.820 Hz
FIDRES           0.244532 Hz
AQ               2.0447233 sec
RG                145.17
DW                62.400 usec
DE                 6.50 usec
TE                298.2 K
D1             1.00000000 sec
TD0                    1
SFO1          400.2524717 MHz
NUC1                  1H
P1                14.50 usec
PLW1          10.71500015 W

F2 - Processing parameters
SI                 32768
SF            400.2500000 MHz
WDW                   EM
SSB       0
LB                 0.30 Hz
GB        0
PC                 1.00
```

1H
4.232
4.214
4.196
4.179
4.176
4.161
4.158
3.890
3.871
3.865
3.846
2.029
2.011
1.987
1.968
1.368
1.363
1.350
1.345
1.332
1.328
0.151
0.121
4.00
1.00
3.17
6.07
0.09
ppm
BRUKER

1H

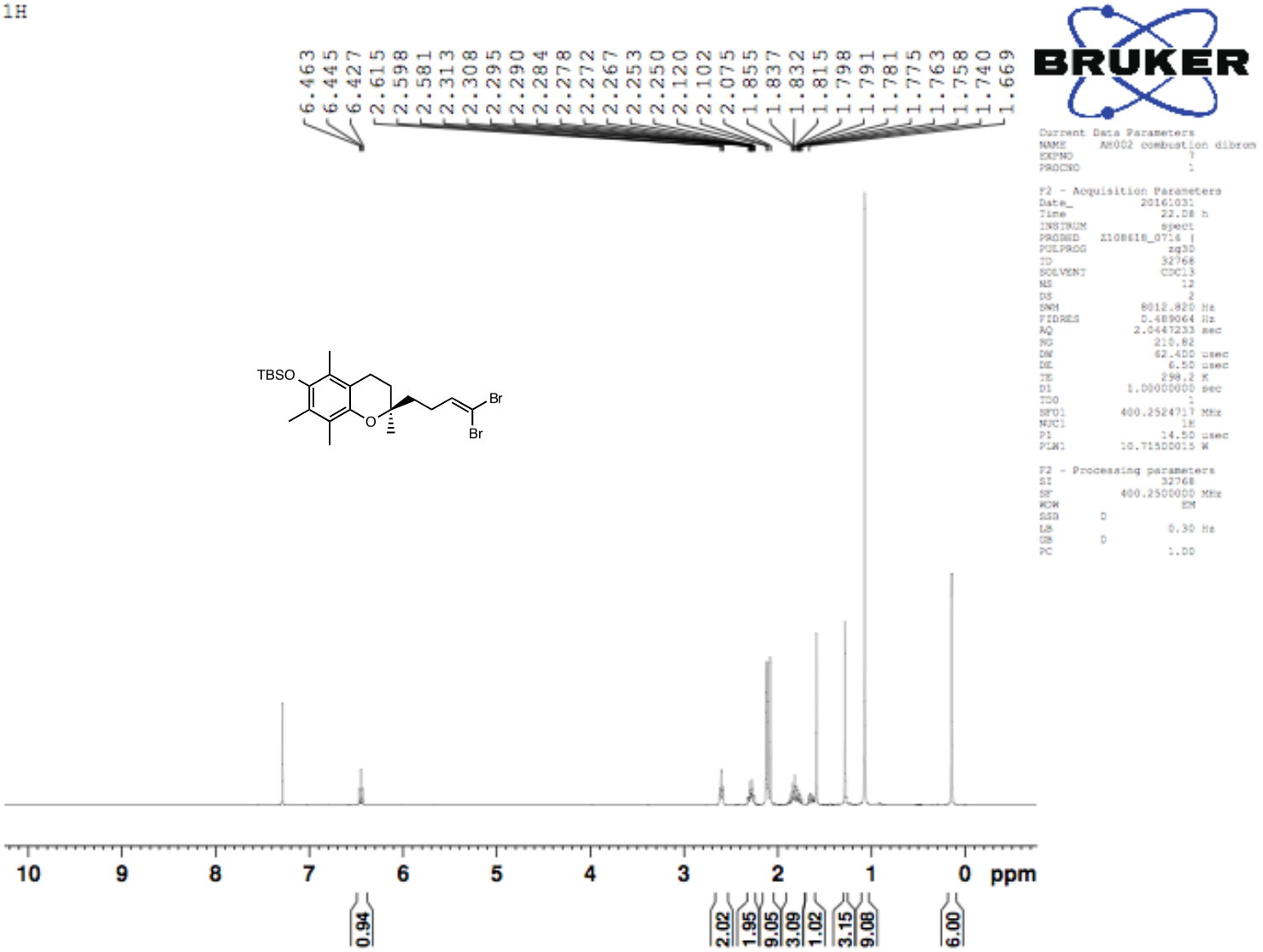
6.463
6.445
6.427
2.615
2.598
2.581
2.313
2.308
2.295
2.290
2.284
2.278
2.272
2.267
2.253
2.250
2.120
2.102
2.075
1.855
1.837
1.832
1.815
1.798
1.791
1.781
1.775
1.763
1.758
1.740
1.669
BRUKER
Current Data Parameters
NAME A8002 combustion dibrom
EXPNO 7
PROCNO 1
F2 - Acquisition Parameters
Date_ 20161031
Time 22.08 h
INSTRUM spect
PROBHD Z108618_0716 (
PULPROG zg30
TD 32768
SOLVENT CDCl3
NS 12
DS 2
SWH 8012.820 Hz
FIDRES 0.489064 Hz
AQ 2.0447233 sec
RG 210.82
DW 62.400 usec
DE 6.50 usec
TE 298.2 K
D1 1.00000000 sec
TD0 1
SFO1 400.2524717 MHz
NUC1 1H
P1 14.50 usec
PLW1 10.71500015 W
F2 - Processing parameters
SI 32768
SF 400.2500000 MHz
WDW EM
SSB 0
LB 0.30 Hz
GB 0
PC 1.00
TBSO
O
Br
Br
10
9
8
7
6
5
4
3
2
1
0
ppm
0.94
2.02
1.95
9.05
3.09
1.02
3.15
9.08
6.00

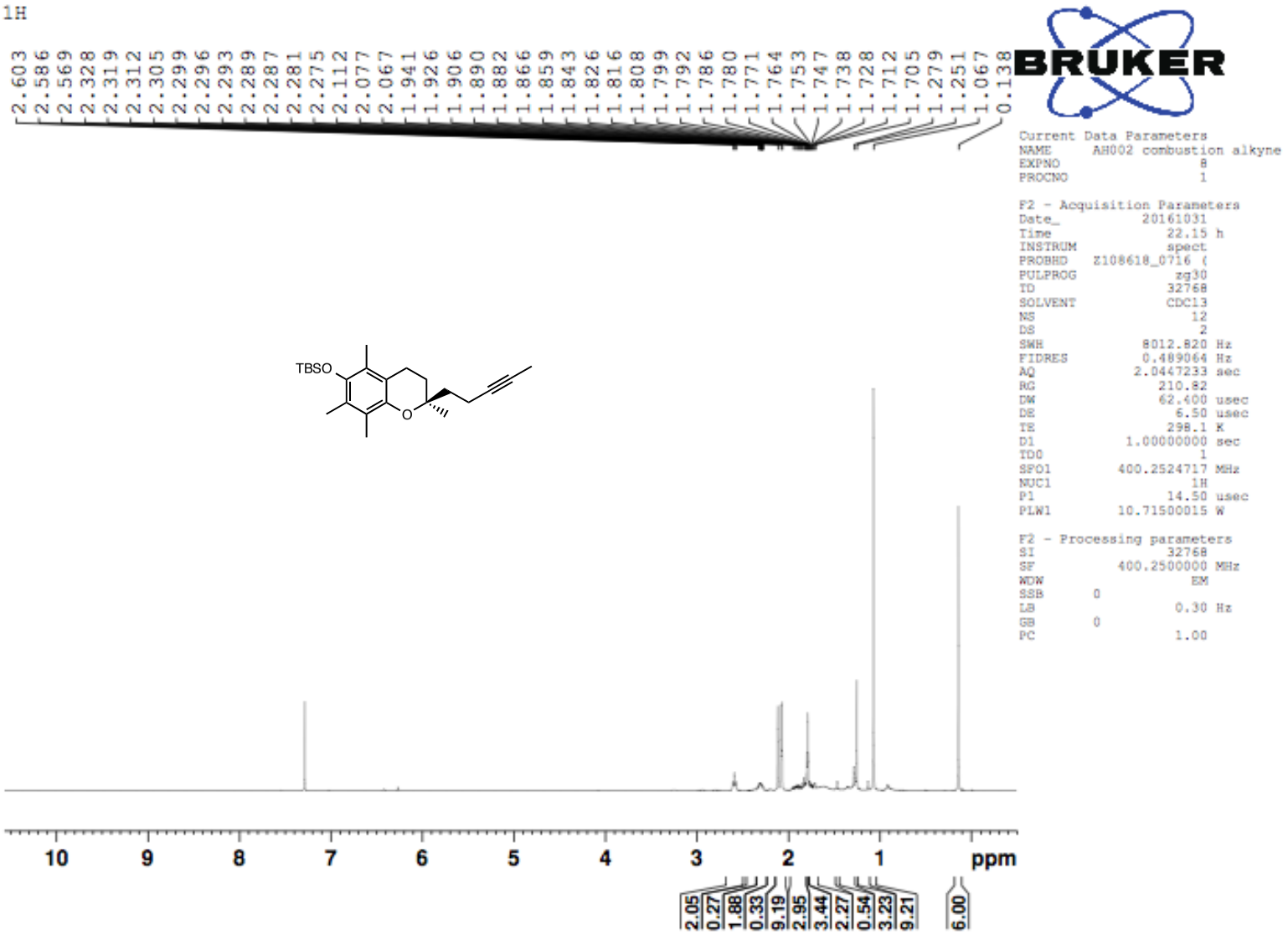
1H
2.603
2.586
2.569
2.328
2.319
2.312
2.305
2.299
2.296
2.293
2.289
2.287
2.281
2.275
2.112
2.077
2.067
1.941
1.926
1.906
1.890
1.882
1.866
1.859
1.843
1.826
1.816
1.808
1.799
1.792
1.786
1.780
1.771
1.764
1.753
1.747
1.738
1.728
1.712
1.705
1.279
1.251
1.067
0.138
BRUKER
Current Data Parameters
NAME AH002 combustion alkyne
EXPNO 8
PROCNO 1
F2 - Acquisition Parameters
Date_ 20161031
Time 22.15 h
INSTRUM spect
PROBHD Z108618_0716 (
PULPROG zg30
TD 32768
SOLVENT CDCl3
NS 12
DS 2
SWH 8012.820 Hz
FIDRES 0.489064 Hz
AQ 2.0447233 sec
RG 210.82
DW 62.400 usec
DE 6.50 usec
TE 298.1 K
D1 1.00000000 sec
TD0 1
SFO1 400.2524717 MHz
NUC1 1H
P1 14.50 usec
PLW1 10.71500015 W
F2 - Processing parameters
SI 32768
SF 400.2500000 MHz
WDW EM
SSB 0
LB 0.30 Hz
GB 0
PC 1.00
TBSO
O
10
9
8
7
6
5
4
3
2
1
ppm
2.05
0.27
1.88
0.33
9.19
2.95
3.44
2.27
0.54
3.23
9.21
6.00

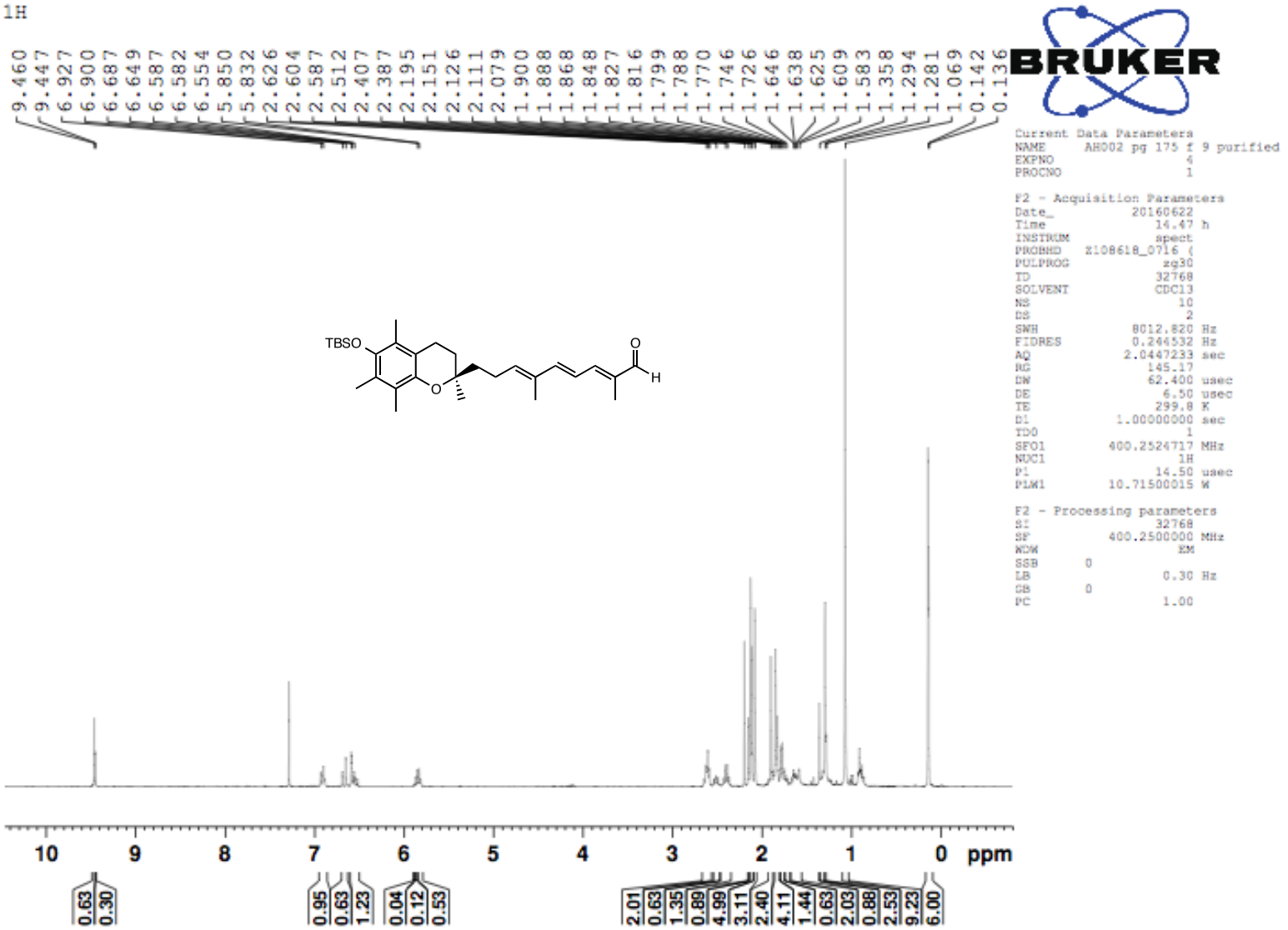
1H
9.460
9.447
6.927
6.900
6.687
6.649
6.587
6.582
6.554
5.850
5.832
2.626
2.604
2.587
2.512
2.407
2.387
2.195
2.151
2.126
2.111
2.079
1.900
1.888
1.868
1.848
1.827
1.816
1.799
1.788
1.770
1.746
1.726
1.646
1.638
1.625
1.609
1.583
1.358
1.294
1.281
1.069
0.142
0.136
BRUKER
TBSO
O
O
H
Current Data Parameters
NAME AH002 pg 175 f 9 purified
EXPNO 4
PROCNO 1
F2 - Acquisition Parameters
Date_ 20160622
Time 14.47 h
INSTRUM spect
PROBHD Z108618_0716 (
PULPROG zg30
TD 32768
SOLVENT CDCl3
NS 10
DS 2
SWH 8012.820 Hz
FIDRES 0.244532 Hz
AQ 2.0447233 sec
RG 145.17
DW 62.400 usec
DE 6.50 usec
TE 299.8 K
D1 1.00000000 sec
TD0 1
SFO1 400.2524717 MHz
NUC1 1H
P1 14.50 usec
PLW1 10.71500015 W
F2 - Processing parameters
SI 32768
SF 400.2500000 MHz
WDW EM
SSB 0
LB 0.30 Hz
GB 0
PC 1.00
10
9
8
7
6
5
4
3
2
1
0
ppm
0.63
0.30
0.95
0.63
1.23
0.04
0.12
0.53
2.01
0.63
1.35
0.89
4.99
3.11
2.40
4.11
1.44
0.63
2.03
0.88
2.53
9.23
6.00

1H

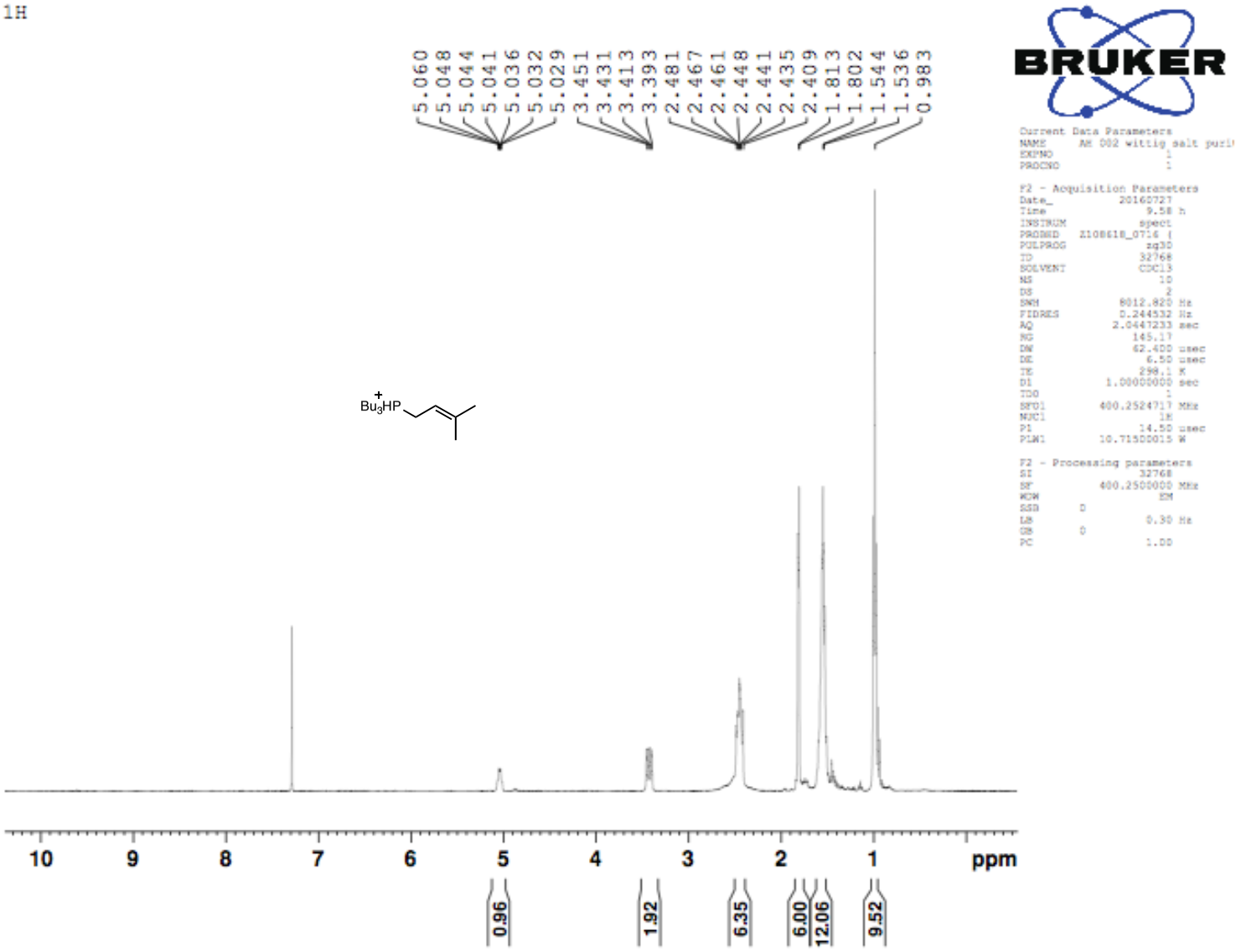

BRUKER

Current Data Parameters
NAME AK 002 wittig salt purif
EXPNO 1
PROCNO 1

F2 - Acquisition Parameters
Date_ 20160727
Time 9.58 h
INSTRUM spect
PROBHD Z108618_0716 (
PULPROG zg30
TD 32768
SOLVENT CDCl3
NS 10
DS 2
SWH 8012.820 Hz
FIDRES 0.244532 Hz
AQ 2.0447233 sec
RG 145.17
DW 62.400 usec
DE 6.50 usec
TE 298.1 K
D1 1.00000000 sec
TD0 1
SFO1 400.2524717 MHz
NUC1 1H
P1 14.50 usec
PLW1 10.71500015 W

F2 - Processing parameters
SI 32768
SF 400.2500000 MHz
WDW EM
SSB 0
LB 0.30 Hz
GB 0
PC 1.00

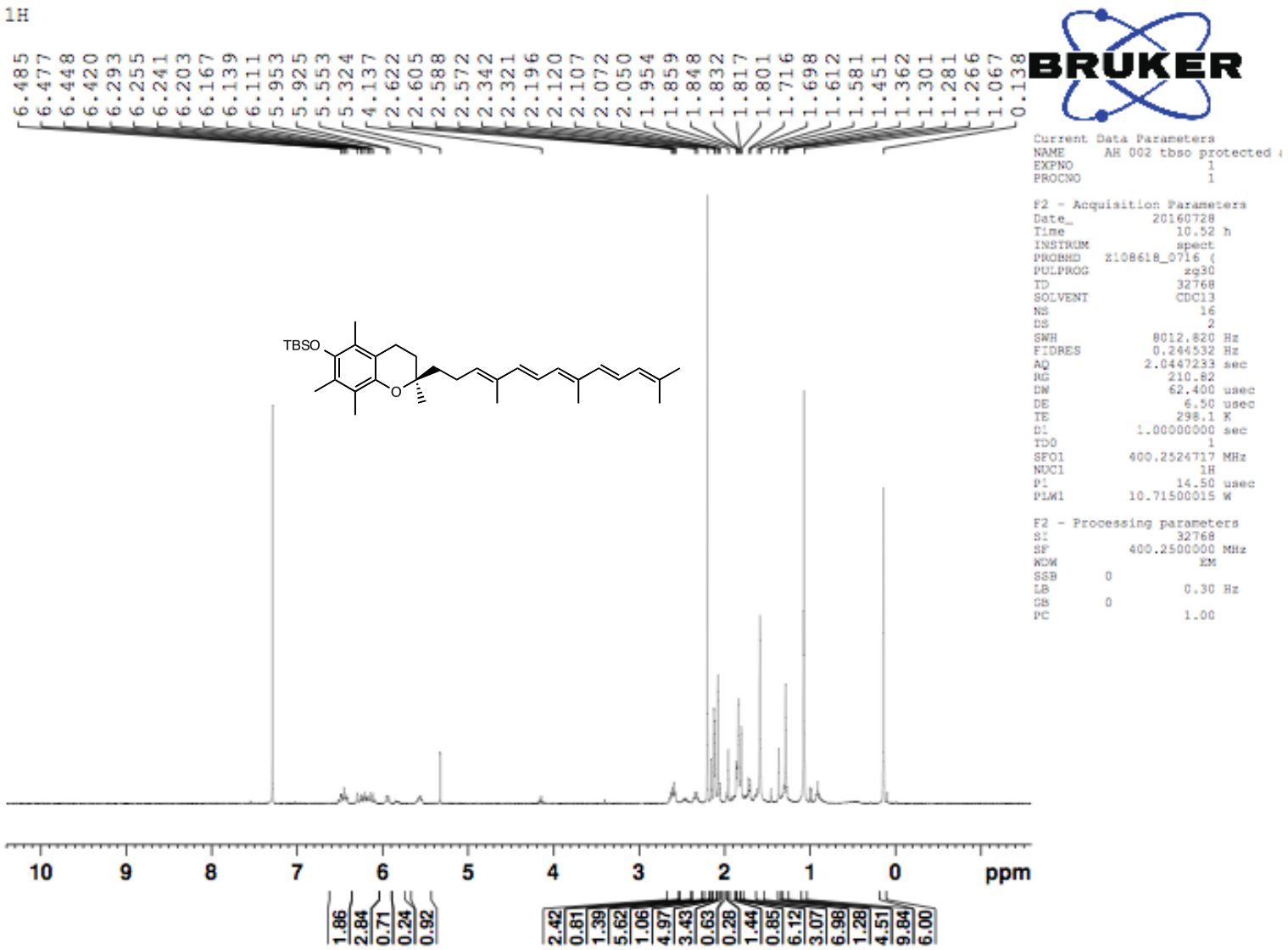
1H
6.485
6.477
6.448
6.420
6.293
6.255
6.241
6.203
6.167
6.139
6.111
5.953
5.925
5.553
5.324
4.137
2.622
2.605
2.588
2.572
2.342
2.321
2.196
2.120
2.107
2.072
2.050
1.954
1.859
1.848
1.832
1.817
1.801
1.716
1.698
1.612
1.581
1.451
1.362
1.301
1.281
1.266
1.067
0.138
BRUKER
TBSO
O
Current Data Parameters
NAME AH 002 tbso protected
EXPNO 1
PROCNO 1
F2 - Acquisition Parameters
Date_ 20160728
Time 10.52 h
INSTRUM spect
PROBHD Z108618_0716
PULPROG zg30
TD 32768
SOLVENT CDCl3
NS 16
DS 2
SWH 8012.820 Hz
FIDRES 0.244532 Hz
AQ 2.0447233 sec
RG 210.82
DW 62.400 usec
DE 6.50 usec
TE 298.1 K
D1 1.00000000 sec
TD0 1
SFO1 400.2524717 MHz
NUC1 1H
P1 14.50 usec
PLW1 10.71500015 W
F2 - Processing parameters
SI 32768
SF 400.2500000 MHz
WDW EM
SSB 0
LB 0.30 Hz
GB 0
PC 1.00
10
9
8
7
6
5
4
3
2
1
0
ppm
1.86
2.84
0.71
0.24
0.92
2.42
0.81
1.39
5.62
1.06
4.97
3.43
0.63
0.28
1.44
0.85
6.12
3.07
6.98
1.28
4.51
9.84
6.00

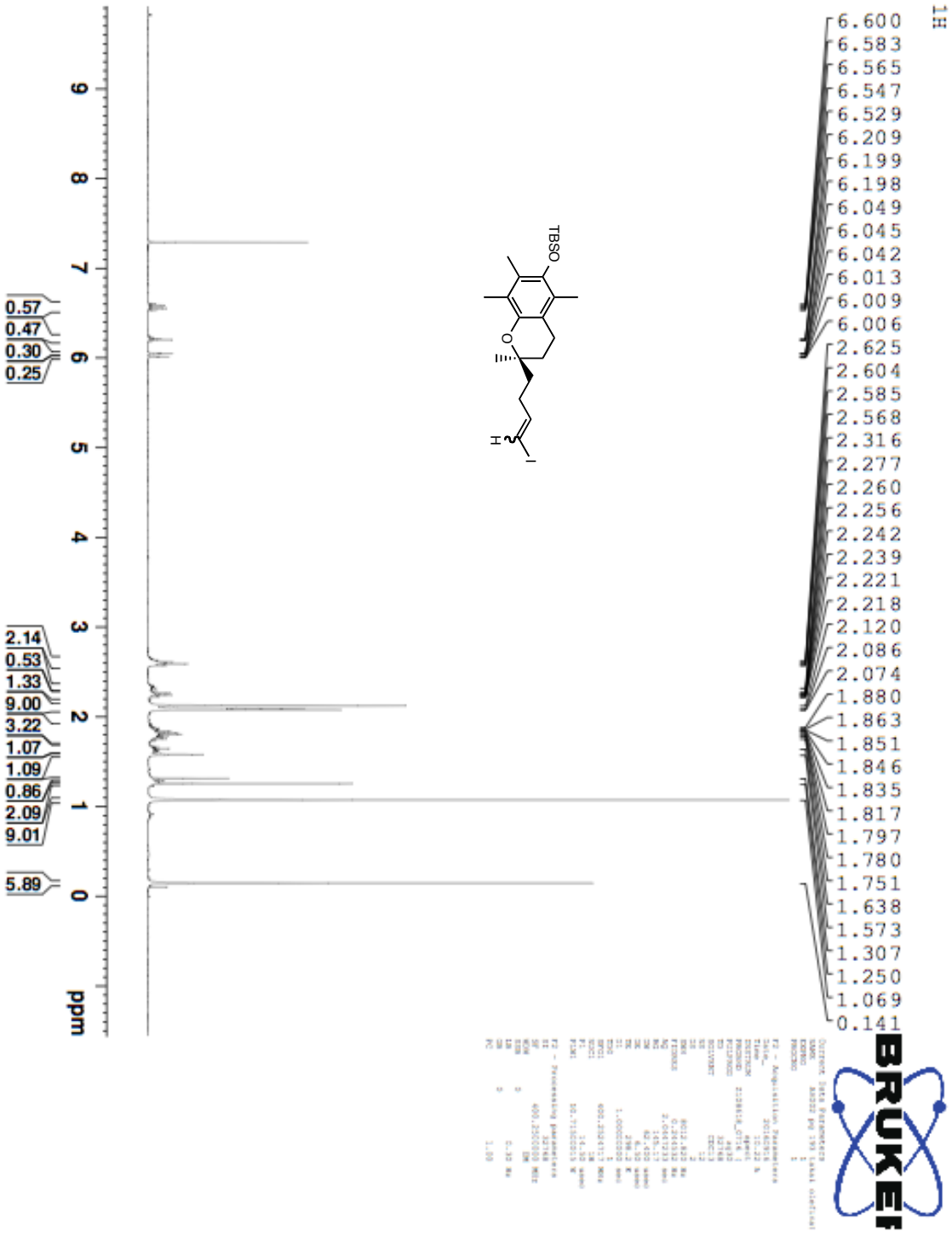
1H
6.600
6.583
6.565
6.547
6.529
6.209
6.199
6.198
6.049
6.045
6.042
6.013
6.009
6.006
2.625
2.604
2.585
2.568
2.316
2.277
2.260
2.256
2.242
2.239
2.221
2.218
2.120
2.086
2.074
1.880
1.863
1.851
1.846
1.835
1.817
1.797
1.780
1.751
1.638
1.573
1.307
1.250
1.069
0.141
TBSO
O
H
0.57
0.47
0.30
0.25
2.14
0.53
1.33
9.00
3.22
1.07
1.09
0.86
2.09
9.01
5.89
ppm
BRUKER

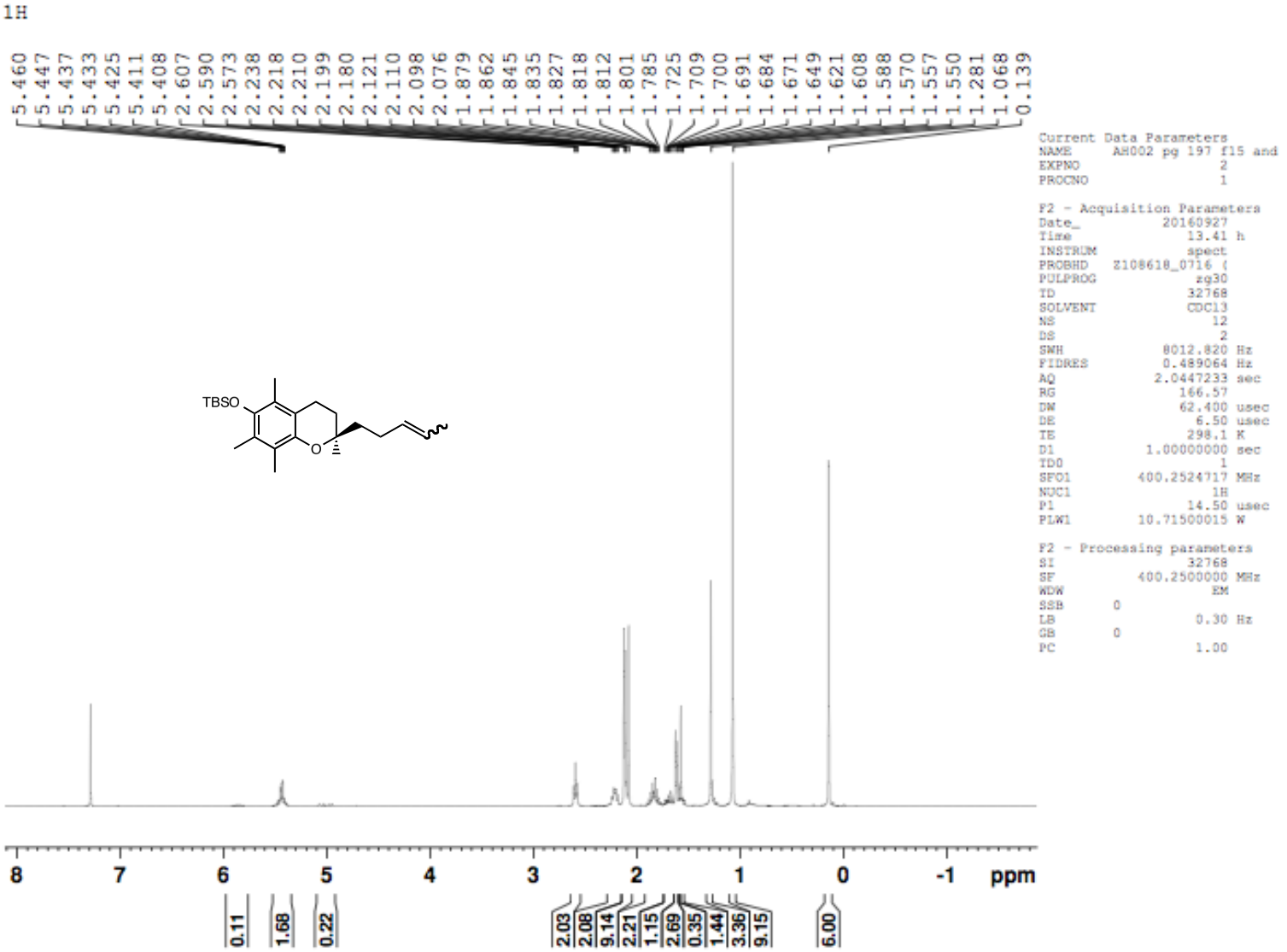


```
Current Data Parameters
NAME      AH002 pg 197 f15 and
EXPNO                        2
PROCNO                       1

F2 - Acquisition Parameters
Date_              20160927
Time                 13.41 h
INSTRUM              spect
PROBHD    Z108618_0716 (
PULPROG              zg30
TD                   32768
SOLVENT              CDCl3
NS                      12
DS                       2
SWH               8012.820 Hz
FIDRES            0.489064 Hz
AQ                2.0447233 sec
RG                   166.57
DW                   62.400 usec
DE                    6.50 usec
TE                   298.1 K
D1                1.00000000 sec
TD0                      1
SFO1            400.2524717 MHz
NUC1                    1H
P1                   14.50 usec
PLW1             10.71500015 W

F2 - Processing parameters
SI                   32768
SF              400.2500000 MHz
WDW                     EM
SSB          0
LB                    0.30 Hz
GB           0
PC                    1.00
```